NASA TECHNICAL MEMORANDUM

NASA TM X-53395

February 10, 1966

NASA TM X-53395

GPO PRICE $

CFSTI PRICE(S) $

Hard copy (HC) $5.00

Microfiche (MF) 1.00

ff 653 July 65

PROGRAM PLAN FOR EARTH-ORBITAL LOW G HEAT TRANSFER AND FLUID MECHANICS EXPERIMENTS

By M.E. Nein and C.D. Arnett
Propulsion and Vehicle Engineering Laboratory

NASA

George C. Marshall Space Flight Center, Huntsville, Alabama

TECHNICAL MEMORANDUM X-53395

PROGRAM PLAN FOR EARTH-ORBITAL LOW G HEAT TRANSFER AND FLUID MECHANICS EXPERIMENTS

By

M. E. Nein and C. D. Arnett

George C. Marshall Space Flight Center
Huntsville, Alabama

ABSTRACT 25307

A feasibility study for orbital experiments in fluid mechanics and heat transfer is presented.

The need for fluid mechanic and heat transfer experiments under low gravity and space vacuum conditions is analyzed. The limitations of earth based experiments are discussed and approaches for the design of an orbital experiment module are given. It is shown that orbital experiments in cryogenic fluid mechanics and heat transfer can be conducted with scale models of future systems. The concepts advanced in this paper can serve as a basis for detailed design of a flight system and the timely accomplishment of integrating these experiments into the earth orbital Apollo missions.

author

NASA - GEORGE C. MARSHALL SPACE FLIGHT CENTER

NASA-GEORGE C. MARSHALL SPACE FLIGHT CENTER

TECHNICAL MEMORANDUM X-53395

PROGRAM PLAN FOR EARTH-ORBITAL LOW G HEAT TRANSFER AND FLUID MECHANICS EXPERIMENTS

By

M. E. Nein and C. D. Arnett

PROPULSION DIVISION
PROPULSION AND VEHICLE ENGINEERING LABORATORY
RESEARCH AND DEVELOPMENT OPERATIONS

TABLE OF CONTENTS

PROGRAM PLAN FOR EARTH-ORBITAL LOW G HEAT TRANSFER AND FLUID MECHANICS EXPERIMENTS

LIST OF TABLES

LIST OF ILLUSTRATIONS

LIST OF ILLUSTRATIONS (Cont'd)

LIST OF ILLUSTRATIONS (Cont'd)

PROGRAM PLAN FOR EARTH-ORBITAL LOW G HEAT TRANSFER AND FLUID MECHANICS EXPERIMENTS

By

M. E. Nein and C. D. Arnett

George C. Marshall Space Flight Center

Huntsville, Alabama

SUMMARY

The design of space flight vehicles with long stay time in the low gravity and hard vacuum environment of space requires a thorough understanding of fluid mechanics and heat transfer phenomena effected by these conditions. This paper presents the results of a feasibility analysis of orbital experiments that are required to support analytical investigations and to develop general correlations which can aid in the design of future cryogenic space storage and propellant transfer systems. On the basis of individual experiments in the various disciplines, a modular concept for an experiment station is derived. It is shown that small scale experiments can be used to investigate these phenomena with sufficient confidence for application to full scale space flight systems.

A development schedule for integration of the experiment module into the Earth Orbital Apollo missions is presented. It is shown that utilization of the Lunar Excursion Module (LEM) as an experiment carrier affords maximum benefit from astronaut participation in the conduct of experiments. The pursuit of the modular concept is recommended since experiments can be incorporated with maximum effectiveness depending on mission requirements.

INTRODUCTION

The behavior of space vehicle propellants under conditions of low gravity and of propellant container thermal protection systems under space vacuum is being studied extensively by NASA and others. Although considerable information has been obtained by experimentation in drop towers, aircraft, and vacuum chambers, earth-based simulation is insufficient. For low gravity simulation, the available time at reduced g level is too short to eliminate standard g flow transients that persist into the low g phase and obscure results. In addition, experimental package sizes that can be accommodated in drop towers require small models which in turn yield results that are questionable for a full understanding of the phenomena. Similarly, since it is impossible in present ground facilities to subject a cryogenic storage tank simultaneously to all flight environments of vibration, rapid pressure changes, acceleration, and radiation, the use of vacuum chambers to study the propellant storage conditions in space provides only a partial understanding of some of the major problems.

It is necessary to conduct several basic orbital experiments that can provide a more complete understanding of the heat transfer and fluid mechanics phenomena of long duration space flight. These experiments will also establish a set of reference conditions from which the validity of earth-based low g and space vacuum simulation can be determined.

The experiments proposed by MSFC as a single payload package are:

Boiling Heat Transfer (MSFC-#5)*
Cryogenic Propellant Transfer (MSFC-#6)*
Spaceborne Propellant Storage System (MSFC-#7)*

Although the primary objectives of these experiments are indicated by their titles, these experiments will investigate the following additional related areas:

1. Bubble growth and dynamics
2. Propellant settling and ullage control

*MSFC Experiment Review Board Number

3. Orbital sloshing
4. Liquid "suction dip" prevention
5. Stratification and stratification destruction
6. Venting of cryogenic fluids under zero-g

In addition it is proposed to incorporate previously approved flight experiments in the areas of boundary layer jump up and low gravity nucleonic mass gaging, since the experimental requirements can be obtained within this payload package.

Acknowledgement is made of major contributions to this document by Messrs. J. Cody, H. Hyde, H. Trucks, and T. Winstead in the areas of superinsulation, propellant transfer, and stratification.

RESEARCH MODULE CONCEPT

Our philosophy is to develop a low gravity heat transfer and fluid mechanics research module around standardized boiling, propellant transfer, and cryogenic propellant storage modules. These three systems will be designed so that the scaling and modeling laws will enable related experiments to be performed using the basic modules with their instrumentation, transfer, venting, photographic, heating, attitude control, and miscellaneous systems intact. FIG 1 illustrates this concept and lists the known related satellite experiment systems that could be incorporated.

The module concept will provide a standardized test system to obtain the necessary technology to design an orbital tanker, a cryogenic upper stage, or any space system that stores, transfers or utilizes cryogenics. This approach will generate the best experiment mission flexibility by employing standardized research modules and implementing the satellite experiments as payloads become available. A well planned program based upon this philosophy will guarantee that all payloads are fully utilized at a minimum cost, for as a satellite experiment is developed, it is not necessary to develop a new flight test system. This approach also assures reliable data interpretation due to the extended familiarization possible with a standardized system. Also, scientific astronaut participation in experiments performed in a standardized module would enhance the probability of obtaining more accurate experimental data. Any of these modules could be "plugged in or out" depending upon mission requirements. This philosophy requires long term use of these modules by government and industry for high effectiveness.

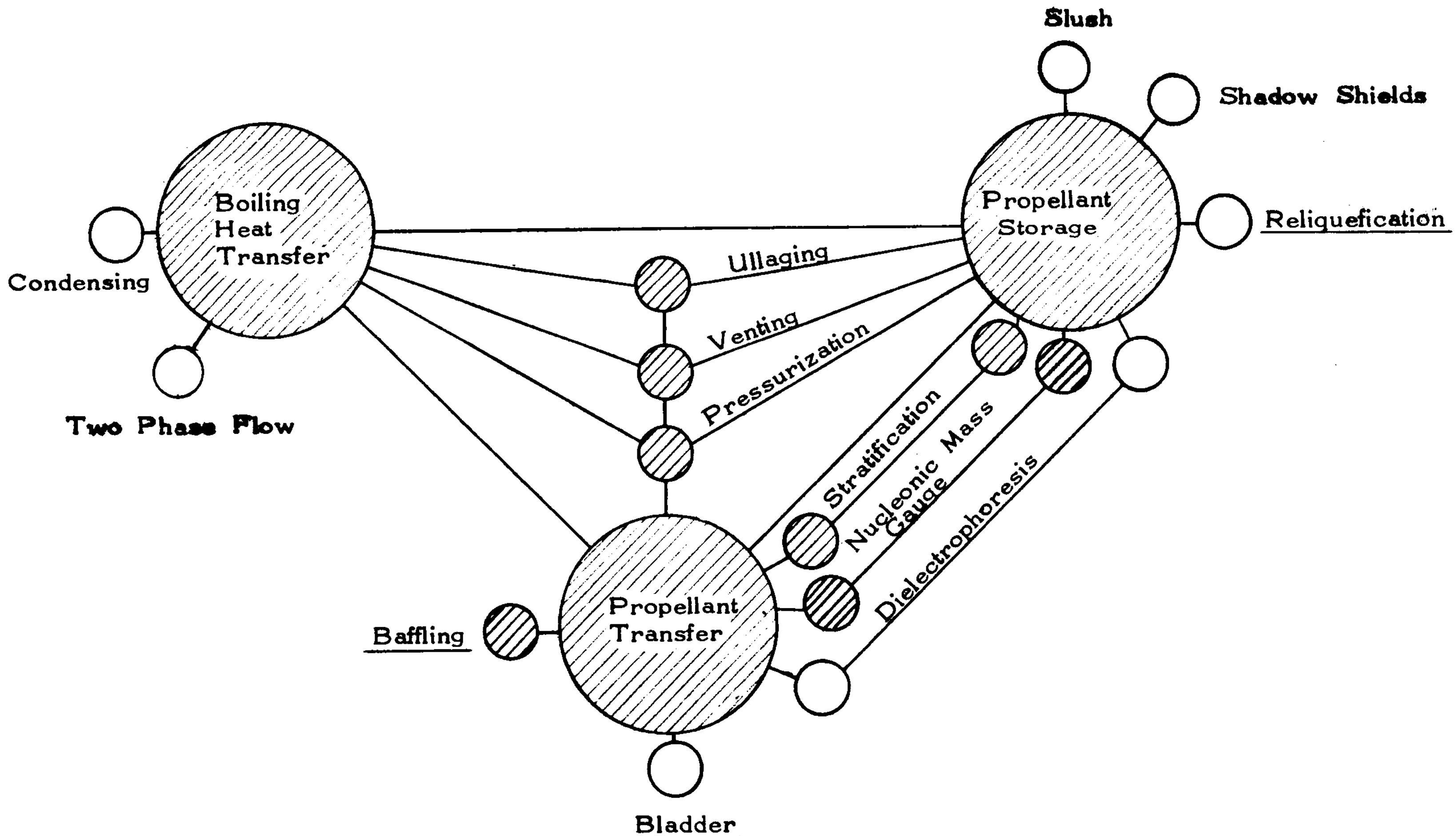

FIG 1 RESEARCH MODULE CONCEPT

EXPERIMENT DEFINITION

Boiling Heat Transfer

Interest in heat transfer to boiling cryogenic fluids has increased rapidly primarily because of the growing number of space applications. Because cryogenic boiling is characterized by small temperature driving forces and small heat fluxes, cryogens can hardly be stored and transferred without the occurrence of boiling and the associated problems of vapor removal, tank pressure control, tank boil over, etc. While these conditions may be looked at by a space vehicle designer as undesirable and complicating, other aspects of cryogenic boiling are desirable for heat transfer equipment design. For instance the direct transition of nucleate boiling to stable film boiling without exceeding burnout temperatures for many materials affords the design of high power density evaporators such as may be used in life support and cooling equipment.

However, theory and limited experimentation show dependence of the boiling phenomena on the local acceleration and thus require detailed studies to understand the influence of the gravity forces on the mechanism of boiling.

Analyses of the boiling phenomena under reduced gravity have been conducted in drop towers and aircraft flying through low gravity trajectories. However, due to the short durations and possible effects of residual flow currents, the behavior of bubbles and vapor films under long duration low gravity cannot be assessed. Any comparison between nucleate boiling under short term and long term zero gravity will depend on the motion of the vapor as it is generated. If it remains in the vicinity of the heating surface, the nucleate boiling, as such, no longer continues. Subcooled liquid at the heating surface is difficult to maintain without gross convection. Due to the poor removal of vapor, small bubbles coalesce and form a large film of vapor that in itself adds resistance to heat transfer. Present drop tower data does not indicate any deviation of the nucleate boiling flux curve under low gravity from the curve at standard gravity. However, the low gravity durations are too short to allow development of a vapor layer as could occur under long term low g conditions.

Deviation of the peak flux, the film boiling regime, and the incipient boiling flux at low gravity from the standard gravity conditions are indicated by analytical and experimental results, even for the short duration tests. FIG 2 shows the results obtained with liquid nitrogen in a 1.4 sec drop tower facility of the University of Michigan, as an illustration of the phenomena.*

Because of these limitations encountered with earth-based low gravity experimentation, it is necessary to conduct basic experiments during long term low gravity space flight to provide reliable reference conditions for future analyses. The basic considerations for planning the orbital boiling heat transfer experiment are given in Appendix A.

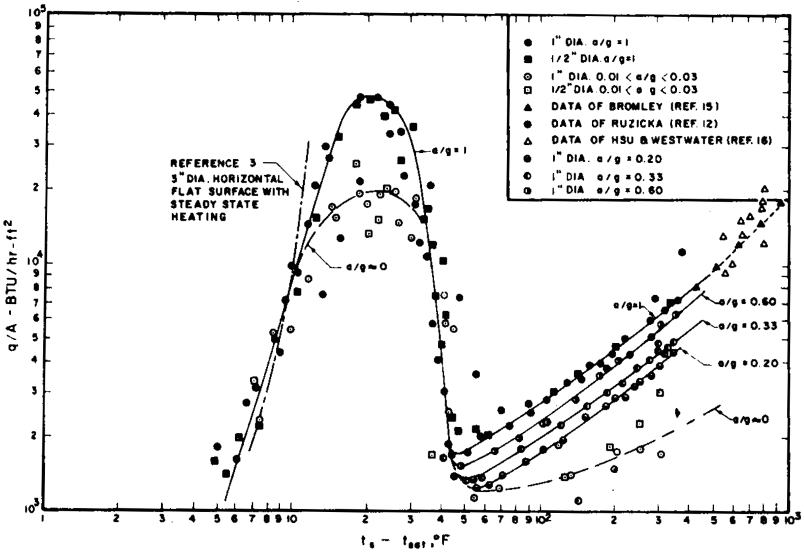

FIG 2 Film Boiling Under Standard and Fractional Gravity and Nucleate Boiling at Standard Gravity and Free Fall. Liquid Nitrogen.

* Note that the upper limit of nucleate boiling, which represents the end of the controlling regime of the evaporative micro layer mechanism, is definitely affected by the gravity condition. At this point free convection forces within the vapor layer adjacent to the wall become controlling and thus gravity effects appear even in short duration tests.

Spaceborne Cryogenic Propellant Storage

As extended mission times of one week or more are contemplated, the need for high energy propellants such as liquid hydrogen becomes more important. However, most high energy propellants are cryogenics with low boiling points and evaporate readily. To fully utilize high energy propellants, thermal protection systems must be designed to protect cryogenics for long periods of time in space. Insulation, stratification, and venting systems are to be analyzed by this experiment.

Insulation

Multi-layer, highly reflective insulation or high performance insulation (HPI) solves part of the problem of long term cryogenic storage. Moreover, the product of thermal conductivity times density for HPI is so low that they are desirable even where high performance is not critical. HPI alone, however, is not sufficient to reduce boiloff to acceptable levels. In fact, the total heat leaks through ducting and structural supports can be equal to or greater than that through the sidewall insulation.

Numerous design studies and structural and thermal tests have been performed by various organizations, and at least two HPI systems are presently being ground tested and could probably be successfully flight tested. The proposal presented herein utilizes what is now the most feasible HPI system.

The basic objective of the HPI flight experiment is to obtain experimental data that can be used to design, with a high degree of confidence, a workable insulation system that will sustain all flight environments and perform as predicted after application to flight type tankage. A secondary objective is to demonstrate the performance of a multi-layer insulation system that has been subjected to the overall vehicle operating regimes from ground hold to space environments.

It is necessary to design the insulation system for the entire vehicle operating regime. Thus this experiment is being designed considering ground hold, ascent flight, and orbital environments. These three regimes will be dealt with by careful consideration of thermal analysis, structural design, and material application to produce the best integrated design.

At the present time, the designer has very little data on high performance insulations that have been subjected to flight conditions. Even though vibration, acoustical, ascent g loading, and rapid evacuation tests have been performed on many insulation samples, all flight conditions have never been simultaneously simulated on a tank at liquid hydrogen temperature. In addition, no vacuum facilities in the country can reproduce the time-ambient pressure history the Saturn class vehicles encounter. The following data are of primary importance for the insulation test:

1. Insulation pressure decay during boost.
2. Applied apparent thermal conductivity of high performance insulation in orbit.
3. Ground hold boiloff.
4. Ratio of total boiloff to vacuum boiloff.
5. Required time to evacuate insulation to $< 10^{-5}$ mmHg.
6. Thermal degradation after the insulation has been subjected to simultaneous high g loading, vibration, acoustics and rapid evacuation.
7. Analysis of residual gas within the high performance insulation layers.

Due to the wide variation possible in insulation layups, vehicle designs, support systems, etc., it is neither desirable or possible to test all configurations in space. Parameter variations and basic information will be obtained on the ground prior to flight. Thus, the basic design will be derived from ground tests and verified in flight. Likewise, the design of any future vehicle will be proven by ground tests of all parameters with modification of the data as appears necessary from the results of the proposed orbital experiment.

The main goal of the analysis of the orbital data will be to obtain a reliable value of sidewall conductivity (K) for the particular insulation layup and to determine the effect of vehicle ascent on insulation de-gassing. The flight value of sidewall K will be compared with the curve of insulation K vs T obtained from ground tests as shown below.

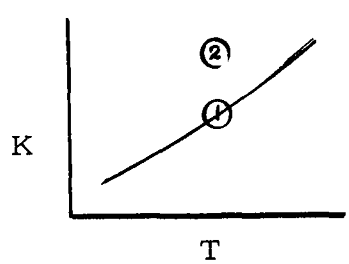

If the flight value of K lies on point (1), values of K obtained from ground tests of various insulation layups and variations would be used with confidence for design purposes. If the flight value of K lies, for instance, at point (2) an appropriate correction factor would be applied to the ground test thermal conductivity before these values are used for design of some future vehicle. An isothermal shroud is recommended for the superinsulation test tank in order to be more certain of the average temperature of the external insulation layer and, therefore, obtain a more reliable value of T_{mean} in the above curve.

The overall tank performance will be obtained by measuring total propellant boiloff. The contribution of the penetrations will be subtracted from this leaving the total heat entering the tank through the sidewall. This will be used to evaluate the sidewall K. The contribution of the insulation penetrations to total heat leak will be evaluated by careful instrumentation during flight and comparison of these results with ground test results. These data may be improved by applying electrical heat or cooling the penetration with vent gas.

Stratification

In the past few years, numerous studies of thermal stratification in cryogenic propellant tanks have been conducted. These investigations may be categorized into groups of stratification prediction and stratification reduction at one-g (and greater) and at near-zero g, for consideration of turbulent and laminar boundary layer flow along the tank sidewalls.

Thermal stratification causes the pressure within a cryogenic storage tank to be considerably higher than would be the case if the propellant were uniformly mixed. A typical example is shown in FIG 3 . The tank may be vented to alleviate the problem of increased ullage pressure. There are periods of time during space vehicle operation, such as the boost phase and the period following orbital injection, in which venting is either undesirable, not possible, or requires auxiliary systems for ullaging and/or liquid/vapor separation. Accurate prediction of stratification is required during these periods to determine tank design pressure levels and auxiliary system requirements.

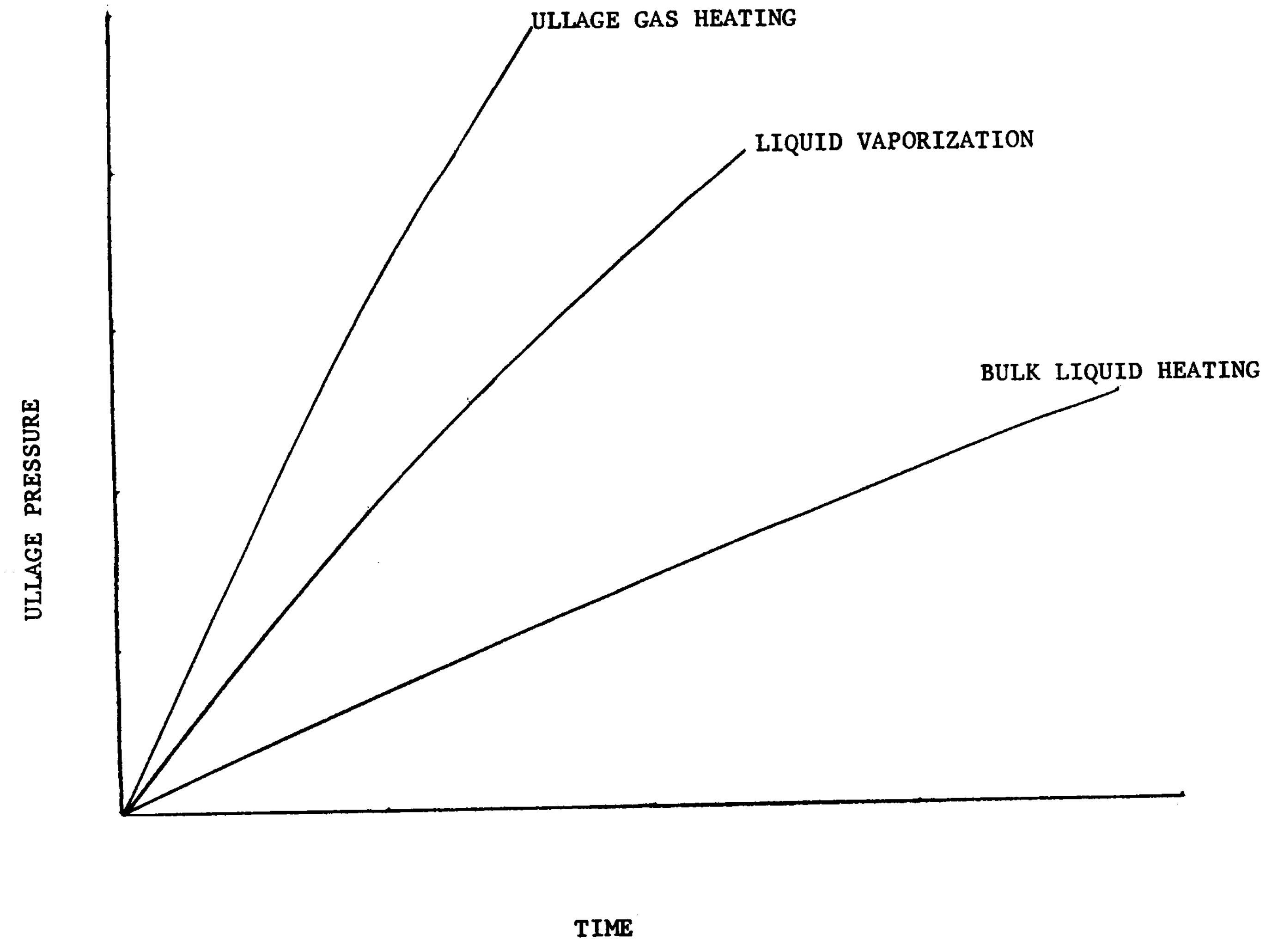

FIG 3

PRESSURE RISE RATE VERSUS TIME FOR THREE THEORETICAL MODELS OF HEAT ADDITION

The basic differences in stratification under high gravitational acceleration and very low gravitational acceleration are the type of boundary layer flow and the ullage location and geometry. Consequently, somewhat different methods of prediction are required for the two conditions.

Several analytical models have been developed for one-g stratification prediction. These models predict the temperature distribution within a cryogenic propellant tank subjected to both sidewall and bottom heating. These formulations are limited with respect to their application to other gravitational conditions; however, the analytical techniques have been extended to apply at near-zero g.

In most of the experimental measurements to date, correlations with basic dimensionless groups (Grashof, Prandtl, etc.) have been attempted. The utility of the correlations is, of course, in the application of the results of limited experimental measurements to a variety of similar, but different, situations and conditions. As a result, there is a wealth of process technology that requires intensive study and representative data for verification.

Results of this experiment with respect to stratification can be generally summarized as a significant set of data to advance the state-of-the-art of cryogenics in space. The fundamental processes of stratification will be demonstrated and will provide an additional basis for acceptance or rejection of the numereous hypotheses of fluid behavior that dictate vehicle design criteria. Also, a demonstration of a low-g stratification reduction device will be of significance, because demonstration of hardware and processes at one-g is only minimal.

These experiments cannot be performed in one-g tests due to small perturbation effects on fluid behavior and the effects of pressurant/liquid heat and mass transfer. Accurate analytical models are not feasible without empirical zero-g data, much of which will be provided by this experiment. A discussion of the pertinent variables, correlation equations, hardware, and instrumentation requirements for the experiment are presented in Appendix B.

Venting

The need for venting cryogenic propellant storage tanks while coasting in space under zero or low acceleration became a real one in the late 1950's, when development of advanced space vehicles capable of engine restarts began.

A cryogenic propellant tank in space absorbs heat, thereby vaporizing some of the already-saturated liquid and tending to increase the tank pressure. The rate of heat addition and, therefore, tank pressure rise can be decreased by insulating the tank; but even with very heavy thermal protection systems, some energy will be transmitted to the propellant. The storage tank must either be strong enough to withstand the resulting pressure rise, or some means must be provided to relieve the tank pressure. The only method of relieving tank pressure employed in practice has been venting of propellant.

Venting can be very simply accomplished on the earth's surface, because the liquid and vapor always occupy known positions within the tank and a simple vent pipe can be employed. This is not practical under low-gravity conditions because the vapor/liquid distribution in the tank can shift easily with small disturbing forces. The following are a number of sources of such disturbing forces.

1. Sloshing induced during the ascent flight could be one of the major sources of energy in the propellant at injection into orbit.
2. During ground hold and ascent, environmental heating will cause thermal convective patterns to form in the liquid, with the hot fluid rising to the top of the liquid due to buoyancy forces and spreading across the surface. If the acceleration is suddenly reduced, as at injection, it is believed that the liquid streamlines will continue vertically instead of continuing to bend over at the liquid surface.
3. Termination of propellant draining from the tank could cause disturbances associated with valve closure or change in direction of fluid momentum near the tank outlet.
4. The tank sidewalls and lower bulkheads will be deflected during boost flight. At injection into orbit the structure will try to return to its undeflected position and, in the process, transmit some of its stored energy to the liquid.
5. Although liquids have low compressibilities, the amount of energy stored in the hydrogen because of the hydrostatic head may have a significant effect on the propellant behavior at injection.

6. During orbital coast, several other types of disturbances may contribute to fluid motion such as: aerodynamic drag, gravity gradient, solar pressure, attitude control operation, or crew movements.

Settling rockets have been used in current venting applications but have two undesirable features: they affect vehicle guidance and control, and are excessively heavy for very high acceleration levels or coast times. It is important, therefore, to study ways of separating vapor from a two-phase mixture of cryogenic propellant in order to insure venting of vapor only.

The heat exchange vent system has been judged the most promising and will be utilized for this experiment. A conceptual feasibility design has been developed incorporating the most nearly optimum design and operating features. Some of these features are summarized below:

1. The heat exchange system consists of a flow regulator valve through which the incoming vent-side fluid is expanded to a lower temperature and pressure, a heat exchanger in which the cooled vent stream exchanges heat with the warmer tank fluid, and a turbine through which the vent stream leaving the exchanger is further expanded to supply power to drive the pump that circulates tank-side fluid through the exchanger and within the tank. After leaving the turbine, the vent stream flows through a control valve sensing tank pressure and finally to small thrustors where it is used to supply settling thrust to the stage during coast periods.
2. The heat exchanger is a compact, finned-surface, counter-flow exchanger with a single pass on each of the vent and tank sides.
3. There is a common location for the vent and tank side inlets.
4. The vent stream exchanger exit temperature and pressure are 37 $^{\circ}$R and 6 psia, respectively.
5. The system should be located in the forward dome region of the tank, and suspended from the manhole cover.

Propellant Transfer

Successful extension of the NASA space program to long duration missions, such as manned interplanetary exploration, requires development of an earth orbital launch capability to remove limitations imposed by Saturn V and future earth launch vehicles. Methods for transferring cryogenic propellants from orbital tankers to an S-IVB class vehicle, nuclear vehicle, or a small "kick stage" must be developed to guarantee optimized propellant use. Several potential orbital propellant transfer modes currently exist; however, these conceptual transfer modes cannot be properly evaluated without experimental data or excessive extrapolation of the present state-of-the-art.

The two basic approaches to obtain the experimental data that will be required to adequately design an orbital transfer system are:

1. Earth-based tests with simulated orbital propellant transfer modes.
2. Small scale orbital experiments.

Propellant transfer under standard gravity conditions will provide an indication of maximum transfer rates; however, the complex super position of heat transfer and fluid motion occurring during orbital propellant transfer cannot be properly simulated. Propellant transfer experiments, in addition to investigating major factors that influence the design of an optimum propellant transfer system, can be organized to (a) directly investigate problems pertinent to feasible propellant transfer modes, (b) expose any unknown problems associated with the various propellant transfer modes that will be tested, and (c) provide valuable data concerning cryogenic propellant flow patterns over extended time periods under low gravity.

Problems associated with the overall experiment (i.e., weight allotment, power requirements, time, available propellants, available space) will define limitations of the propellant transfer experiment. It is realized that the acquisition of usable data should not be jeopardized by attempting excessively complicated experiments. For example, propellant transfer times for an experiment must be sufficiently long to allow adequate steady-state operating time for mechanical equipment such as pumps, vapor separators, quality meters, etc., although longer transfer times will necessarily reduce the number of transfer modes which can be experimentally investigated. Within such limitations, the propellant transfer experiment will be designed to obtain maximum information on major factors that influence the selection of an optimum propellant transfer system including gravity level, "suction dip," damping of transfer fluid momentum, vehicle attitude perturbations, vent performance, and transfer mode. In general, the experiment will use pumps and pressure to transfer LH_2 alternately between two geometrically similiar, superinsulated tanks under varying g loads with vented and nonvented receiver tanks. The basic considerations for planning the orbital cryogenic propellant transfer experiment are extensively discussed in Appendix C.

SYSTEM REQUIREMENTS

The systems required to accomplish the experiment tasks are listed in Table I and are shown schematically in FIG 4. Table II lists some representative components that may be used in these systems; flight qualified components will be used where possible. Table III contains system design data. The layout of the boiling tank (FIG 5) illustrates the philosophy of using a fixed focal length movie camera with variable frame speed and back lighting. The heat transfer models are moved into view by a manipulator actuated by the astronaut. The astronaut may also visually monitor the model for bubble growth and adjust the input power for better data acquisition. Figures 6 and 7 are representative sketches of the flat plate and bubble growth heat transfer models. FIG 8 is a layout of the proposed superinsulation tank with HPI techniques shown. A schematic of a zero-gravity vent system is illustrated in FIG 9.

A layout of the research module is shown in Figures 10 and 11, located in a proposed LEM lab, which is being utilized as the main carrier for the module during the definition study phase. A parametric carrier study will be performed during phase B. The preliminary module design will be applicable to various carrier vehicles. A preliminary system weight breakdown is presented in Table IV. A list of instrumentation requirements is presented in Table V.

TABLE I

Low Gravity Heat Transfer and Fluid Mechanics Experiments

BOILING HEAT TRANSFER

Tests	Systems
I. Vertical Plate	1. Tank
	2. LH_2 Transfer
II. Horizontal Plate	3. Vent System
	4. Lights, Cameras
III. Bubble Growth	5. Manipulator
	6. Purge
	7. Instrumentation
	8. Power
	9. Networks
	10. Insulation
	11. Window
	12. Plates (Models)

PROPELLANT TRANSFER

Tests	Systems
I. Pump	1. Two Tanks
	2. Insulation
II. Pressure	3. Lights, Camera
	4. Power
	5. Instrumentation
III. Vent Device	6. LH_2 Transfer
	7. Pump - Two way
IV. Positioning	8. Pressurization
	9. Venting
V. Baffling	10. Vortex Device
	11. Baffles
	12. Heaters (Internal)
	13. Purge
	14. Valves (Submerged)
	15. Spray Nozzle

SPACE BORNE CRYOGENIC PROPELLANT STORAGE

Tests	Systems
I. Stratification	1. Tank
	2. Instrumentation
II. Insulation Evaluation	3. Insulation
	4. Pump
III. Stratification Reduction (Mixing)	5. Pressurization
	6. Zero-Gravity-Vent Device
	7. Transfer
IV. Pressure Rise Rate	8. Mixer
V. Venting	

NOTE:
ALL THREE-WAY SOLENOID
VALVES MAY BE VENTED THROUGH
THE NONPROPULSIVE VENT SYSTEM

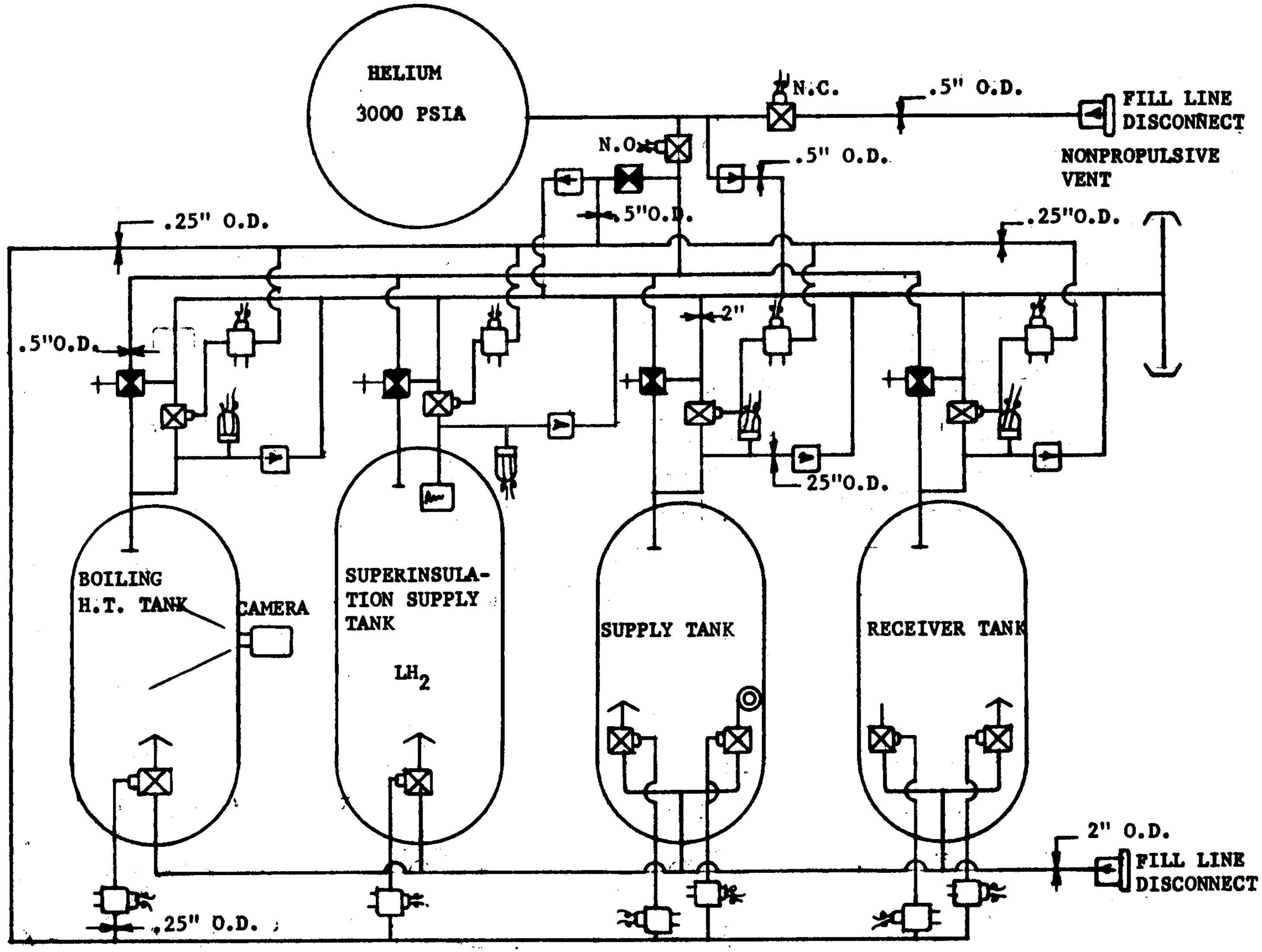

FIG 4 SCHEMATIC OF EXPERIMENTAL SYSTEMS

TABLE II

LIST OF COMPONENTS FOR THE RESEARCH MODULE

COMPONENT	Q	LINE SIZE (O.D.)	TOTAL WEIGHT	N.P.	COST	VENDOR	VENDOR NUMBER	REMARKS
SOLENOID VALVE, Two-Way (-65 to -165°F)	2	1/2"	6.00	N.C. & N.O.		Lanagan	90142	Boeing Spec # 60B52106
REGULATOR (750 psig)	1	1/2"	2.50			Rocketdyne	550278	MSFC Spec # 10M01151 & Drawing # 20M30134
REGULATOR	4	1/2"	20.00			Grove		Hand Operated -- Dome Loaded
SHUTOFF VALVE (LH_2 Submerged)	10	2"	60.00	N.C.		Parker	2630140	MSFC Spec # 20M32014
SOLENOID CONTROL VALVE (-65 to -165°F)	10	1/4"	10.00	N.C.		Marotta	218263	MSFC Spec # 10M01374 & Drawing # 20M30128
RELIEF VALVE (-423°F)	4	1/4"	4.00					This valve will have to be developed.
RELIEF VALVE (-65 to -165°F)	1	1/2"	.75			Fairchild	63-034	Douglas Module Spec # 1A49398
RELIEF VALVE (-65 to -165°F)	1	1/4"	.75			Randall	1107	Boeing Spec # 60B52104
PRESSURE SWITCH (-423°F)	4	1/4"	2.60			Frebank	8008-1	Douglas Spec # 1A18676-1
LIQUID-VAPOR SEPARATOR			/15					
PUMP, SUBMERGED	1	2"	13.00			Pesco	144668-121	

LEGEND: Q - Quantity
N. P.- Normal Position

TABLE III

LOW GRAVITY HEAT TRANSFER AND FLUID MECHANICS EXPERIMENT DESIGN DATA

PARAMETERS	BOILING HEAT TRANSFER	PROPELLANT TRANSFER	CRYOGENIC PROPELLANT STORAGE	PRESSURIZATION
Tankage (Ft.)	1.5 x 4	3' x 6'	3.8 x 7.6	4-4.5 Ft^3 Spheres
Press. (Psia)	25	50	50	3000/200
Temp. (°R)	35 to 530	35 to 530	35 to 530	300 to 530
Flowrate Vent	0.1	.2/1	.2 to 1	
(lb/sec) Fill	0.5	1 to 6	1 to 6	
	±.5			
ΔP Vent Gr.				
(Psid) Flt.	1	1	1	
Fill Gr.				
Flt.	3	3	3	
Models (Ft.)				
Plate	.5 x .5			
Disk	2" Dia.			
Power				
Peak kw	2.9	1		
Total kw hrs	.308	5		
Nozzle ΔP (Psid)		5		
Propellant	LH_2/GH_e	LH_2/GH_e	LH_2/GH_e	GH_e
Camera				
Speed fps	30 to 300	30		
Total footage	5000			
Valves Vent/Relief	1 (15 ± 1/2)	2 (50 ± 3)	1 (30 ± 1/2)	1
(psia) Fill	1	2	1	1
Reg.				1 3000/200
Control	1 (25 ± 3)	2 (47 ± 3, 20 ± 3)	1 (17 ± 1)	1

TABLE III (cont'd)

LOW GRAVITY HEAT TRANSFER AND FLUID MECHANICS EXPERIMENT DESIGN DATA

PUMP S-IVB LH_2 Recirculation

Flowrate	.8 to 1.4	lb/sec
Head	10 to 6	Psia
Power	1	H.P.

Ullaging System

Propellant	Thrust lb_f	I_{sp} $\frac{lb_f}{lbm}$ sec
GN_2	.85	73
GN_2	4	73
Storage	35	294

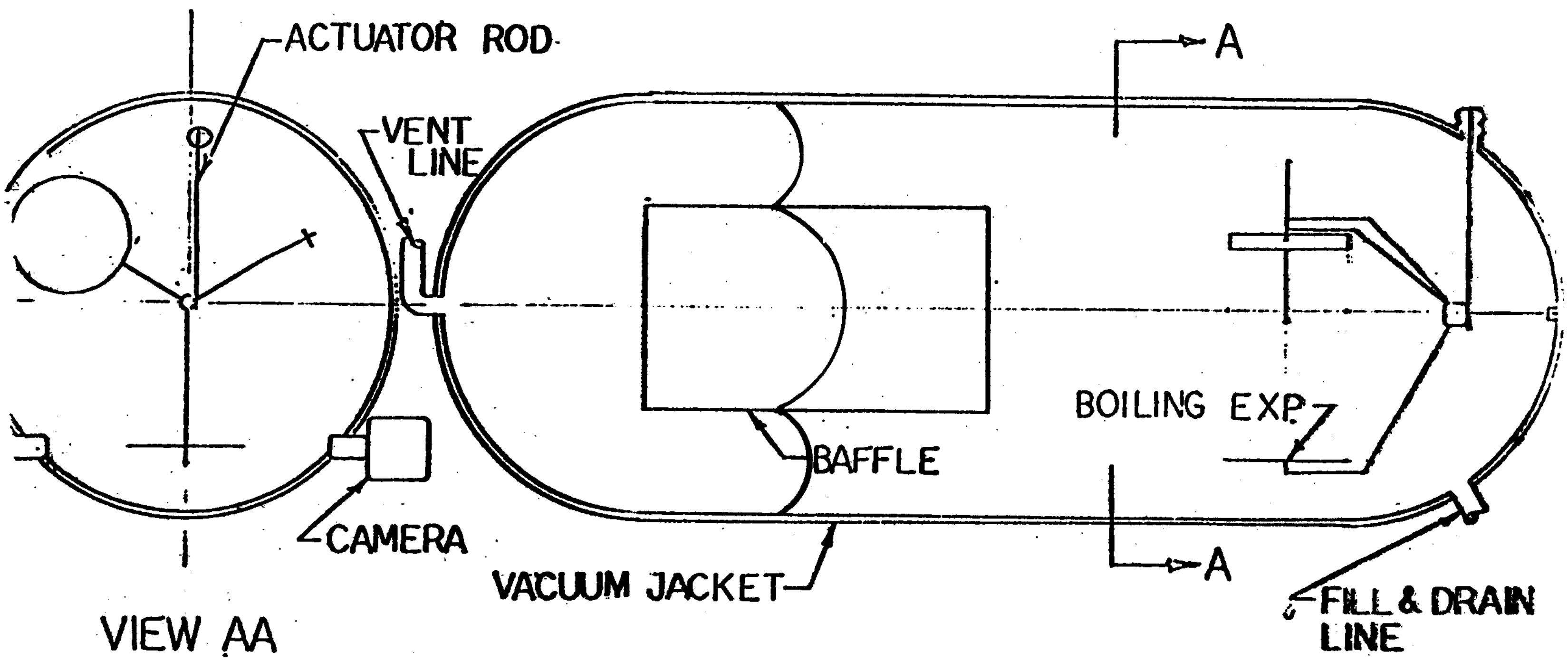

FIG 5

BOILING HEAT TRANSFER TANK

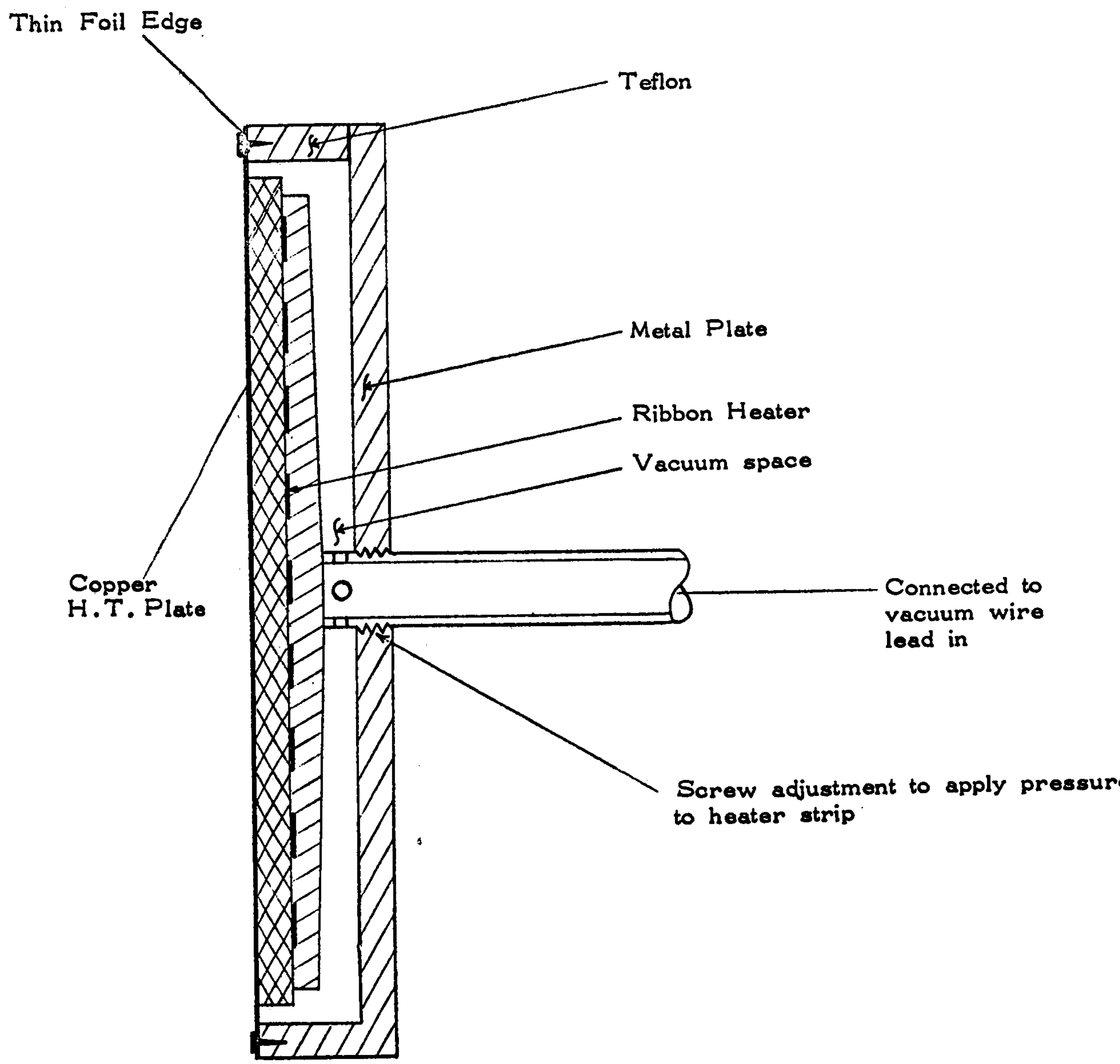

FIG 6

SCHEMATIC OF FLAT BOILING PLATE

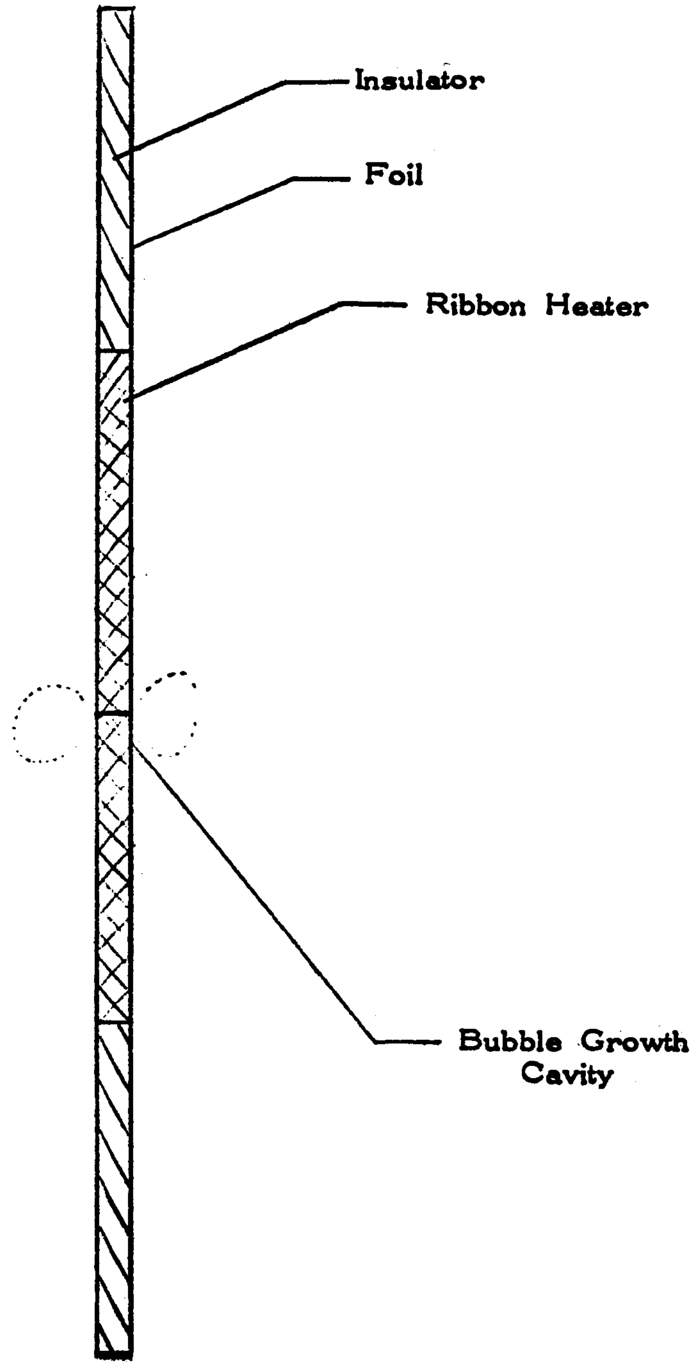

FIG 7

SCHEMATIC OF BUBBLE GROWTH RIBBON

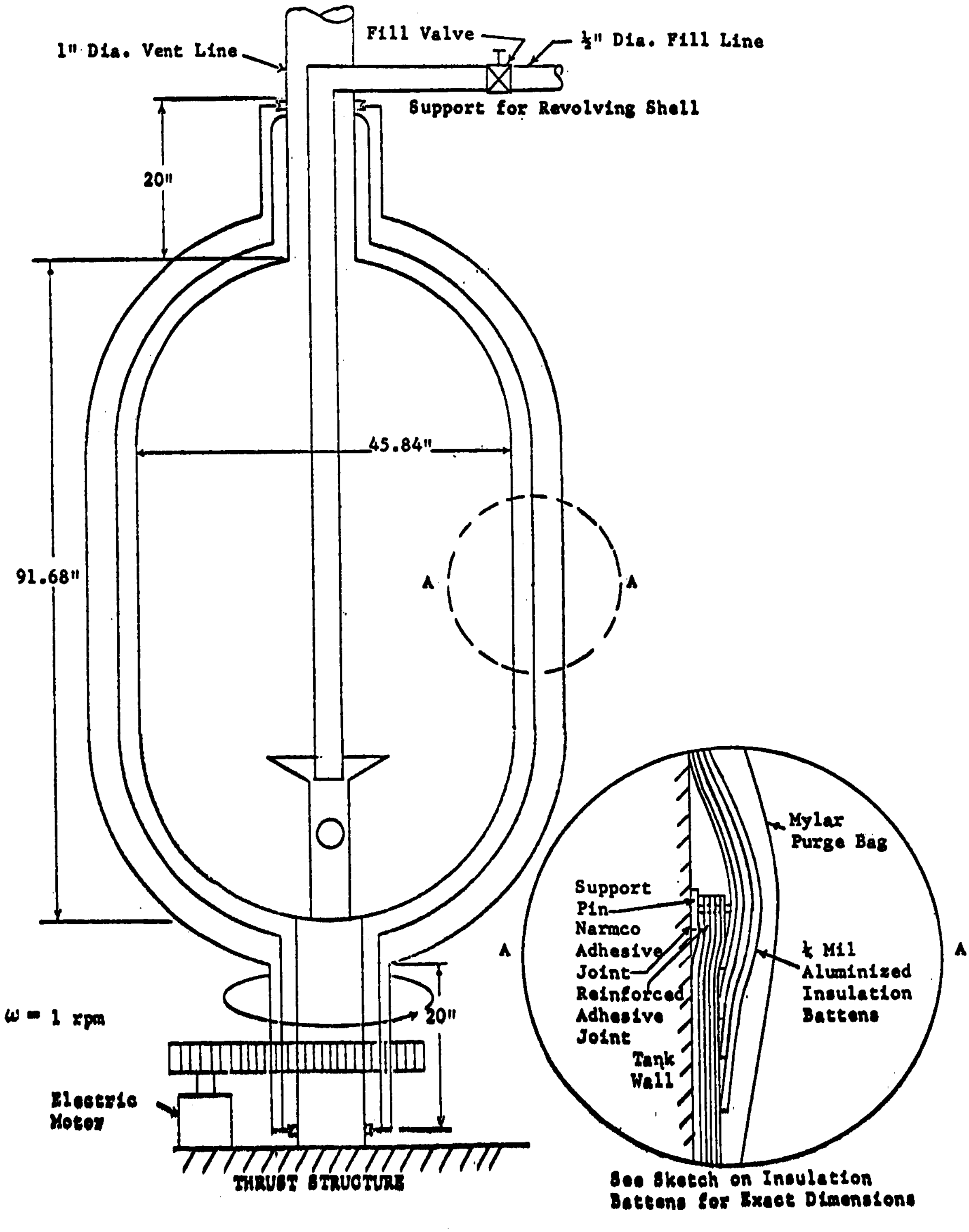

HIGH PERFORMANCE INSULATION SCHEMATIC

FIG 8

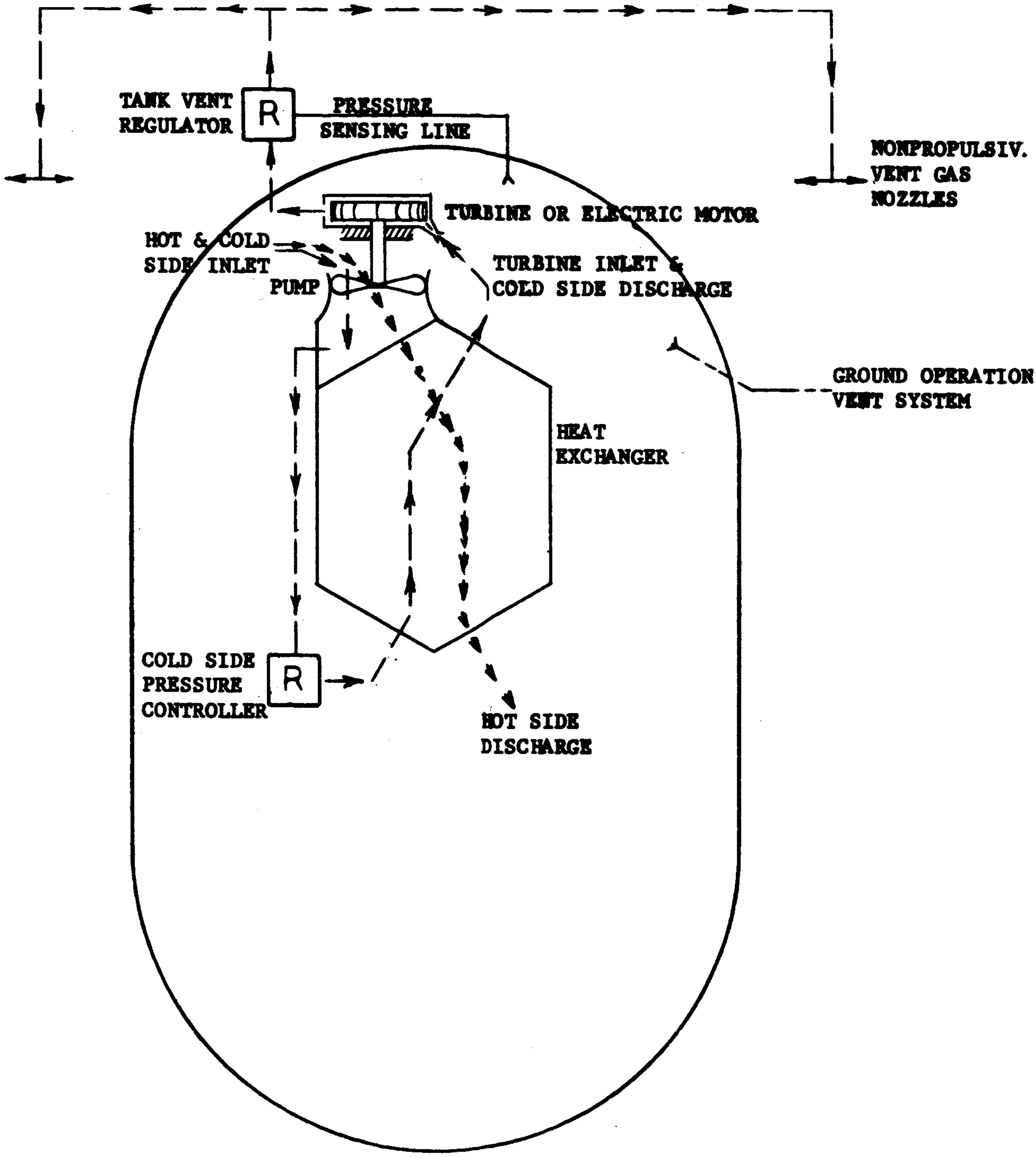

LOW G VENT SYSTEM SCHEMATIC

FIG 9

KEY LOG

EARTH ORBIT LEM

I. Environmental Measurements Sensor
2. Fuel Transfer Receiver Tank
3. Camera
4. Helium Sphere
5. Helium Sphere
6. Mech Properties-Exp Electronics
7. Mirror Housing-Boiling Tank Window
8. Boiling Tank
9.&I0. Environmental Measurements Sensor
II. Environmental Measurments- Electronics
I2. I3.&I4. Power Supply Fuel Cells
I5. I6.&I7. Helium Spheres
I8. Fuel Transfer Supply Tank
I9. Lubrication Exp.- Electronics
20. Environmental Measurements Sensor
2I. Camera- Boiling Tank
22. Super Insulation Tank

VIEW

A-A

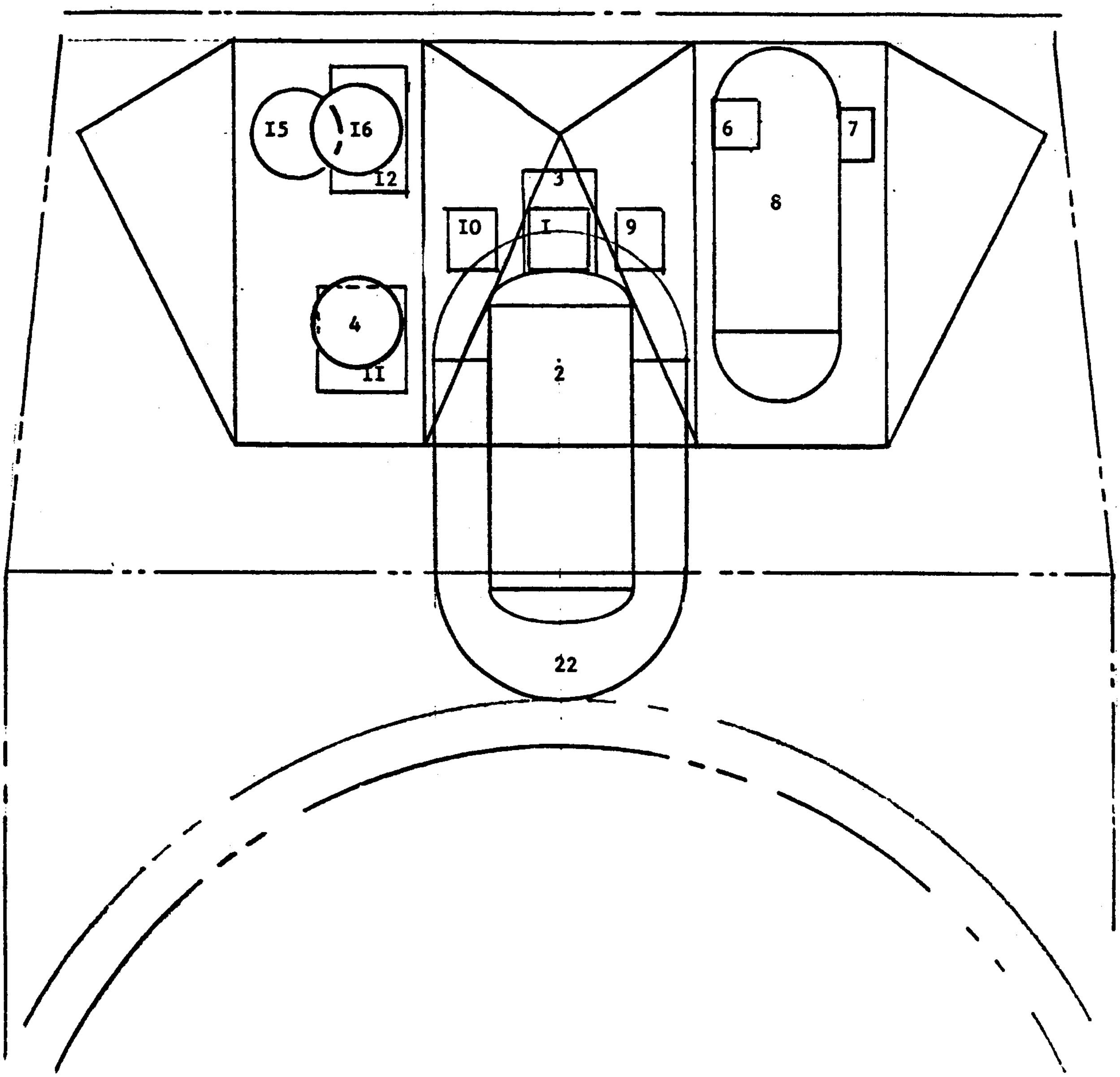

FIG 10

LEM DESCENT STAGE, SIDE VIEW

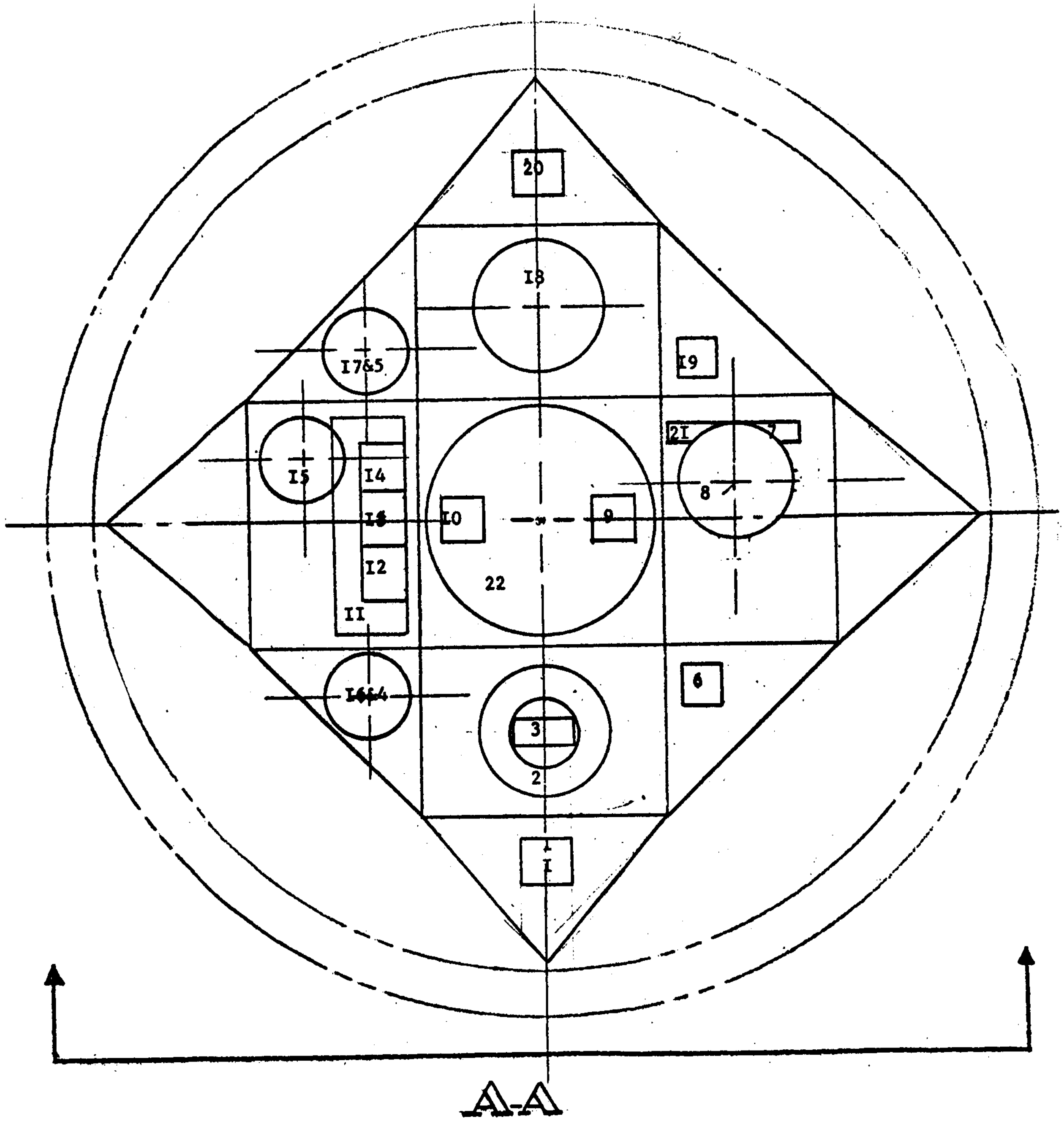

FIG. 11

LEM DESCENT STAGE, TOP VIEW

TABLE IV

Estimated System Weights

	System	Boiling Heat Transfer	Propellant Storage	Propellant Transfer	Pressuri-zation System	Attitude Control Systems
1.	Tankage	19	172	130	572	
2.	Support Structure	19	52	23		
3.	Propellant	30	\300	150	34	
4.	Transfer System	62	67	80	14	
5.	Vent System	67	67	78	4	
6.	Pressurization	20	21	21		
7.	Actuation		66			
8.	Instrumentation + Cameras	50	50	50		
9.	Power		100			
	SUBTOTAL	267	895	533	624	400

TOTAL 2719

TABLE V

INSTRUMENTATION REQUIREMENTS

MEASUREMENT	TYPE	RANGE	QUANTITY
<u>Boiling Heat Transfer Experiment</u>			
Temperature	Platinum	0-800°R ΔT	6
	"	0-1°R ΔT	1
	"	35-40°R	9
	"	35-760°R	2
	"	34-40°R	1
Pressure	-	10-30 psia	1
Voltage	-	28V	2
Amp	-	110 amps	2
TOTAL			24
<u>Propellant Transfer</u>			
Temperature	Copper Constantan	20-400°R	10
	Platinum Resistance	20-400°R	6
	Platinum Resistance	20-200°R	19
Pressure		0-60 psia	2
Flowrate	Gaseous H_2	0 - lb/sec	2
	Liquid LH_2	0 - 6 lb_m/sec	2
Liquid Level	Capacitance Continuous		2
TOTAL			43
<u>Cryogenic Propellant Storage</u>			
Quality Meter	Nucleonic		1
Liquid Level	Capacitance Continuous		1
Temperature	Platinum Resistant	36-60°R	12
	" "	36-100°R	10
	" "	36-380°R	14
	Copper Constantan	300-500°R	15
Pressure	-	0-45 psia	2
	Ion Gauge	10^{-3} 10^{-6} mmHg	3
	Alpha Tron Gauge	10^{-2} 10^{-5} mmHg	4
	Thermocouple Gauge	10^{-2} 10^{-4} mmHg	3
Flowmeters	Gaseous H_2	0-1 lb/hr	1
	Gaseous H_2	0-75 lb/hr	1
Thickness Gauge	Nucleonic	0-2.5"	6
Leak Detector Hg	Electronic	10^{-3} 10^{-10} cc/sec	1
TOTAL		0-100% concen.	74

SEQUENCE OF EVENTS

The sequence of events is shown in FIG 12 through 14. Maximum astronaut participation is required during the experiments to adjust experimental conditions and data aquisition devices since in many areas operating ranges can only be estimated in advance.

Events are scheduled so that as one experiment is being performed, another is establishing equilibrium conditions in preparation for initiation of the experiment. FIG 15 shows an estimate of the percentage of astronaut time required in support of these experiments.

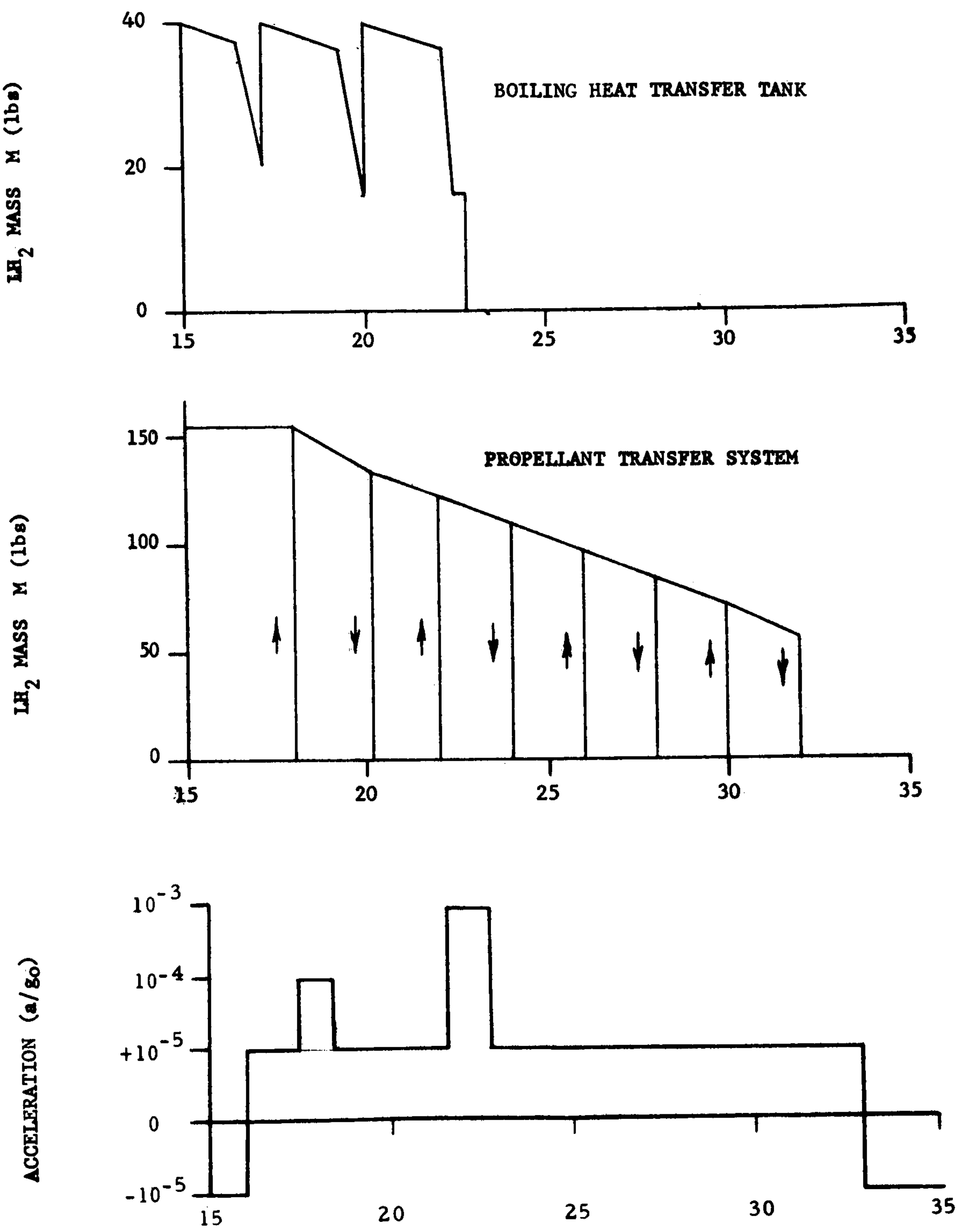

TIME t (Hrs) AFTER INSERTION INTO ORBIT

FIG 12 SEQUENCE OF EVENTS FOR BOILING HEAT TRANSFER AND PROPELLANT TRANSFER

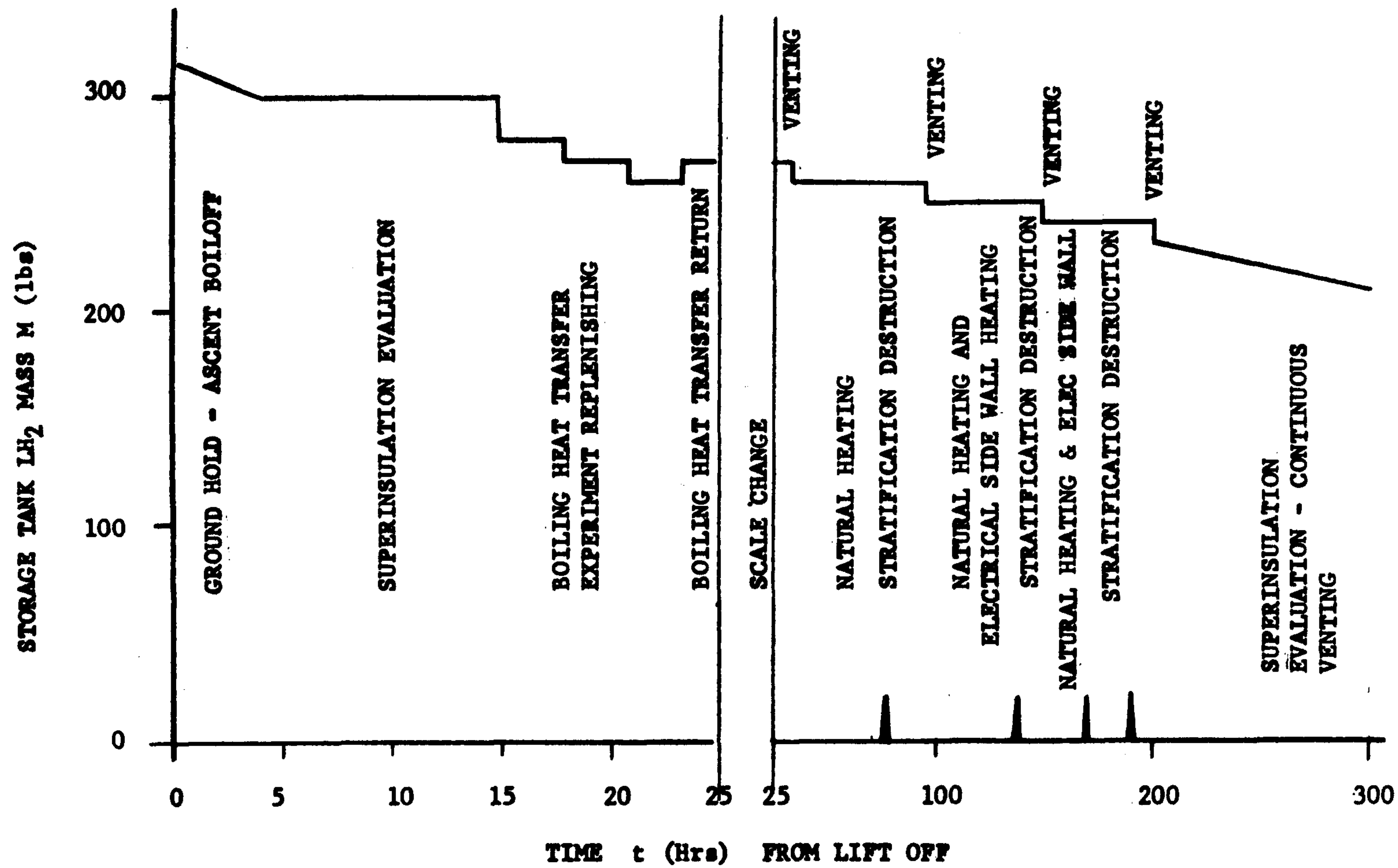

FIG 13

SEQUENCE OF EVENTS FOR SUPERINSULATION AND STRATIFICATION

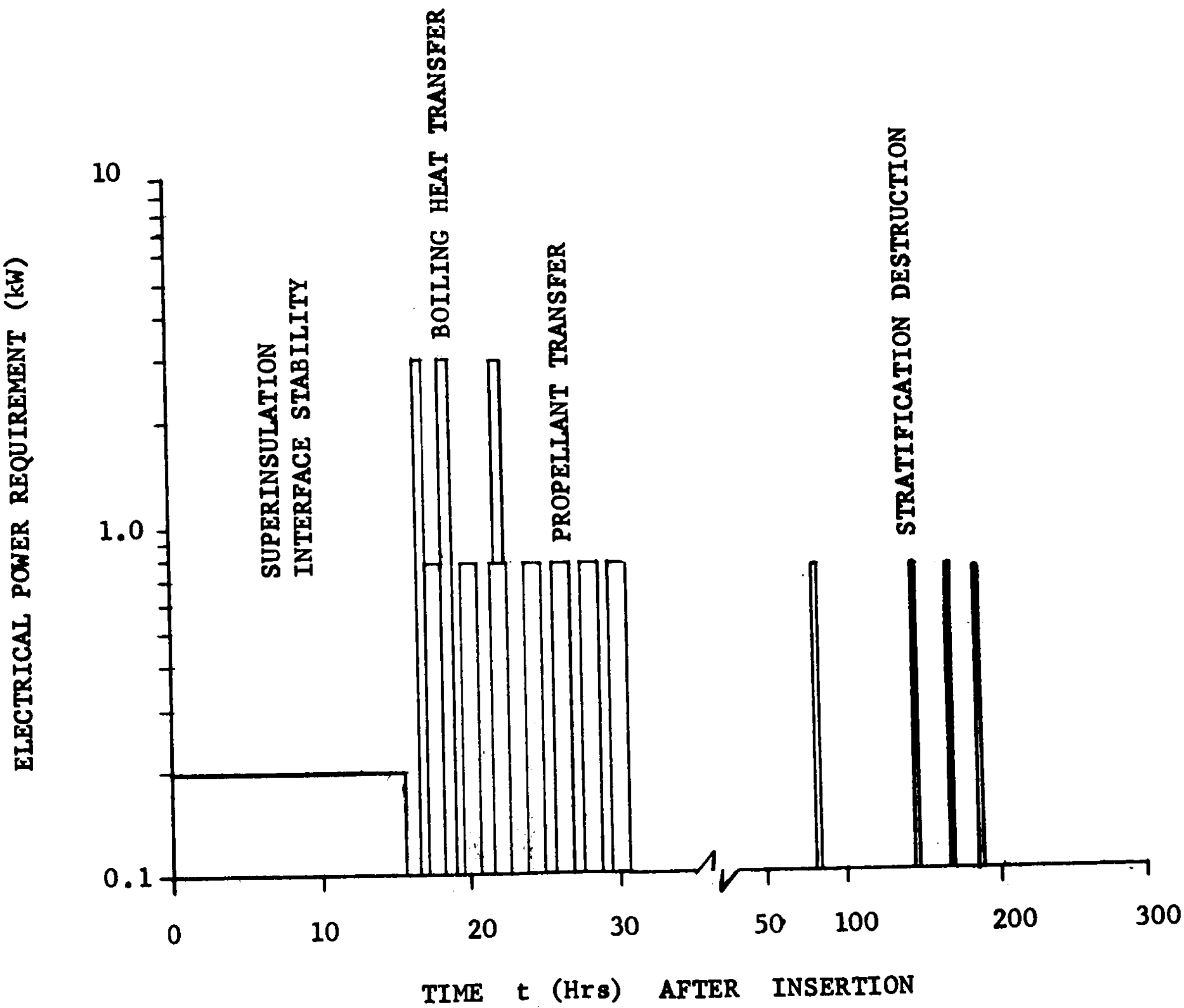

FIG 14 ELECTRICAL POWER REQUIREMENTS

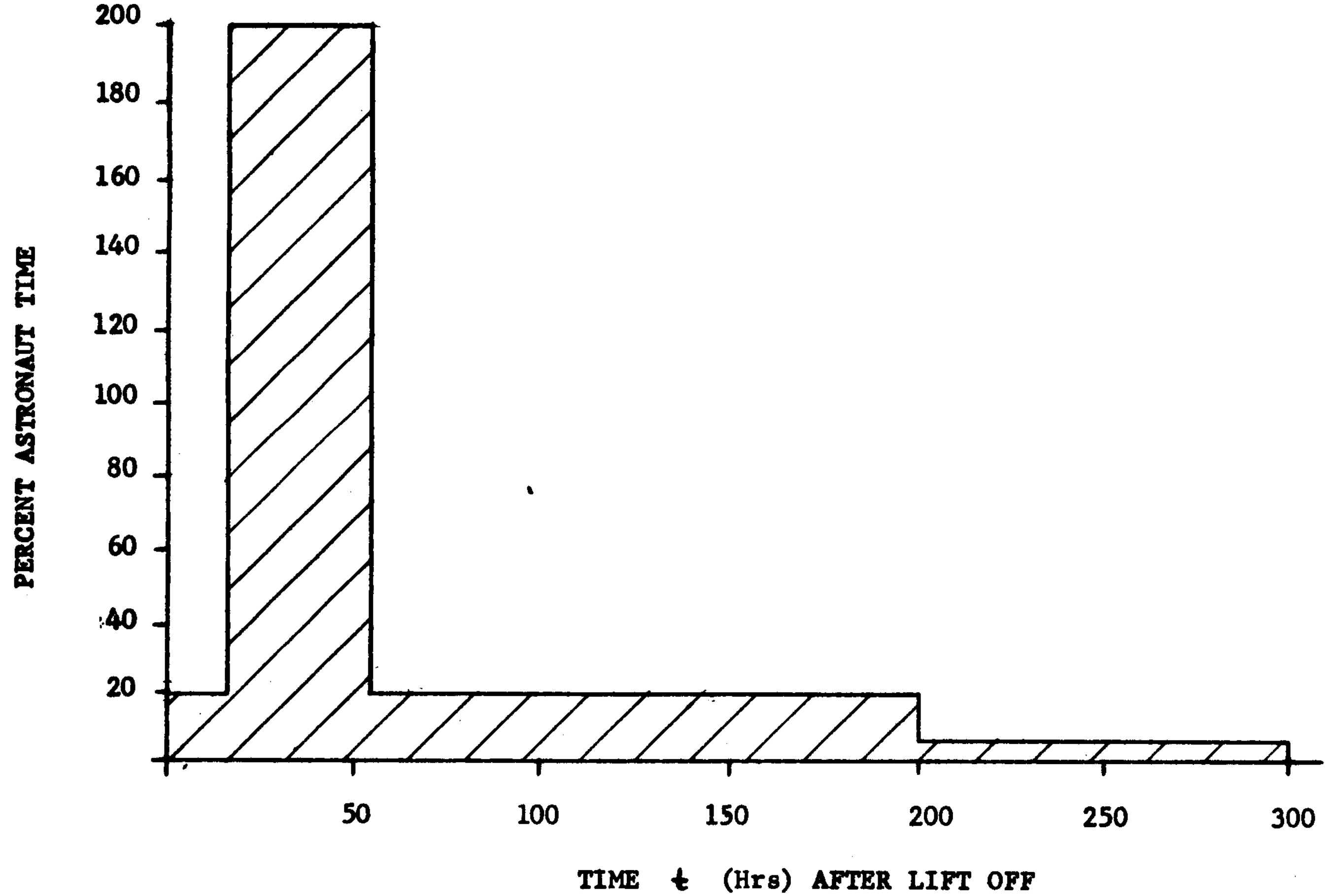

FIG 15 ASTRONAUT PARTICIPATION IN EXPERIMENT CONDUCTION

PROGRAM SCHEDULES

The program scheduling presented in Table VI is based upon the phase philosophy as defined below:

Phase A. Feasibility Study
B. Preliminary Design
C. Release Documentation and Prototype Development
D. Manufacturing, Test, Flight

Out-of-house contract support may be used in phases B, C, or D. Coordination with other NASA centers, universities, and industry on experiment definition and design will be performed under phases A and B. Table VII is the proposed phase B task assignment schedule.

TABLE VI

Low-G Heat Transfer and Fluid Mechanics Experiment

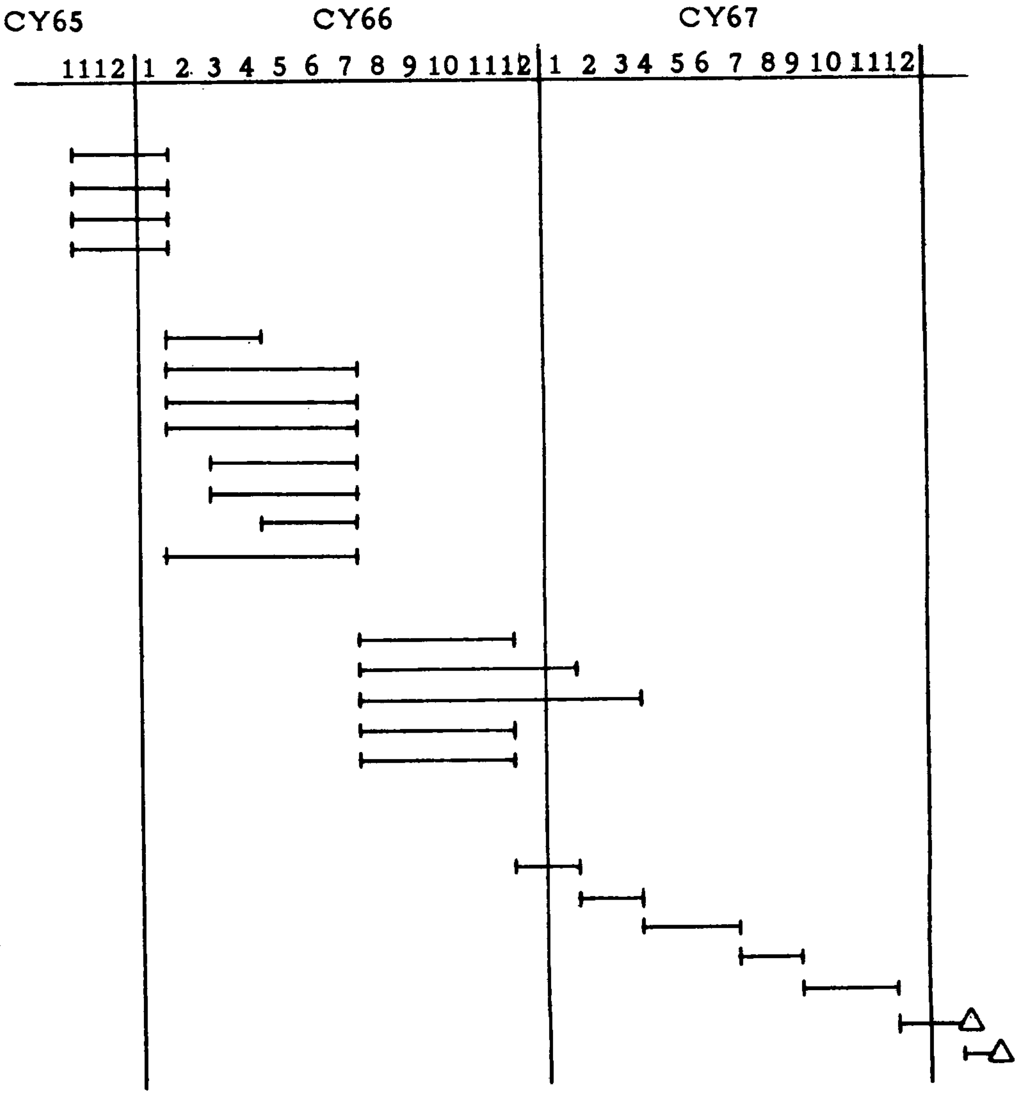

PHASE A

1. Exp. Definition
2. System Definition
3. Tankage & Structure Definition
4. Phase B Scope

PHASE B

1. Finalize Exp. Definition
2. Preliminary Tankage Design
3. Preliminary System Design
4. Preliminary Carrier Integration
5. Soft Mockup
6. Define Support Equipment
7. Long Lead Time Item Define
8. Phase C. Scope

PHASE C

1. Finalize Drawings & Spec's
2. Finalize Carrier Integration
3. Hard Mockup (Shop Queen)
4. Long Lead Time Items
5. Phase D Scope

PHASE D

1. Manufacture: Tankage
   Insulation
   Carrier Integration
   Checkout
   Qual Test
2. Flight
3. Data Evaluation

TABLE VII

PHASE B TASK ASSIGNMENTS

	Agent Responsible	Manpower	Start Date	Due Date
1. Experiments				
a. Definition	PT	2	Feb 1	May 1
b. Procedures	PT	1	Feb 1	May 1
c. Supporting technology contracts	PT	.2	Mar 1	Aug 1
d. Orbit determinations	Aero	.5	Feb 1	May 1
2. Tankage and Structural Design				
Preliminary Tank and Support Designs	SS	3	Feb 1	Aug 1
3. Systems				
Preliminary Specifications and drawings				
a. Pressurization	PM/PT	2	Feb 1	Aug 1
b. Transfer	PM/PT	2	Feb 1	Aug 1
c. Insulation	PTD	1	Feb 1	Aug 1
d. Instrumentation	PT/ASTR	.5	Feb 1	Aug 1
e. Power	PT/ASTR	.2	Feb 1	Aug 1
f. Attitude Control	PT/ASTR	.5	Feb 1	Aug 1

TABLE VII (cont'd)

	Agent Responsible	Manpower	Start Date	Due Date
4. Carrier definition	SS	3	Feb 1	Aug 1
a. Hard points				
b. Environments				
c. Modifications				
5. Mock up	SS		Mar 1	Aug 1
6. Support Equipment	V	1	Mar 15	Aug 1
7. Long Lead Time Items			May 1	Aug 1
8. Phase C Scope		1	May 1	Aug 1

APPENDIX A

BOILING HEAT TRANSFER EXPERIMENT

Appendix A states the assumptions made for the experimental conditions and develops the requirements for test duration, photographic coverage, artificial gravity level, and instrumentation.

For the design of the orbital experiment on pool boiling of a cryogenic fluid the following assumptions are made:

1. Surface configuration of interest:

   Flat plate vertical with respect to the acceleration vector.
   Flat plate horizontal with respect to the acceleration vector.
   Ribbon heater for bubble growth studies.

2. Fluid conditions:

   Saturated fluid
   Subcooled fluid

3. Gravity levels for test:

   $a/g = 10^{-5}$
   $a/g = 10^{-4}$
   $a/g = 10^{-3}$

4. Test points boiling experiment - saturated fluid

   Flat plate vertical at $a = 10^{-5}$ g :

   Natural convection regime: 2
   Close to incipient boiling: 1
   Nucleate boiling regime: 3 (point close to peak)
   Film boiling regime: 2

   Flate plate vertical at $a = 10^{-4}$ g :

   Same-

Flat plate vertical at $a = 10^{-3}$ g :

Nucleate boiling regime: 3
Film boiling regime: 2

Flat plate horizontal up at $a = 10^{-5}$ g :

Nucleate boiling regime: 3

Flat plate horizontal up at $a = 10^{-4}$ g :

Nucleate boiling regime: 3

Flat plate horizontal up at $a = 10^{-3}$ g :

Nucleate boiling regime: 3
Film boiling regime: 2

5. Test points boiling experiment - subcooled fluid

One point for each gravity level in the nucleate regime, three points.

6. Test specimen configuration:

The boiling tests should be conducted with a circular copper disk. A disk size of 6 inches is chosen to avoid edge effects. The disk thickness should be about 0.25 inches to assure a uniform surface temperature from the heater ribbon in back of the plate. A 6-inch plate will also assure that bubble growth under reduced g will accommodate maximum bubble size at departure, assuming hemispherical shape for a single bubble.

Bubble diameter: $D = D_{@\ 1g} (a/g)^{-1/2} \cong 5$ in.

Experiment Sizing

1. **Heat flux and power requirements:**

   a. Boiling:

From theory $(Q/A)\ max = f\ (a/g)^{+0.25}$

$$(Q/A)\ min\ film = f\ (a/g)^{+0.25}$$

For hydrogen vertical flat plate under one g

$$(Q/A)\ max = 50{,}000\ Btu/Hr\ Ft^2$$

Then:

(a/g)	(Q/A)	P (kW)	(Q/A)min Film	P (kW)
1	50,000	2.89	6,000	0.359
10^{-3}	8,900	0.514	1070	0.062
10^{-4}	5,000	0.289	600	0.0359
10^{-5}	2,830	0.163	335	0.0194

   b. Natural Covection: Hydrogen Vertical 6-inch plate

$$(Q/A) = 32.8\ \Delta T^{1.25}\ (a/g)^{+0.25}$$

Assuming $\Delta T = 0.1\ (^{\circ}R)$

(a/g)	Q/A	P (kW)
1	1.84	10^{-4}
10^{-3}	0.321	1.8×10^{-5}
10^{-4}	0.184	1.07×10^{-5}
10^{-5}	0.104	0.6×10^{-5}

2. **Test duration:**

After fluid residual motions have damped out, the test will be conducted in the following manner:

   a. Supply electrical power to heater
   b. Record surface temperature rise, fluid temperature in vicinity of surface, and $(T_w - T_{fluid})$ temperature difference.
   c. When wall temperature approaches constant value, adjust power to new heat flux setting.

The time requirements are:

a. Natural convection laminar boundary layer development. FIG 16 shows the time requirements for laminar boundary layers development on a heated vertical plate in LH_2.

a/g	t (Hrs) $\Delta T = 0.1\ ^oR$, L = 1/2 (ft)
1	0.0085
10^{-3}	0.27
10^{-4}	0.85
10^{-5}	2.7

b. Nucleate boiling:

$$t = -\left(\frac{M\,C_p}{hA}\right) \ln \frac{(T - T_{sat}) - P_{in}/hA}{T_o - P_{in}/hA}$$

$M_{plate} = 2.3$ lbs

$Cp_{cu} = 0.05$ Btu/lb ^oR

$A = 28.4$ in.^{2}

h_{max} @ $(a/g) = 10^{-5}$ 570 Btu/Hr Ft^2 ^oR

$t = 1.9$ sec for Q/A 2830 $\left(\frac{Btu}{Hr\ Ft^2}\right)$

Time constant = 3.7 sec for 63% of max rise, thus time for heating is of no consequence.

c. Film boiling:

Adding sufficient material for plate backing

assume $M_p = 4.6$ lbm

$$t = \frac{4100}{h} \ln \frac{\hat{\Delta T}_{1/2} - P_{in}/hA}{T_o - P_{in}/hA}$$

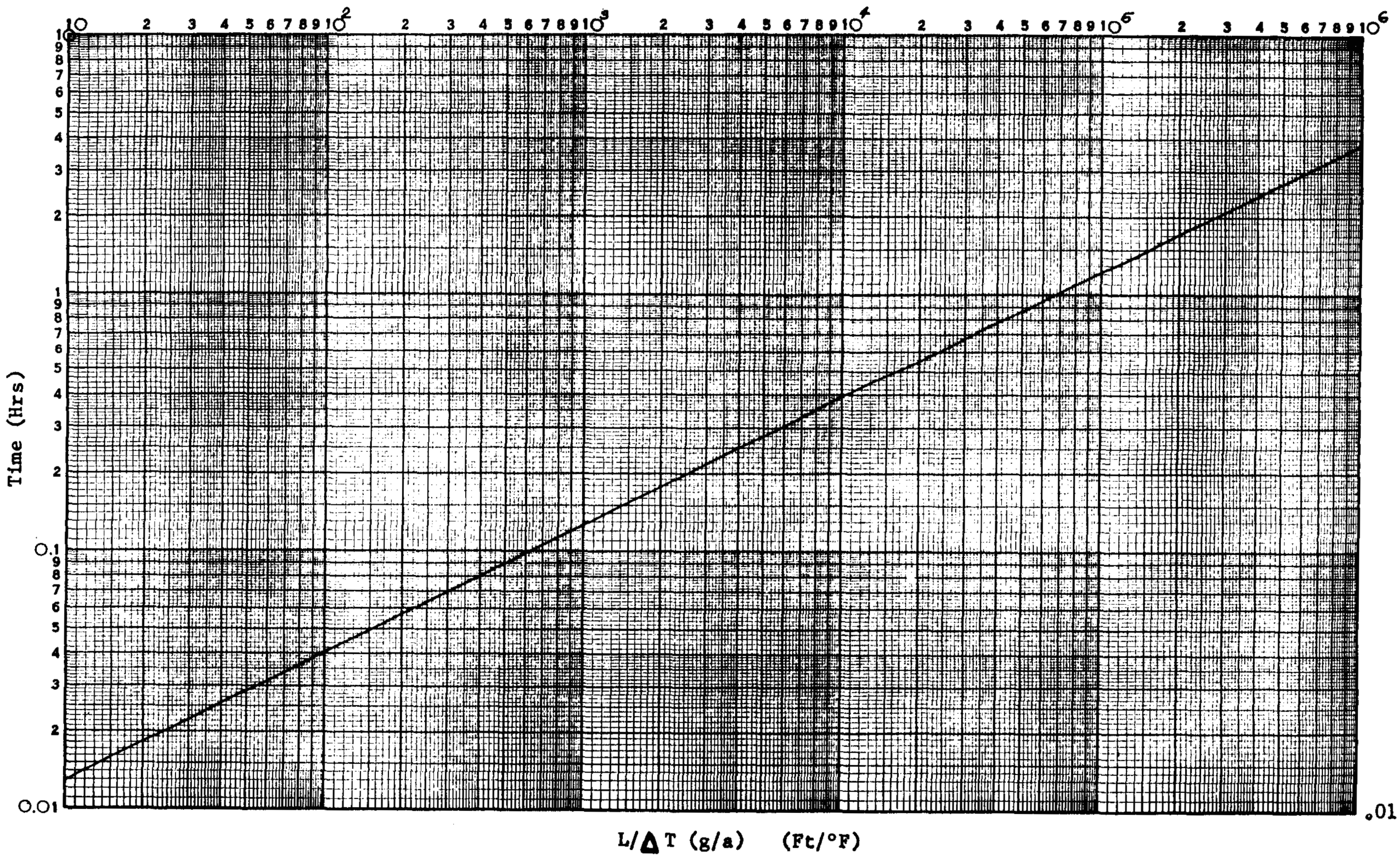

FIG 16 Time To Establish Steady State Laminar Boundary Layer For LH_2

(a/g)	h	P_{in}/hA Assuming $P = P_{max}$	T_1/ T_2	t (sec)
1	50/50	1,000	400/800	40/132
10^{-3}	8.9/8.9	5,600	400/800	34/72
10^{-4}	5/5	10,000	400/800	33/68
10^{-5}	2.82/2.82	17,700	400/800	33/67

d. <u>Bubble growth rate:</u>

Movies by Martin Company show growth of bubble in one g:

frequency $f = 1/3.5 \times 10^{-3} \left(\frac{\text{Bubbles}}{\text{sec}}\right)$

Assuming that $f\,D = \text{const}$

$D = 0.03$ in. (observed bubble diameter)

then $fD = \frac{1}{3.5} \times 3 \times 10 \approx 10$

if D under low $g = D_1 (a/g)^{-1/2}$

then $(fD)_1 = (fD)_2 = f_2 D_1 (a/g)^{-1/2}$

(a/g)	f (ft/sec)	t (sec)
1	285	3.5×10^{-3}
10^{-3}	9	0.11
10^{-4}	2.8	0.36
10^{-5}	0.9	1.1

Thus, allowance of 60 sec for bubble study at each g level appears sufficient.

3. Boiling Experiment Tank Size

During the boiling process it is intended to observe the travel of the bubbles away from the plate. Container walls should be sufficiently distant from the boiling plate to allow bubble travel normal to the gravity vector until buoyancy forces are dominant and cause the bubbles to move parallel to the wall. It is assumed that the center of gravity of a bubble moves at the liquid-vapor interface velocity and that a bubble maintains spherical shape.

Bubble velocity due to buoyancy

$$u = u_m \operatorname{Tan h} \left[\frac{\rho_L - \rho_V}{\rho_V} \left(\frac{a}{g}\right) (g_o) \frac{t}{u_m} \right]$$

$$u_m = \left[\frac{4}{3} \frac{d}{C_D} \left(\frac{a}{g}\right) (g_o) \right]^{1/2}$$

Bubble velocity due to inertial force

$$u = u_i \Big/ \left(\frac{3}{4} u_i \frac{\rho_L}{\rho_V} \frac{C_D}{D} t + 1 \right)$$

For hydrogen bubble @ $a/g = 1$ $\quad$ $D = 0.015$ in.

$u_{terminal} = 1.4$ Ft/Sec

$$u_i = df = \frac{0.03 \times 285}{12} = 0.716 \text{ Ft/Sec}$$

Tank Diameter:

$d \geq 1.5$ Ft

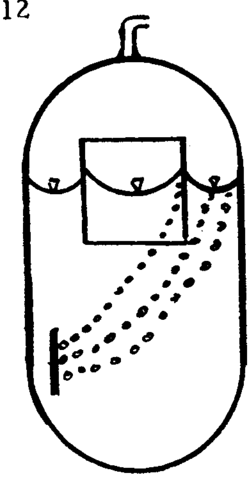

Bubble path intercepts surface prior to intercepting wall

Tank Height:

1.5 ft + height required to contain boiloff mass for one test without clearing ullage control device. See figure on next page.

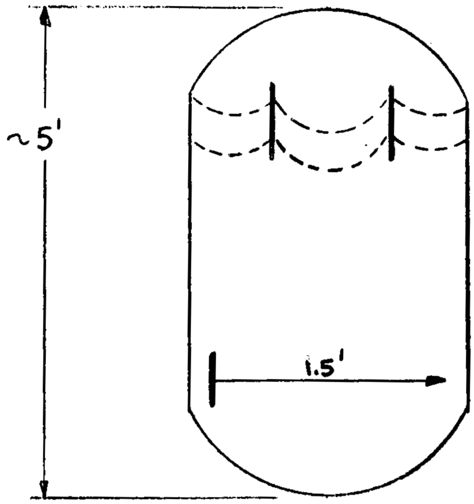

4. Instrumentation:

Temperature Difference

Horizontal Flat Plate:	3 (0 - 800°R)
Vertical Flat Plate :	3 (0 - 800°R)
Ribbon :	1 (or built as platinum resistance thermometer (0 - 1°R)

Absolute Fluid Temperature

In vicinity V. F. plate:	3 (35-40°R)
H. F. plate:	3 "
Ribbon :	3 "

Absolute Plate and Ribbon Temperature

V. F. plate:	1 (35-760°R)
H. F. plate:	1 "
Ribbon :	1 (34-40°R)

Tank Pressure: 1 (10-20 psia)

Voltage and Amperage:

Voltage :	2 (28 V)
Amperage :	2 (0-110 Amp)

Temperature feed back power control - Common to all Configurations

Total Measurements 24

TABLE VIII

TEST SCHEDULE

TEST	(a/g)	TEST POINT	POINT TIME (sec)	POWER (kW)/ POINT	TOTAL TIME	CAMERA-ftp frames/sec x time x point
Vertical Flat Plate Saturated Fluid	10^{-5}	N. C. 2 I. B. 1 N. B. 3 F. B. 2	10,000 640 30 63/63	$0.6x10^{-5}$ $0.6x10^{-5}$ 0.163 (max) 2.9 (33 sec) 0.065 (30 sec) 2.9 (33 sec) 0.135 (30 sec)	10,000* 640 90 63 63	 24x640 24x90 + 400x5x3 24x30 400x5
H. F. P. (sat.)	10^{-5}	N. B. 3	30	0.163 (max)	90	24x90 + 400x5x3
V. F. P. subcooled	10^{-5}	N. B. 1	30	0.163 (max)	30	24x30 400x5
H. F. P. subcooled	10^{-5}	N. B. 1	30	0.163 (max)	30	24x30 400x5
Bubble growth	10^{-5}	—	1	$0.6x10^{-5}$	60	400x60
Subtotal		13		154.9 kW sec	2346	62480
V. F. P. saturated fluid	10^{-4}	N. C. 2 I. B. 1 N. B. 3 F. B. 2	3600 200 30 63/68	$1.07x10^{-5}$ $1.07x10^{-5}$ 0.289 (max) 2.9 (33 sec) 0.115 (30 sec) 2.9 (38 sec) 0.23 (30 sec)	3600* 200 90 63 68	 24x200 24x90 + 400x5x3 24x30 400x5
H. F. P. sat. fluid	10^{-4}	N. B. 3	30	0.289 (max)	90	24x90 400x5x3
V. F. P. (subcool)	10^{-4}	N. B. 1	30	0.289 (max)	30	24x30 + 400x5
Bubble Growth	10^{-4}	—	0.36	$1.07x10^{-5}$	60	400x60
				195.8 kW sec	1001	30,560

TABLE VIII (Cont'd)

TEST	(a/g)	TEST POINT	POINT TIME (sec)	POWER (kW) / POINT	TOTAL TIME	CAMERA-ftp $\frac{\text{frames}}{\text{sec}}$ x time x point
V. F. P. sat. fluid	10^{-3}	N. B. 3	30	0.514 (max)	90	24x90 400x5x3 400x5
		F. B. 2	64/102	2.9 (34 sec) 0.208 (30 sec) 2.9 (72 sec) 0.41 (30 sec)	64 102	
H. F. P. sat. fluid	10^{-3}	N. B. 3	30	0.514 (max)	90	24x90 400x5x3 400x5
		F. B. 2	64/102	2.9 (34 sec) 0.208 (30 sec) 2.9 (72 sec) 0.41 (30 sec)	64 102	
V. F. P. subcooled fluid	10^{-3}	N. B. 1	30	0.514 (max)	30	
Bubble growth	10^{-3}	—	.11	1.8×10^{-5}	60	400x60
				757.6 kW sec	602	34160

Total Film Requirements	127200 Frames ≈ 5000 Ft.
Power Requirement	0 - 2.9 kW
Total Energy	0.308 kW Hrs
Total Test Time	3949 sec + time for adjustment of exp. + time for fluid settling

* These values are too high for auxiliary propulsion system.
Rate observation may be required in lieu of steady state measurements

DEFINITION OF SYMBOLS

Symbol	Definition	Units
A	Surface Area	ft^2
C_P	Specific Heat at Constant Pressure	$\frac{Btu}{lb\ ^oR}$
C_D	Drag Coefficient	—
D	Bubble Diameter	in.
f	Frequency	$\frac{1}{sec}$
g_o	Conversion Constant	$\frac{ft\ lbm}{sec^2\ lbf}$
a/g	Acceleration	—
h	Heat Transfer Coefficient	$\frac{Btu}{Hr\ ft^2\ ^oR}$
L	Heated Length	ft
M	Mass	lb
P	Electrical Power	kW
Q/A	Heat Flux	$\frac{Btu}{Hr\ ft^2\ ^oR}$
ρ	Density	$\frac{lbm}{ft^3}$
t	Time	sec
T	Temperature	^oR
ΔT	Temperature Difference	^oR
u	Velocity	$\frac{ft}{sec}$
N. C.	Nucleate Boiling	
I. B.	Incipient Boiling	
F. B.	Film Boiling	

BIBLIOGRAPHY

Boiling Heat Transfer Experiment

Clark, J. A.; and Merte, H., Jr.: Investigation and Study of Transient Heat Transfer. University of Michigan Progress Reports to NAS8-20228

Merte, H., Jr.; and Clark, J. A.: Boiling Heat Transfer with Cryogenic Fluids at Standard, Fractional and Near Zero Gravity. Transactions of the ASME Journal of Heat Transfer-Paper # 63-HT-28

Tuck, G.: LH Boiling Threshold. GD/Astronautics - Report # 55 D 859-3, General Dynamics, Convair Division

McCrary, Leon: Bubble Accumulation in Simulated Boiling. GD/Astronautics - Report # 55 D 859-6, General Dynamics, Convair Division

O'Hanlon, T. W.: LH_2 Film Boiling. GD/Astronautics - Report # 55 D 859-2, General Dynamics, Convair Division

Lewis, Eugene W.; Merte, Herman, Jr.; and Clark, John A.: Effects of Zero Gravity on Fluid Dynamics and Heat Transfer. The 55th National Meeting - American Institute of Chemical Engineers, Hustion, Texas, February 7 - 11, 1965. A publication of the Heat Transfer Laboratory, Department of Mechanical Engineering, The University of Michigan, Ann Arbor, Michigan.

Zuber, Novak: Recent Trends in Boiling Heat Transfer Research, Part I: Nucleate Pool Boiling. Advanced Technology Laboratories, General Electric Company, Schenectady, New York

Yang, Wen-Jei; and Clark, J. A.: Part I: Growth and Collapse of Bubbles. Heat Transfer and Thermodynamics Laboratory, University of Michigan.

Graham, Robert W.; Hendricks, Robert C.; and Ehlers, Robert C.: Analytical and Experimental Study of Pool Heating of Liquid Hydrogen over a Range of Accelerations. Technical Note D-1883, Lewis Research Center, Cleveland, Ohio von Glahn, Uwe H.: A Correlation of Film-Boiling Heat-Transfer Coefficients Obtained with Hydrogen, Nitrogen, and Freon 113 In Forced Flow. Technical Note E-1841, Lewis Research Center, Cleveland, Ohio

Lewis, James P.; Goodykoontz, Jack H.; and Kline, John F.: Boiling Heat Transfer to Liquid Hydrogen and Nitrogen in Forced Flow. Technical Note D-1314, Lewis Research Center, Cleveland, Ohio

Bergles, A. E.; and Rohsenow, W. M.: The Determination of Forced-Convection Surface-Boiling Heat Transfer. Massachusetts Institute of Technology, Cambridge, Mass. Paper No. 63-HT-22

Pomerantz, M. L.: Film Boiling on a Horizontal Tube in Increased Gravity Fields. Bettis Atomic Power Laboratory, Pittsburg, Pa.

Schwartz, B. S.; and Adelberg, M.: Some Thermal Aspects of a Contained Fluid in a Reduced Gravity Environment. Douglas Aircraft Company, Symposium on Fluid Mechanics and Heat Transfer Under Low Gravitational Conditions, June 24-25, 1965, Palo Alto, California

APPENDIX B

SPACEBORNE CRYOGENIC PROPELLANT STORAGE

I. Insulation

Concepts

Ground hold boiloff should be obtained in the installed condition to account for the various conditions and extraneous heat leaks. Using this value, a base line heat leak can be established for normalizing heat input during ascent and orbital environments.

Ratio of total boiloff to vacuum boiloff is a very important analytical and design tool, enabling, for a given ratio of penetration to side wall heat flux, insulation system performance prediction with confidence for different size systems. If pumping paths, batten lengths, and overlap areas are designed on a large tank similar to those of the experimental tank, similar insulation performance could be expected for any given size tank. In all cases, and particularly for small size tanks, heat leaks through piping and supports must be carefully calculated or measured to determine final system thermal performance. Heat leaks due to penetrations can be determined from FIG 17. Note that pipe wall thickness, coefficient of thermal conductivity of the pipe material, and length of insulation material have a significant effect on heat input to the liquid hydrogen.

Insulation pressure decay during vehicle ascent is extremely important. Purge bag rupture is desirable after about 85 seconds of flight to provide as much pumping area as possible. A Dacron material purge jacket with a pre-set rupturing zipper will be used. Rupture will occur at a given ΔP across the purge jacket. This system has been tested and proven to be workable.

The required time for the insulation pressure to decay to less than 10^{-5} mmHg determines the transient boiloff loss from ground hold to final orbital conditions. Apparent thermal conductivity of the insulation is proportional to the interstitial gas pressure within the insulation as illustrated by FIG 18 which indicates the need for rapid evacuation and obtaining an ultimate pressure of less than 10^{-5} mmHg in orbit. If the ultimate pressure level of 10^{-5} mmHg is not achieved, a steady-state boiloff penalty will result. The proposed

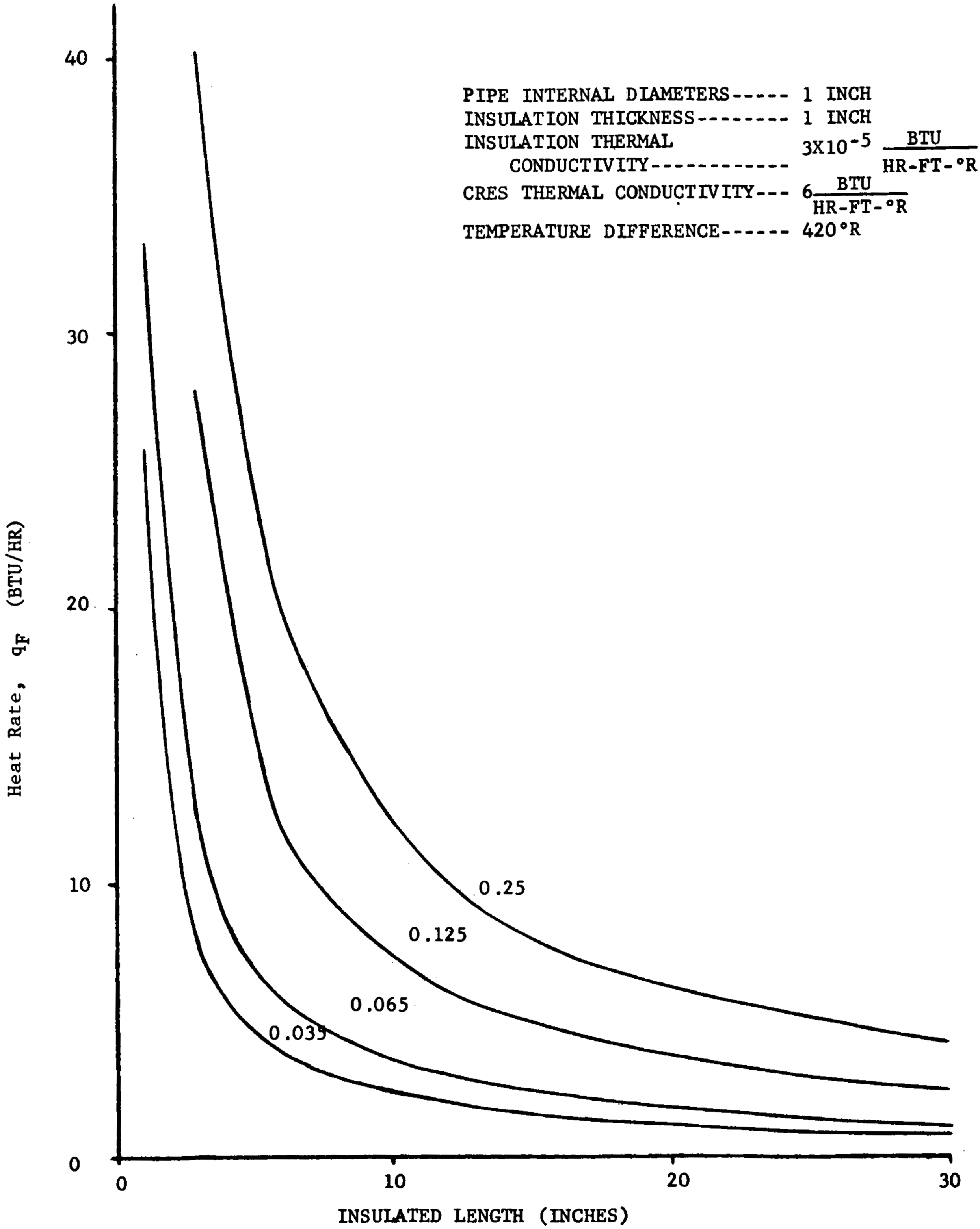

FIG 17 PENETRATION HEAT LEAK AS A FUNCTION OF INSULATED LENGTH

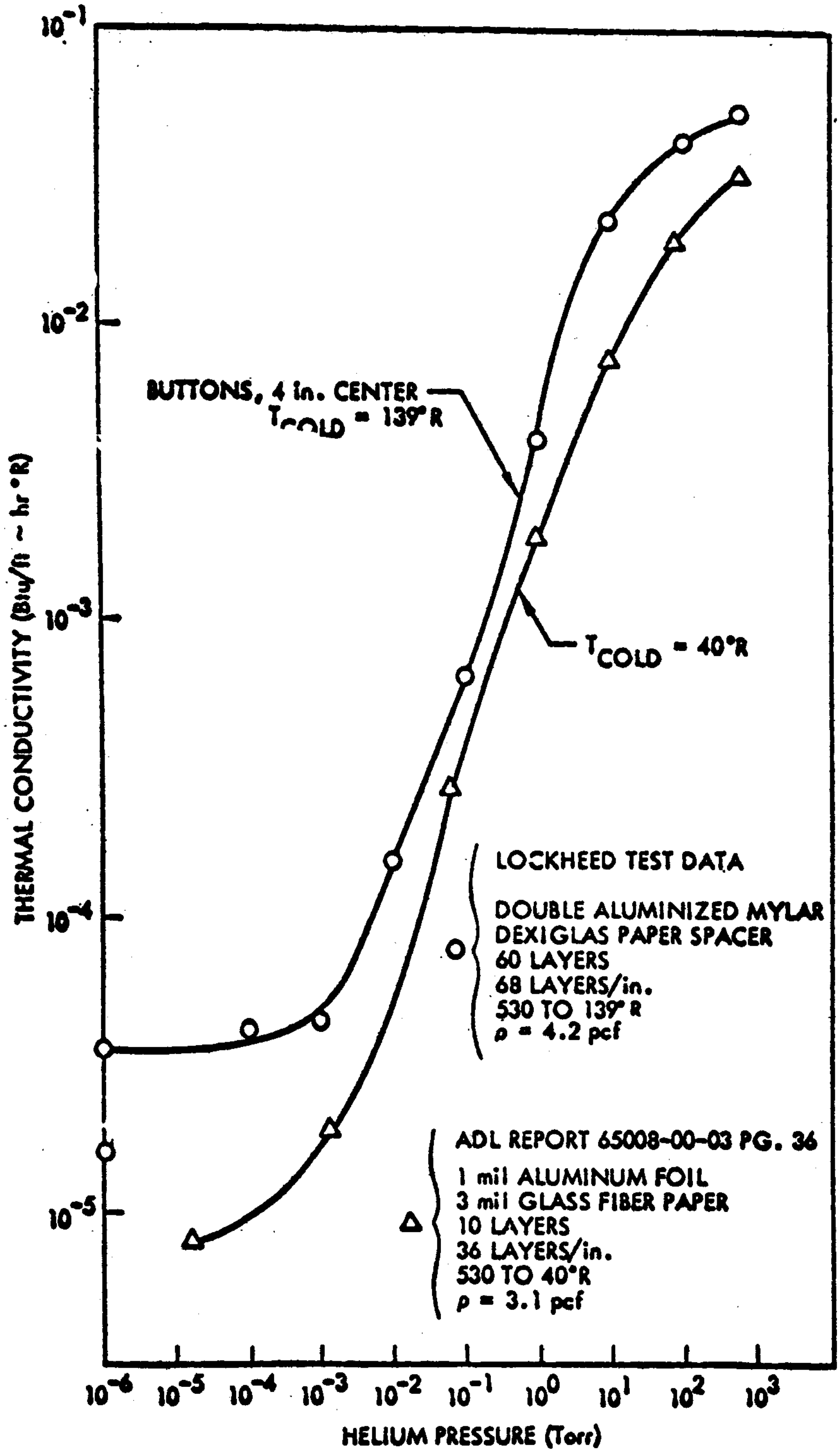

FIG. 18 THERMAL CONDUCTIVITY VERSUS HELIUM PRESSURE FOR TYPICAL SUPERINSULATIONS

insulation batten and purge jacket are designed so that ultimate insulation performance will be achieved during ground hold, ascent, and orbital environments. FIG19 is a plot of the ratio of total heat flux to vacuum heat flux versus vacuum chamber pump down time. This curve was obtained using a 14-inch diameter sphere. Even though the tank diameter and the application of the insulation to the tank were not the same as the proposed experimental tank, the shape of the heat flux curve is typical.

Thermal degradation of aluminized Mylar insulation has never been measured after the insulation has been exposed to simultaneous high-g loading, vibrations, acoustics, and rapid evacuation. Many tests have been performed on component tanks where combinations of the above effects were present. The extent of thermal degradation incurred when the insulation is subjected to the combined effects of the above environmental conditions is needed for system design and evaluation. A flight experiment is the only way to obtain this data for application to larger tankage on future space flights.

In many cases, however, the error in instrumentation used to measure performance parameters can preclude measurement of the thermal degradation due to other factors. FIG 20 is a sketch of the tank proposed for this experiment. FIG 21 shows the approximate type of instrumentation to be used. An error analysis was performed to determine if the above scheme would provide useable information. A test case using the above sketch and other information is included showing the error analysis and development and the accuracy expected on the proposed test tank. Analyses to date indicate that harmful thermal degradation can be measured. FIG 22 shows the variable temperature gradient to be expected because of vehicle orientation and earth orbit. A rotating shield could be used to reduce this temperature variation and thus improve measuring accuracy of the insulation performance.

Heat enters the cryogenic fluid through the penetration insulation due to radiation tunneling and parallel conduction down the layers, as well as heat flow normal to the insulation layers. However, radiation tunneling and parallel heat conduction are not exclusive to the insulation around the penetrations. Any purged multi-layer insulation system must be applied to the tank wall so that the purge gas can vent during vehicle ascent and orbital operations. Consequently,

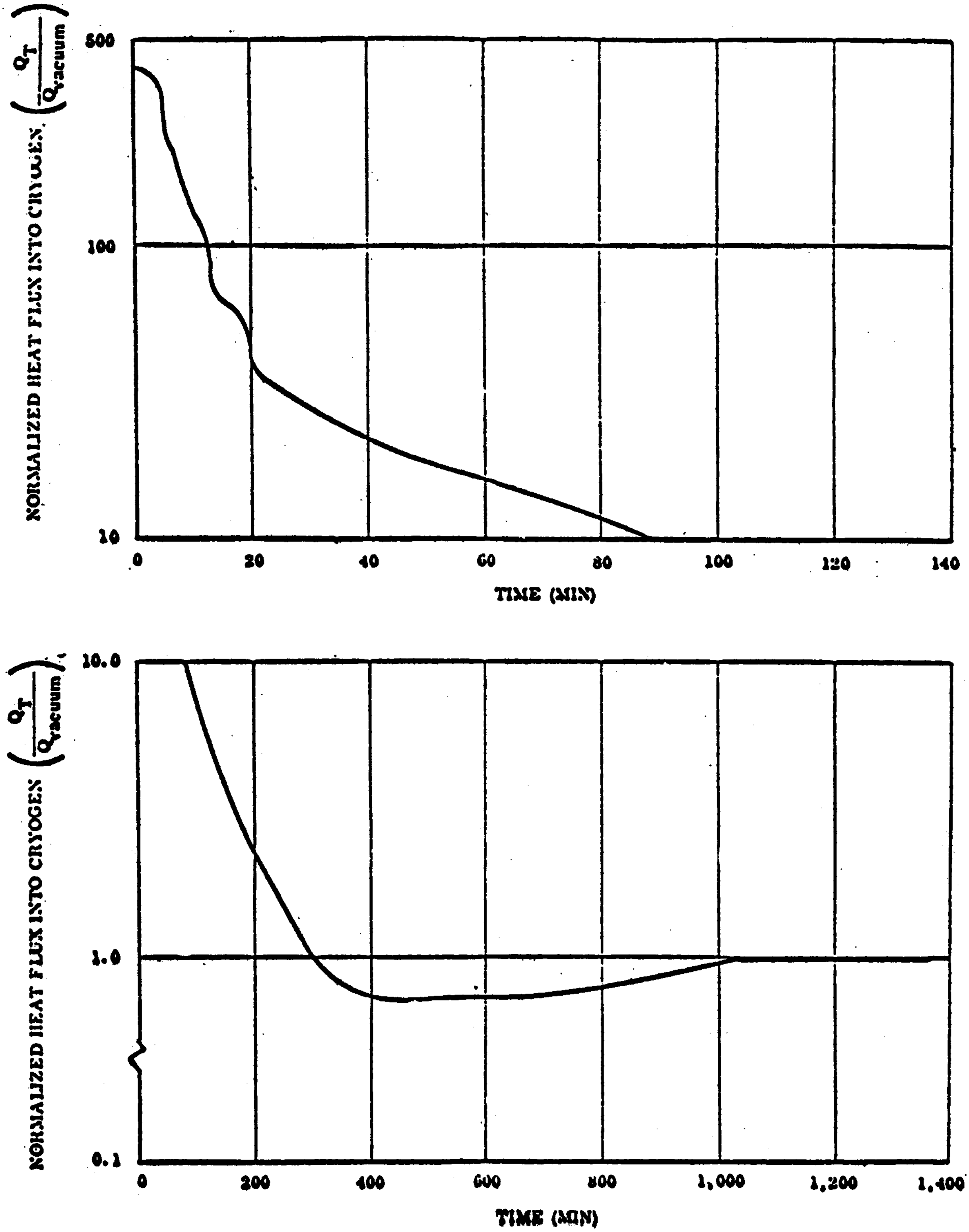

FIG 19 EFFECT OF DEPRESSURIZATION OF INSULATION ON BOIL-OFF RATE

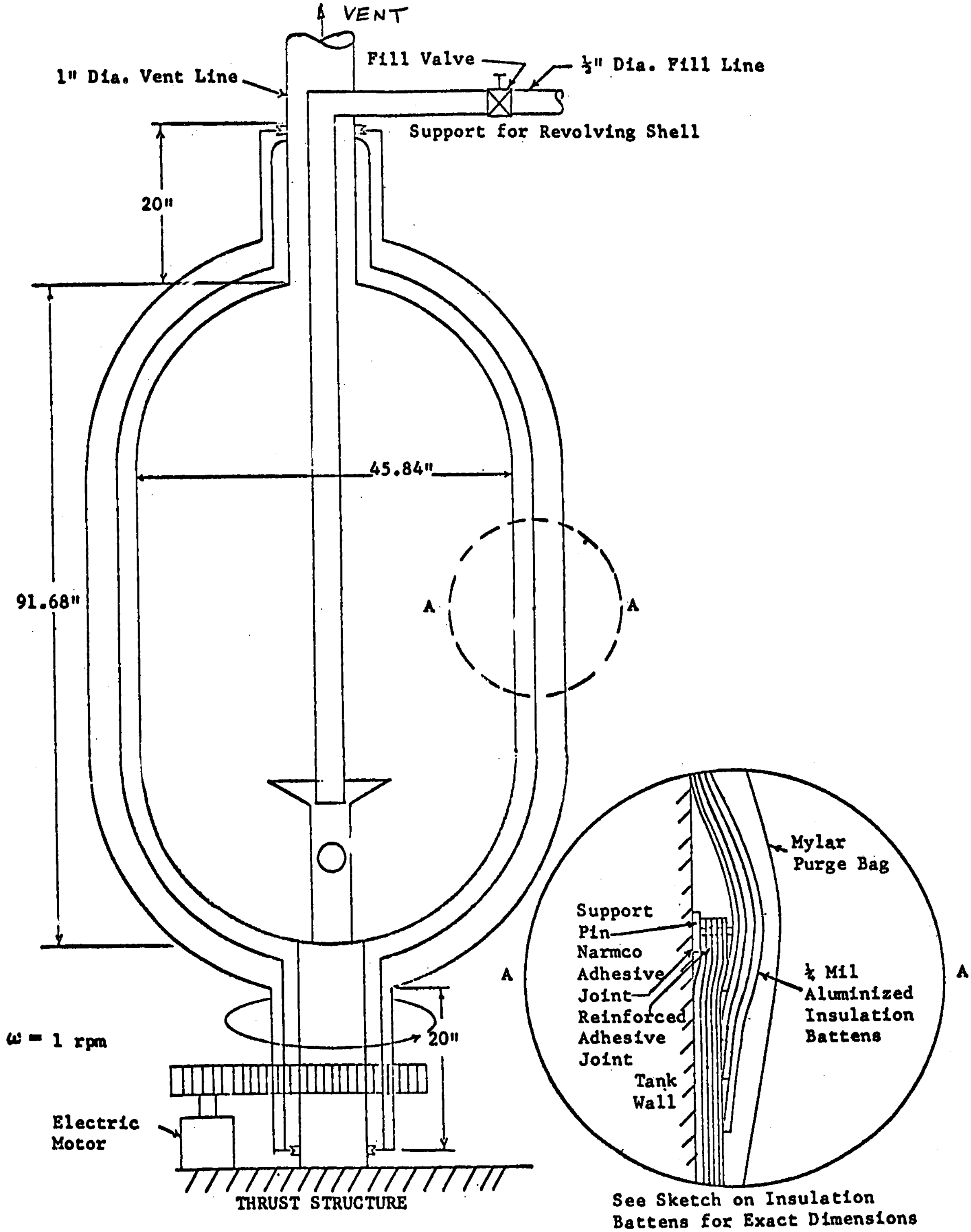

HIGH PERFORMANCE INSULATION SCHEMATIC

FIG 20 TYPICAL SUPERINSULATION SYSTEM AND TANK ASSEMBLY SCHEMATIC

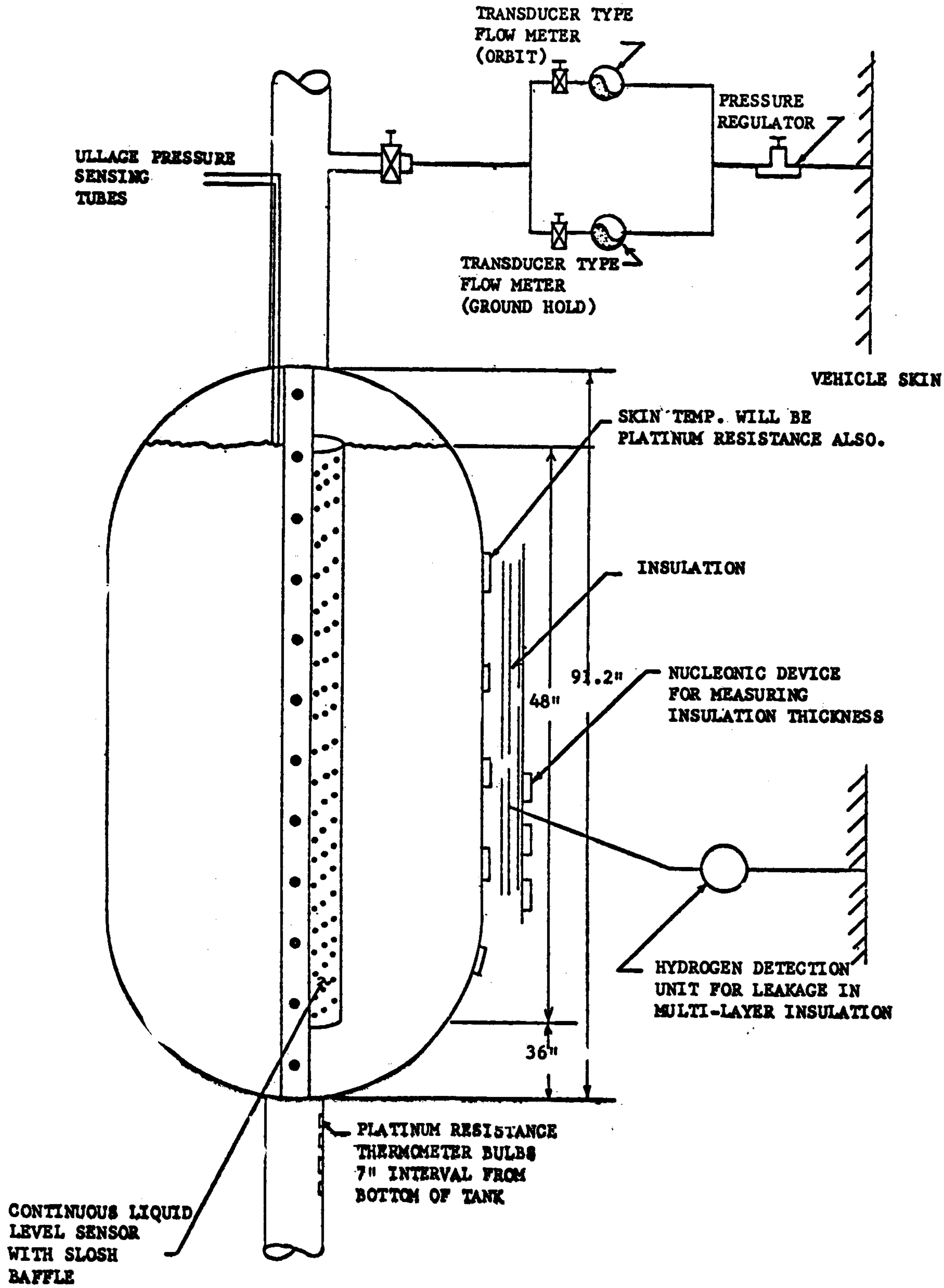

FIG 21 TYPICAL INSTRUEMENTATION REQUIREMENTS FOR SUPERINSULATION TANK

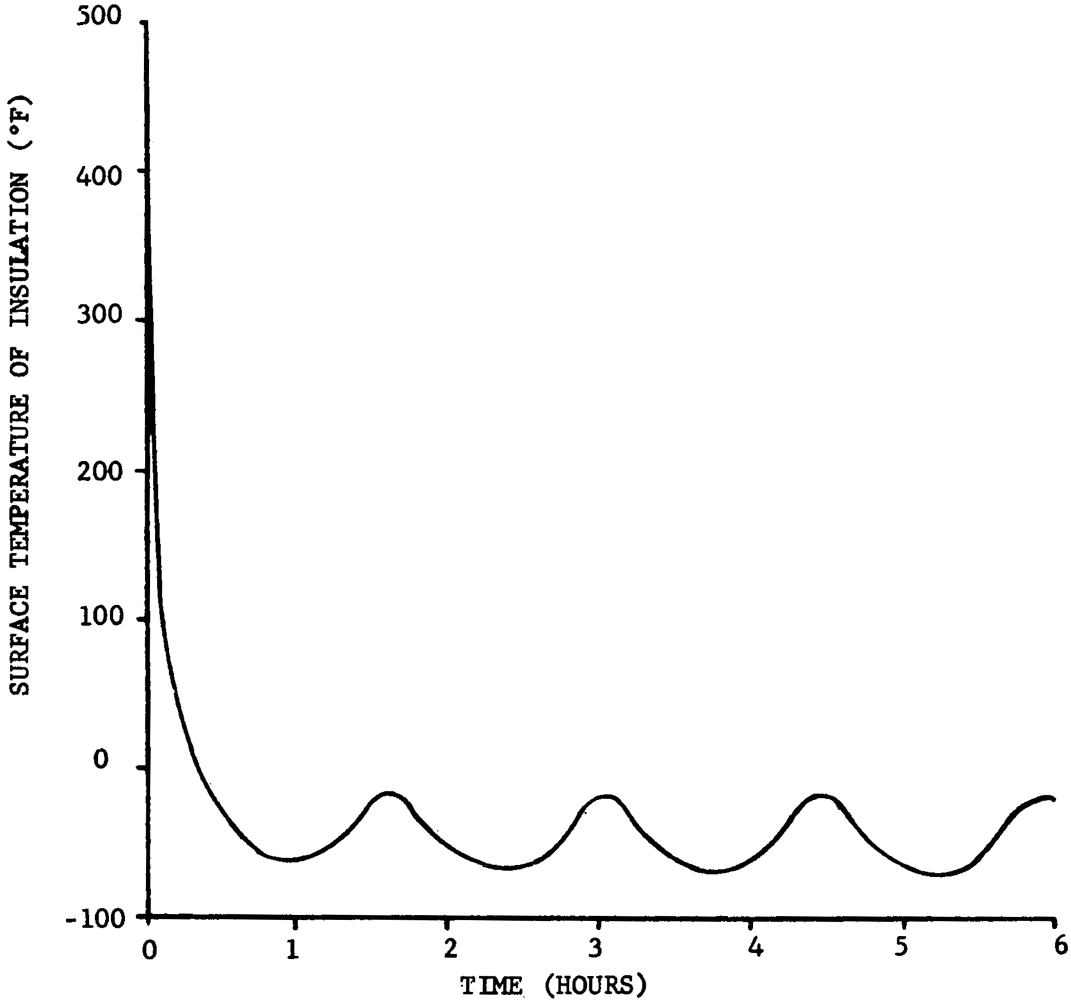

FIG 22 INSULATION SURFACE TEMPERATURE VERSUS TIME

the insulation must be applied in the form of shingles or battens. Therefore, radiation tunneling and conduction effects are present in the side wall insulation as well as around the penetrations. In fact, it has been estimated that the parallel heat flow in the insulation around a penetration will be about 2.6% of the parallel heat flow in the side wall insulation.

The feasibility of measuring the radiation tunneling and lateral conduction for a multi-layer insulation batten installed on a cryogenic tank to be subjected to the ascent environment produced by a rocket vehicle is doubtful. For instance, thermocouples attached to insulation layers would be subjected to the rapidly venting gas flow during ascent, as well as to high g and vibrational loads. It is believed that radiation tunneling and conduction effects can best be evaluated by a series of ground tests where laboratory quality instrumentation can be used and various geometry effects can be investigated.

The insulation batten tank can be installed so that the wrapping technique (batten size, overlap, etc.) can be used on tanks of different size. The apparent side wall thermal conductivity obtained from the orbital experiment can then be extrapolated for design purposes. Furthermore, the basic sidewall thermal conductivity of the insulation used for the orbital experiment can be determined in a ground test by subjecting an identical insulation system to the thermal boundary conditions measured during the orbital experiment.

Ascent Boiloff

The superinsulation tank will be instrumented internally for temperature, pressure, and liquid level. Therefore, the internal energy of the fluid can be determined at any time. The tank wall and supports will be instrumented with temperature sensors in order to determine the energy change of the structure.

During the boost phase, the tank must be closed for safety reasons. Therefore, equivalent ascent boiloff must be evaluated from the internal energy change of the fluid during boost. During the insulation outgassing period (time unknown), the heat entering the tank will be relatively high so the internal energy rates should not be too difficult to measure. Once the rate of change of internal energy becomes relatively constant, the tank can be vented to relieve the pressure. To reduce errors only one vent-down should be made. Therefore, the most profitable vent-down will be after the steady orbital heating condition has been reached.

Heat rate versus time can be readily obtained from internal energy versus time. However, determination of the thermal performance of the insulation during the ascent portion of flight will be extremely complicated. The difficulty arises because the thermal conductivity of the insulation is a function of temperature and pressure The pressure in the insulation is also a function of gas temperature due to the dependance of gas diffusion on temperature. Therefore, a combined transient heat transfer and fluid mechanics problem must be solved simultaneously for the thermal performance of the insulation. FIG 23 is indicative of the expected thermal sequence in the high performance insulation tank.

Penetration Heat Leak Determination

To investigate the feasibility of determing penetration heat leak by measuring the temperature gradient in the penetration at the cold boundary, the following cursory study was made. Four computer runs were made to investigate the effects of variable thermal conductivity, warm boundary temperature, and heat transfer through the insulation on the cold boundary temperature gradient.

1. The penetration and insulation geometry can be seen on FIG 20. The support penetration is constructed from titanium alloy. FIG 24 presents the thermal conductivity of titanium versus temperature. Two cases each were run for warm boundary temperatures of $200^{\circ}R$ and $520^{\circ}R$.

2. To determine the variable conductivity effect on the temperature gradient, cases were run with warm boundary temperatures of 200° and $520^{\circ}R$, assuming perfect insulation. To investigate the insulation effect on the gradient, two cases were run (same two warm boundary temperatures as above) with one-inch thick insulation ($K = 1 \times 10^{-4}$ Btu/hr $^{\circ}R$) installed on the penetration as shown in FIG 25. The insulation conductivity was degraded by approximately one order of magnitude to account for uncertainty in insulation wrapping techniques, etc.

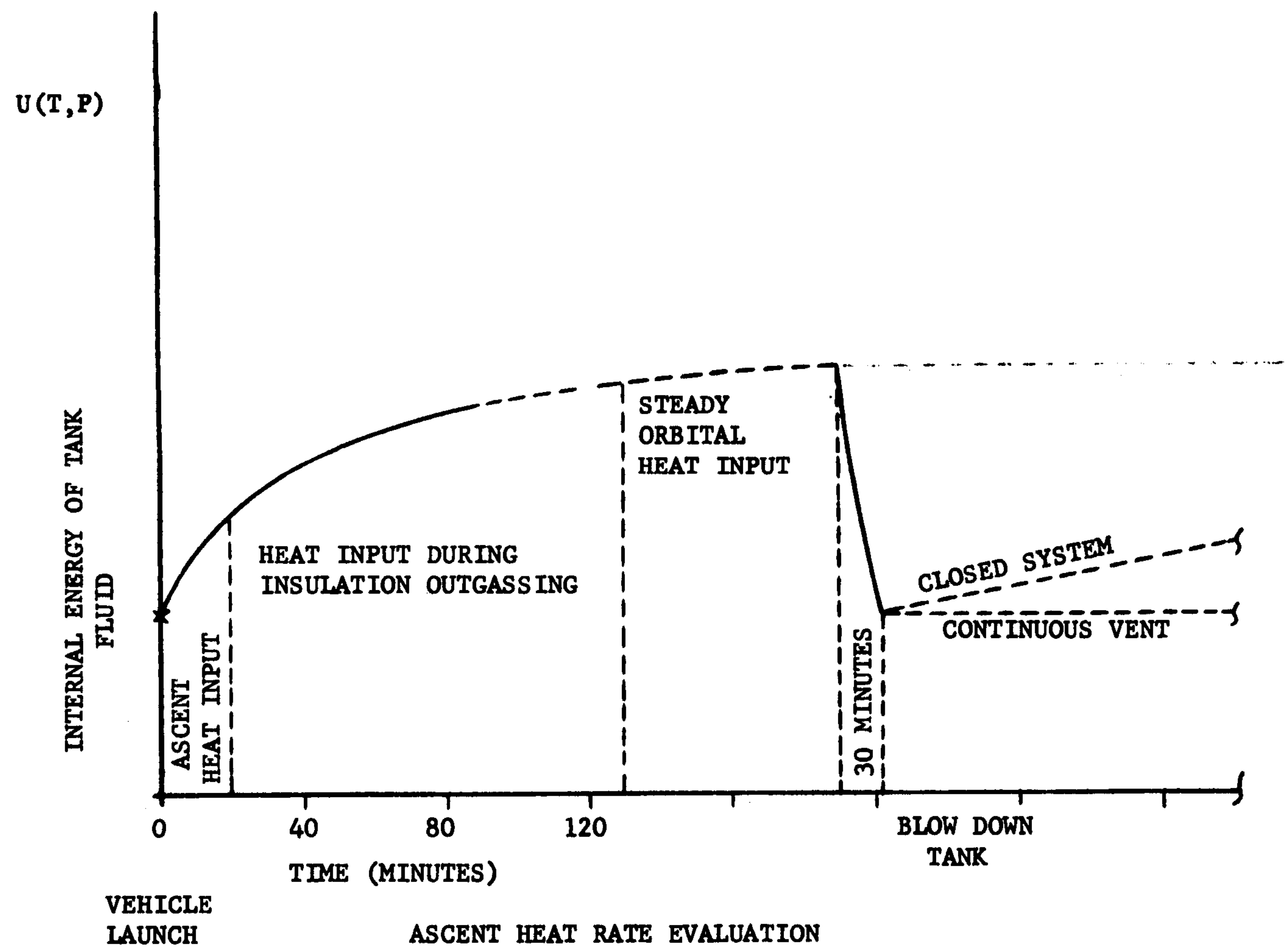

FIG 23 TYPICAL HEAT INPUT HISTORY FOR A FLIGHT TYPE SUPERINSULATED TANK

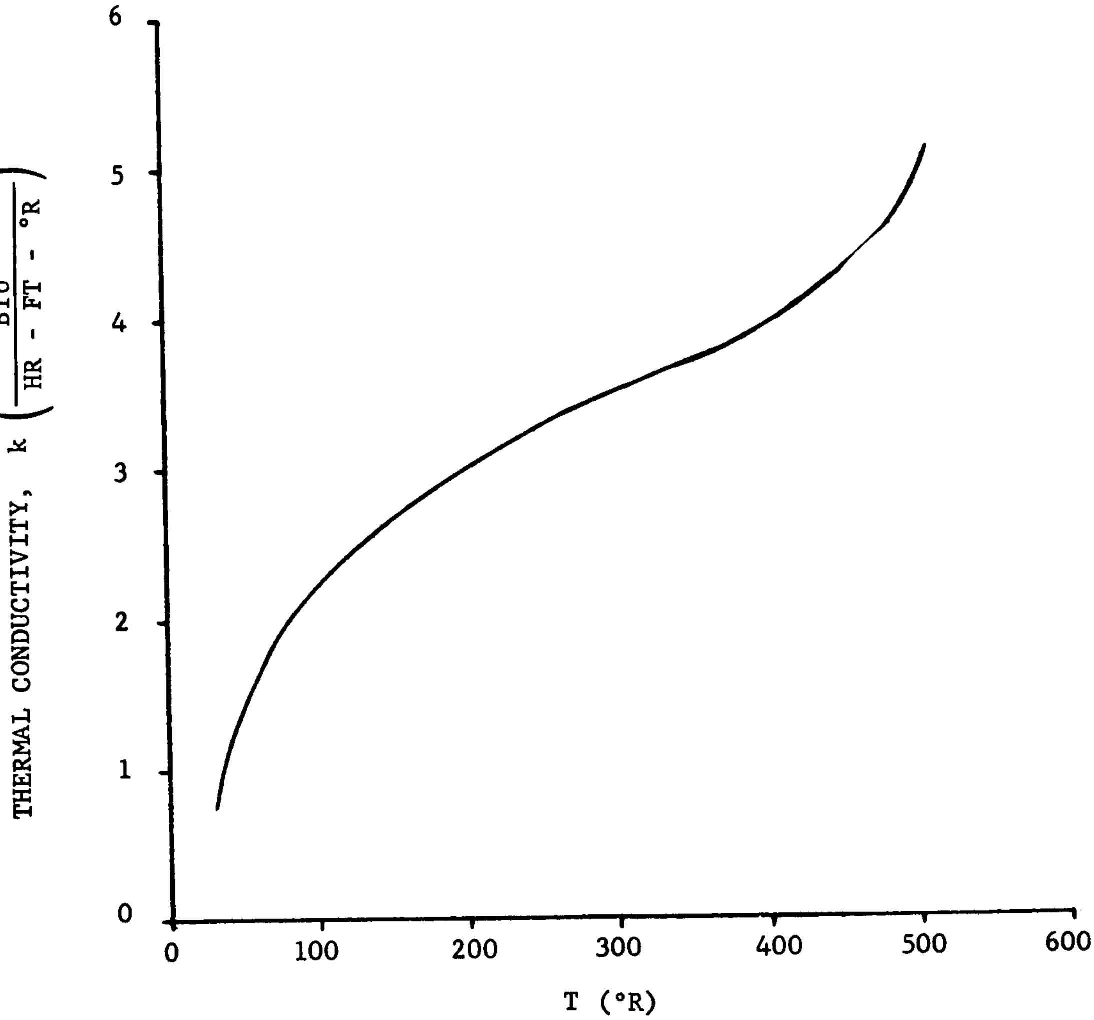

THERMAL CONDUCTIVITY OF A TITANIUM ALLOY

FIG 24 VARIATION OF THERMAL CONDUCTIVITY OF TITANIUM ALLOY WITH TEMPERATURE

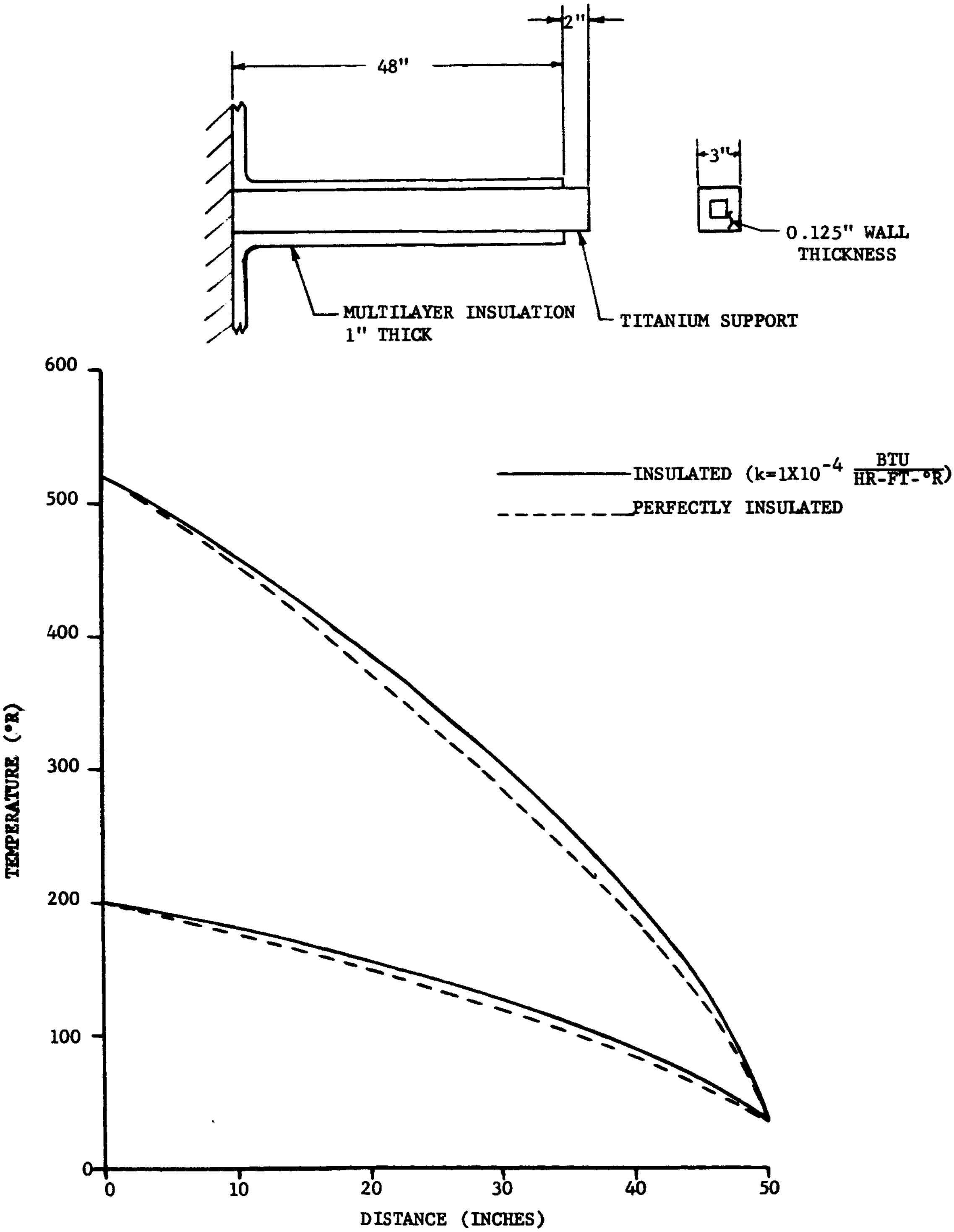

EFFECT OF WARM BOUNDARY TEMPERATURE ON COLD BOUNDARY TEMPERATURE GRADIENT.

FIG 25 WARM BOUNDARY TEMPERATURE EFFECT ON TEMPERATURE GRADIENT IN PENETRATION

3. As can be seen from FIG 25, the variable thermal conductivity of the metal penetration has the greatest effect on the temperature gradient, not the heat transfer through the insulation. Futhermore, the magnitude of the cold boundary temperature gradient is a strong function of the warm boundary temperature. Considerable error could be introduced when attempting to evaluate the penetration heat leak by measuring a large variable temperature gradient, as one would expect to encounter with high warm boundary temperatures. However, if the warm boundary temperature is reduced by cooling the penetration, the cold boundary temperature gradient will also be reduced and can be measured more accurately.

4. Cooling the penetration not only simplifies measuring the cold boundary temperature gradient, but also decreases the ratio of penetration heat leak to side wall heat leak, thus reducing errors in evaluating side wall thermal performance.

5. Based on the above considerations, the support penetrations on the multi-layer insulation experimental tank should be cooled to reduce errors and facilitate measuring penetration heat leak.

SIDE WALL BATTEN THERMAL DEGRADATION

Thermal degradation for a batten area of 50 square feet is about 3 Btu/hr as compared to ideal insulation application. Thermal degradation is due primarily to parallel conduction down the multi-layers. Lockheed test data were used to determine the radiation tunneling effect down the battens.

One cylindrical batten on the high performance insulation tank has been analyzed to determine if the overlap causes serious thermal degradation. The following symbols define the various parameters.

A_1 = area with one thickness

$A2$ = area with two thicknesses

X_1 = 1 inch thickness

X_2 = 2 inch thickness

$T_{A_{avg}}$ = 0.2 (380-37)

$T_{B_{avg}}$ = 0.8 (380-37)

Circ A = $D_{2_{avg}} \pi$

Circ B = $D_{1_{avg}} \pi$

$D_{1_{avg}}$ = 3.90 ft.

$D_{2_{avg}}$ = 4.07 ft.

T_{s_o} = 380°R

T_{s_i} = 37°R

L_1 = (50-12.5) = 37.5 inches

L_2 = 12.5 inches

D_{1_s} = 3.99 ft.

D_{2_s} = 4.15 ft.

$k_{\underline{1}}$ = 3 x 10^{-5} Btu/hr-ft-°R

$Q_{\underline{1}}$ = perpendicular heat leak

Q_{11c} = parallel conducted heat leak

Q_{11T} = parallel tunneling heat leak

$$Q_1 = k\,\Delta T\left(\frac{A_1}{X_1} + \frac{A_2}{X_2}\right)$$

$$= 3 \times 10^{-5}\ (380-37)\left[\frac{(3.90)(37.5)(\cancel{12})}{(1)(\cancel{12})} + \frac{\pi(4.07)(12.5)(\cancel{12})}{(2)(\cancel{12})}\right]$$

$$= (.01029)\left[(459.2) + 79.87\right]$$

$$Q_1 = 5.54 \text{ Btu/hr}$$

$$Q_{11c} = N(K_{AL}\,t_{AL} + K_{mylar}\,t_{mylar})\left(\frac{T_{A_{avg}}\text{CircA}}{L_A} + \frac{T_{B_{avg}}\text{Circ B}}{L_B}\right)$$

$$Q_{11c} = 72\left(145 \times \frac{1}{12\text{x}10^6} + .07 \times \frac{.00025}{12}\right)\left[\frac{.2(343)(\ \pi\ )(4.07)(12)}{14} + \frac{.8\pi(343)3.90}{\frac{20}{12}}\right]$$

$$Q_{11c} = 72\left(121 \times 10^{-7} + 14.6 \times 10^{-7}\right)\left(751 + 2016\right)$$

$$Q_{11c} = 977.63 \times 10^{-7}\quad (27767)$$

$$Q_{11c} = 2.70 \text{ Btu/hr}$$

$Q_{11T} = 0.29\ Q_{11c}$ From LMSC A 70394 Page 24

$$Q_{11T} = 0.29\ (2.72)$$

$$Q_{11T} = .79 \text{ Btu/hr}$$

$$Q_T = 5.54 + 2.70 + .79$$

$$Q_T = 9.03 \text{ Btu/hr}$$

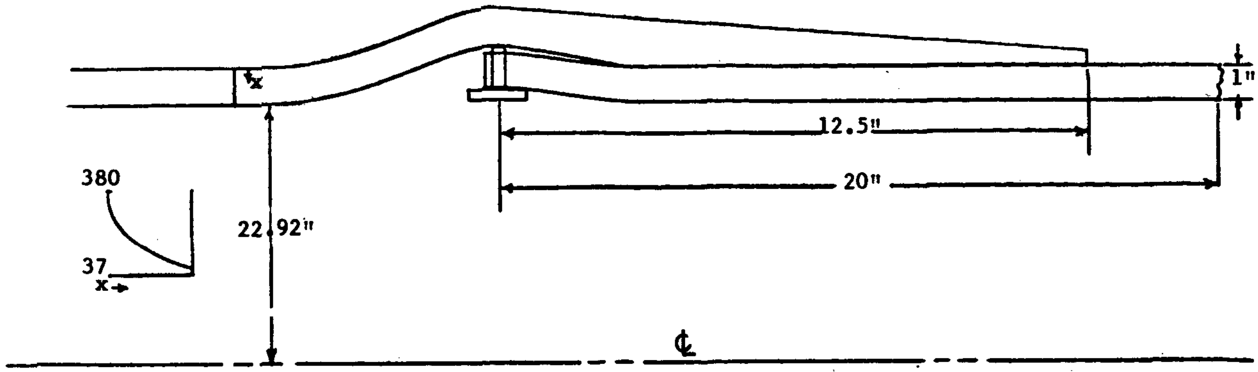

BATTEN SURFACE AREA:

$A = D_s L$

$D_s = 45.84 + 2" = 47.84"$

$A = \frac{(45.84)}{.2}\frac{(50)}{12}$

$A = 49.97\ ft^2$

$Q_I = kA \frac{\Delta T}{\Delta X}$

$Q_I = (3 \times 10^{-5})(50)\frac{(343)}{1"}(12)$

$Q_{II} = 6.17$ Btu/hr

$\frac{Q_B}{Q_I} = \frac{9.03}{6.17}$

$\frac{Q_B}{Q_I} = 1.46$

$Q_B - Q_I = 9.03 - 6.17$

$Q_B - Q_I = 2.86$ Btu/hr for 50 sq. ft. batten

Error Analysis

An analysis was made to estimate the errors involved in evaluating the thermal conductivity of multi-layer insulation installed on an orbiting LH_2 tank. Three methods for obtaining heat input data to the LH_2 were considered, and the errors associated with each method have been estimated. The objective was to determine the method that produces the least error in determining the effective thermal conductivity of the multi-layer insulation system.

The investigation of each case assumes a constant heat flux to the system. The effects of non-uniform transient heat flux will be discussed later. Table IX presents a comparison of typical errors between the constant vent system and the closed vent system. The three techniques are as follows:

A. No Vent Case: For this method, the tank vent is closed. The tank and cryogen are allowed to absorb heat over a period of time. Tank pressure, fluid temperature, and tank structure temperature will be recorded to obtain heat input to the system.

B. Alternate Venting: This procedure is essentially the same as Case A except the tank will be vented down after a period of absorbing heat, and the stored heat will be determined by measuring the energy in the vent gas. Pressure and temperatures within the tank will also be recorded and will serve as a check on the vent gas data.

C. Constant Pressure Continuous Venting: This technique allows the tank to continuously vent to space at constant fluid pressure. The fluid pressure and temperature will be measured along with the heat leaving the system through the vent.

An error analysis of the three data collecting techniques is as follows:

Case A:

For a finite time span the energy equation for Case A is:

$$\int_{\theta_1}^{\theta_2} \dot{Q} d\theta = U_{g_2} M_{g_2} - M_{g_1} U_{g_1} + M_{f_2} U_{f_2} - M_{f_1} U_{f_1} + M_T \int_{T_1}^{T_2} C_{p_T} dT_T \qquad (1)$$

TABLE IX

COMPARISON OF TYPICAL ERRORS

No Vent System (10 Day Orbit)
(Steady Conditions)

Estimated Conditions:

$\dot{Q} = 26$ Btu/hr, $A = 91$ ft^2, $\dot{Q}/A = .286$ Btu/hr-ft^2

Penetration Heat Leak:
Assume one support @ 4 Btu/hr and fill and vent @ 8 Btu/hr

$Q_p = 12$ Btu/hr

$$Q_p/Q_w = \frac{12}{26-12} = 0.86$$

Mass of System: (Propellant + Structure) = 465 lbs.

$$Q/M = \frac{(26)(10)(24)}{465} = 13.5 \text{ Btu/lb}$$

Temperature Error: $\pm .2$

From FIG (1), the error in Q is $\sim \pm 7\%$

Entering FIG (4) @ $\pm 7\%$ with $Q_p/Q_w = .86$ gives an error in conductivity of $\sim \pm 18\%$

Continuous Vent System
(Steady Conditions)

Estimated Conditions:

$\dot{Q} = 20$ Btu/hr, $A = 91$ ft^2.

Penetration Heat Leak:
Assume one support @ 4 Btu/hr and fill and vent @ 1 Btu/hr

$Q_p = 5$ Btu/hr

$$Q_p/Q_w = \frac{5}{20-5} = .33$$

$$\dot{W} = \dot{Q}/h_{fg} = \frac{20}{190} = .105 \text{ lbs/hr}$$

Range on Flow Meter (0-.4) lbs/hr with an error of $\pm 2\%$ full scale

For a flow of 0.105 lbs/hr the % error is $\frac{.008}{.105} = .076$, or 7.6%

Error in Quality $\sim \pm 1\%$

Error in $\dot{Q} \cong 8.6\%$

Entering FIG (4) @ $\pm 8.6\%$ with $Q_p/Q_w = .33$ gives an error in conductivity of $\sim \pm 12.5\%$

Where: M = Mass

U = Internal Energy

T = Temperature

$\dot{Q}$ = Heat Rate

θ = Time

Subscripts:

g = gas

f = liquid

T = tank and associated structure (supports, etc)

1 = state point (1)

2 = state point (2)

Introducing enthalpy into equation (1) and integrating gives:

$$Q = M_{g_2} h_{g_2} - M_{g_1} h_{g_1} + M_{f_2} h_{f_2} - M_{f_1} h_{f_1} - V_T (P_1 - P_2) + M_T Cp_T (T_2 - T_1) \qquad (2)$$

Where: Q = Total heat absorbed

V = Volume of tank

P = Pressure

h = enthalpy

The error in overall heat input "Q" can be expressed as:

$$\frac{dQ}{Q} = -2V_T \frac{dP}{Q} + M_{g_2} \frac{dh_{g_2}}{Q} + h_{g_2} \frac{dM_{g_2}}{Q} - M_{g_1} \frac{dh_{g_1}}{Q} - h_{g_1} \frac{dM_{g_1}}{Q} + M_{f_2} \frac{dh_{f_2}}{Q} + h_{f_2} \frac{dM_{f_2}}{Q} - M_{f_1} \frac{dh_{f_1}}{Q} - h_{f_1} \frac{dM_{f_1}}{Q} + 2 M_T Cp_T \frac{dT_T}{Q} \qquad (3)$$

The relationship, dh = cp dT can be introduced with very little error. Therefore, equation (3) becomes:

$$\frac{dQ}{Q} = -V_T\frac{dP}{Q} + M_{g_2}C_{p_g}\frac{dT_{g_2}}{Q} + h_{g_2}\frac{dM_{g_2}}{Q}$$

$$- M_{g_1}C_{p_g}\frac{dT_{g_1}}{Q} - h_{g_1}\frac{dM_{g_1}}{Q} + M_{f_2}C_{p_f}\frac{dT_{f_2}}{Q} \qquad (4)$$

$$+ h_{f_2}\frac{dM_{f_2}}{Q} - M_{f_1}C_{p_f}\frac{dT_{f_1}}{Q} - h_{f_1}\frac{dM_{f_1}}{Q} + 2M_TC_{p_T}\frac{dT_T}{Q}$$

It can now be seen that the error in $\dot{Q}$ is not only dependent on the measurement accuracy but also on the repeatability of the instrumentation. For instance, if the temperature error "dT" is constant ($dT_{g2} = dT_{g1}$, $dT_{f2} = dT_{f1}$) during the change from state point one to state point two and the error in mass measurement "dM" is also assumed constant, the error in "Q" can be written:

$$\frac{dQ}{Q} = -2\ V_T\frac{dP}{Q} + (M_{g_2} - M_{g_1})\frac{dT_g}{Q}$$

$$(5)$$

$$+ (M_{f_2} - M_{f_1})C_{p_f}\frac{dT_f}{Q} + (h_{g_2} - h_{g_1})\frac{dM_g}{Q}$$

$$+ (h_{f_2} - h_{f_1})\frac{dM_f}{Q} + 2\ M_TC_{p_T}\frac{dT_T}{Q}$$

However, if the instrumentation is not repeatable, i.e., there are sign changes in dT and dM the error in Q is maximized and becomes:

$$\frac{dQ}{Q} = 2\ V_T\frac{dP}{Q} + M_{g_2}C_{p_g}\frac{dT_{g_2}}{Q} + M_{g_1}C_{p_g}\frac{dT_{g_1}}{Q}$$

$$+ M_{f_2}C_{p_f}\frac{dT_{f_2}}{Q} + M_{f_1}C_{p_f}\frac{dT_{f_1}}{Q} + h_{g_2}\frac{dM_{g_2}}{Q} - h_{g_1}\frac{dM_{g_1}}{Q}$$

$$+ h_{f_2}\frac{dM_{f_2}}{Q} - h_{f_1}\frac{dM_{f_1}}{Q} + 2\ M_TC_{p_T}\frac{dT_T}{Q} \qquad (6)$$

If both liquid and gas temperature measurements are given the same band accuracy, equation (6) becomes:

$$\frac{dQ}{Q} = 2\, V_T \frac{dP}{Q} + \left[(M_{g_2} + M_{g_1})\, C_{p_g} + (M_{f_2} + M_{f_1})\, C_{p_f} \right] \frac{dT}{Q} + (h_{g_2} - h_{g_1}) \frac{dM_g}{Q} + (h_{f_2} - h_{f_1}) \frac{dM_f}{Q} + 2\, M_T C_{p_T} \frac{dT_T}{Q} \qquad (7)$$

Since instrumentation errors fluctuate with a given band accuracy, equation (7) is the applicable equation for estimating error in overall heat input. It can be shown that the most significant term in equation (7) is:

$$(M_{f_2} + M_{f_1})\, C_{p_f} \frac{dT}{Q} \; .$$

Introducing the parameter "(Q/M_s)", equation (7) will reduce to:

$$\frac{dQ}{Q} = \left(\frac{M_{f_2} + M_{f_1}}{M_s} \right) \frac{dT}{M_s} \qquad (8)$$

Where M_s = total mass of fluid, tank struts, etc.

Equation (8) is presented in graphical form on FIG 26. The total heat input Q is a function of heating rate and orbit time. This relationship is presented on FIG 27.

It can be seen from FIG 27 that a heating rate of $Q/A = .29$ Btu/hr-ft^2 and an orbit time of 10 days gives a Q/M of 14. For a Q/M of 14 Btu/lb and a temperature error of 0.1, FIG 26 shows that the error in overall heating rate will be approximately $\pm$ 7%. The above numbers are representative of a 4' diameter LH_2 tank with a length-to-diameter ratio of 2. The insulation system was assumed to be one inch of multi-layer insulation.

Case B:

The analysis of Case B is essentially the same as Case A, with the exception of measuring the heat leaving the system through the vent.

NO VENT CASE

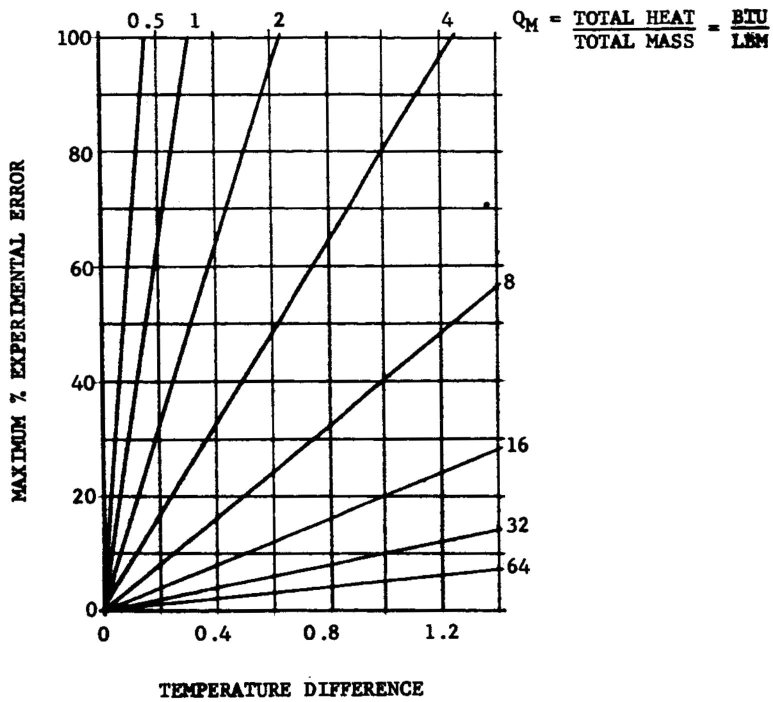

FIG 26 ERRORS DUE TO TEMPERATURE AND Q/M

NO VENT CASE

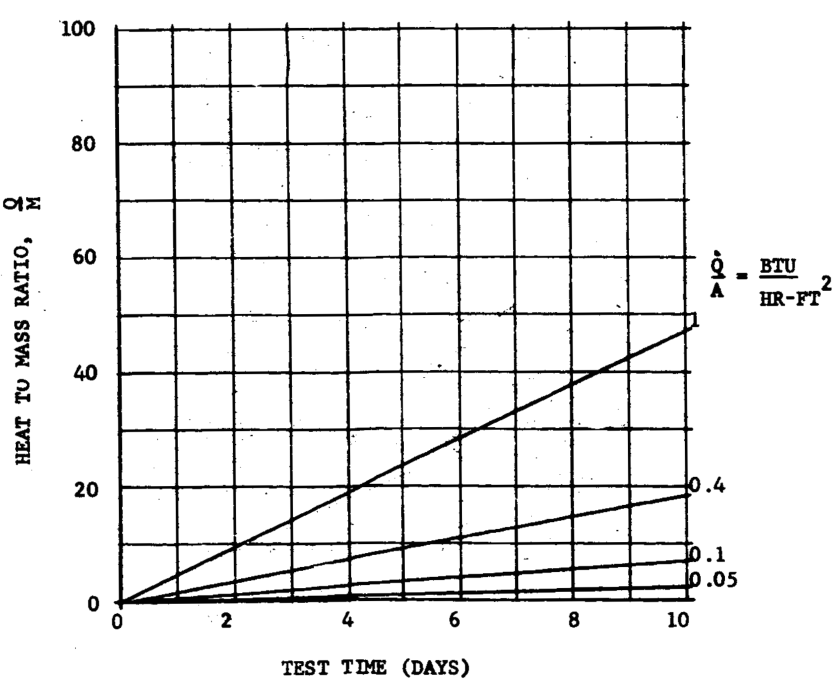

FIG 27 Q/M VS TEST TIME AND HEAT FLUX (Q/A)

During the vent-down time, the heat balance on the system is:

$$Q = \int_{\theta_1}^{\theta_2} h_g dM_s + M_{g_2} h_{g_2} - M_{g_1} h_{g_1} + M_{f_2} h_{f_2} - M_{f_1} h_{f_1}$$

$$- V_T(P_1 - P_2) + M_T C_{p_T} (T_2 - T_1) \qquad (9)$$

Equation (8) is the same as equation (2) with the exception of the vent term $(\int_{\theta_1}^{\theta_2} h_g dM_s)$. The vent term is a path function and cannot be analytically integrated. However, if the vent cycle is rapid the Q through the insulation will be small.

Neglecting Q, equation (9) reduces to:

$$-\int_{\theta_1}^{\theta_2} h_g dM_s = M_{g_2} h_{g_2} - M_{g_1} h_{g_1} + M_{f_2} h_{f_2} - M_{f_1} h_{f_1}$$

$$- V_T(P_1 - P_2) + M_T C_{p_T} (T_2 - T_1) \qquad (10)$$

The error on the right hand side of equation (10) is the same as given in equation (9). Therefore, the vent term, when measured, will serve as a check on the heat balance. One must realize that relatively rapid depressurization of the tank introduces an error in the term $M_T\ C_{p_T}\ (T_2 - T_1)$ because the structure tank, supports, etc., will not be in thermal equilibrium with the tank contents during blowdown. This condition could be helped by venting in steps and stirring the fluid after each step. However, if there is appreciable stratification, this could cause a rapid pressure increase in the tank.

Case C:

For this case, an energy balance on the tank gives the following expression for the heat rate.

$$\dot{Q} = \frac{\rho_f - \rho_v + \rho_g}{\rho_f - \rho_g} (h_g - h_f)\, \dot{w} + M_f \frac{dT_f}{d\theta} + M_g \frac{dT_g}{d\theta}$$

$$+ M_T C p_T \frac{dT_T}{d\theta} \qquad (11)$$

Where: ρ = density

$\dot{w}$ = flow rate

Subscripts: v = vent

If $\rho_v = \rho_g$ the density term in equation (16) will be small. Furthermore, for a small ullage volume, the energy term for the gas will also be small. Equation (11) can be written:

$$\dot{Q} = h_{fg}\,\dot{w}_v + M_f\,Cp_f\,\frac{dT}{d\theta} \tag{12}$$

The error in $\dot{Q}$ can now be expressed as:

$$\frac{d\dot{Q}}{\dot{Q}} = h_{fg}\,\frac{d\dot{w}}{\dot{Q}} + \frac{M_f\,Cp_f}{\dot{Q}}\left[\pm\left(\frac{dT_f}{d\theta}\right)_A \pm \left(\frac{dT}{d\theta}\right)_M\right]$$

$$+\ \frac{dT_f}{d\theta}\left(\frac{dM_f}{\dot{Q}}\right) \tag{13}$$

Where $\left(\frac{dT_f}{d\theta}\right)_A$ = Actual temperature gradient in the liquid

$\left(\frac{dT_f}{d\theta}\right)_M$ = Measured temperature gradient in the liquid

The term $\left(\frac{dT_f}{d\theta}\cdot\frac{dM_f}{\dot{Q}}\right)$ is a product of small quantities and is therefore, negligible.

For small changes in $\dot{Q}$ and/or ullage pressure the term $(dT_f/d\theta)_A$ will be small, and it is expected that a temperature sensor would follow these small changes accurately. Based on this reasoning, the temperature terms in equation (13) can be neglected and the error on heating rate is directly proportional to the error in measuring flow rates. It is expected that gas flow rates can be measured with an accuracy of $\pm$ 2% of full scale. The errors involved in using a time-averaged surface temperature are to be investigated when the transient temperature data become available.

An evaluation of multi-layer insulation, from bulk thermodynamic data obtained from the LH_2 tank requires that all extraneous heat leaks (penetrations, etc.) be accounted for. Furthermore, a temperature map of the outer surface of the insulation must be available, as well as the tank wall temperature distribution. Assuming that these data can be measured, the error in evaluating the thermal conductivity can be expressed as:

$$\frac{dK}{K} = \frac{\sum_{i=1}^{n} A_i \left(\pm\, dT_{si} \pm dT_{wi}\right)}{\sum_{i=1}^{n} A_i \left(T_{si} - T_{wi}\right)} + \left(\frac{d\dot{Q}}{\dot{Q}}\right)_w \qquad (14)$$

Where $(d\dot{Q}/\dot{Q})_w$ = error in evaluating heating rates through tank wall

K = thermal conductivity of multi-layer insulation

A = incremental area

T = temperature

$\dot{Q}$ = heat rate

Subscripts: n = number of times tank area is subdivided

s = surface of insulation

w = tank wall

To investigate the effect of penetration heat leak on the error in evaluating thermal conductivity, the following approach is used:

Define the ratio N such that:

$$\dot{Q}_p / \dot{Q}_w = N \qquad (15)$$

Where $\dot{Q}_p$ = penetration heat leak (and/or any heat entering the fluid that does not pass through the insulation)

$\dot{Q}_w$ = side wall heat rate

Another error associated with the venting cases (both Cases B and C) is the error in determining the quality of the vent gas. FIG 28 is an estimate of the error in heat rate as a function of quantity of liquid vented and the accuracy of measuring the % liquid in the gas. For the sample case presented in Table IX, the continuous vent system introduces errors in Q of approximately $\pm$ 8.6%.

As mentioned previously, the analysis presented above only considers errors associated with the heat entering the LH_2 tank. If the incident heat flux is variable (which will be the case in low earth orbit), the transient effects must be accounted for or eliminated if accurate thermal conductivity data is to be obtained. Furthermore, the thermal conductivity of multi-layer insulation is a strong function of warm boundary temperature. Therefore, to obtain conductivity data from boiloff and temperature data collected from an unsymmetrically heated tank, one would need to know the relationship between conductivity and temperature. This relationship is available for the Linde multi-layer insulation system operating under ideal conditions (calorimeter data), and similar data could be generated for other multi-layer systems. However, if the system is degraded during boost, the ideal values may no longer apply and the error introduced cannot be determined.

To reduce circumferential gradients, it is recommended that the tank be enclosed in a shroud of high conductivity material (aluminum). Calculations are now in progress to determine the effects of various coatings on the shroud temperature gradients and transient temperature variations. If the coatings do not sufficiently eliminate the circumferential gradients, another possiblity would be to design the tank and shroud so that the shroud could be rotated about the tank with sufficient speed to assure a constant temperature. The transient temperature variations will be of a steady periodic nature. The amplitude of the temperature fluctuations can be reduced by controlling the optical properties of the shroud surface. Small amplitude periodic fluctuations of temperature can be averaged over several orbits and the average surface temperature of the insulation can be used for conductivity evaluation.

Now: $\dot{Q}_w = \dot{Q} - \dot{Q}_p$

The maximum error in $\dot{Q}_w$ is:

$$\frac{dQ_w}{Q_w + Q_p} = \frac{d\dot{Q}}{\dot{Q}} + \frac{dQ_p}{Q_w + Q_p} \qquad (16)$$

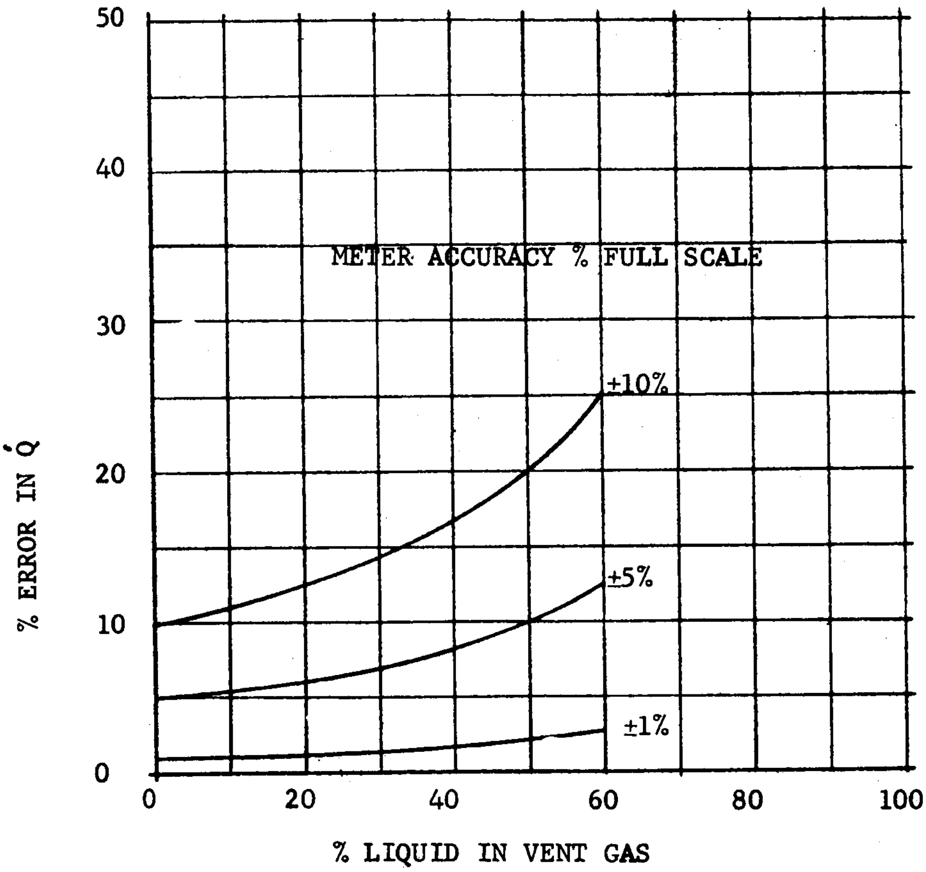

FIG 28 ERROR IN HEAT RATE VS ENTRAINED LIQUID IN THE VENT GAS

substitution of equation (15) and simplifying gives:

$$\left(\frac{d\dot{Q}}{\dot{Q}}\right)_w = (1 + N)\ \frac{d\dot{Q}}{\dot{Q}} + N\ \frac{d\dot{Q}_p}{\dot{Q}_p} \tag{17}$$

Substituting equation (17) into equation (14) gives:

$$\frac{dK}{K} = \frac{\sum_{i=1}^{n} A_i\ (\pm\ dT_{si} \pm\ dT_{wi})}{\sum_{i=1}^{n} A_i\ (T_{si} - T_{wi})} + (1 + N)\ \frac{d\dot{Q}}{\dot{Q}} + N\ \frac{d\dot{Q}_p}{\dot{Q}_p} \tag{18}$$

Obviously, from equation (18), the error in thermal conductivity can be reduced by reducing the penetration and/or extraneous heat leaks. FIG 29 presents the error in thermal conductivity as a function of the right hand side of equation (18). To generate the curves in FIG 29 the following values were assumed:

$dT_s = \pm\ 1^o$

$dT_{sw} = \pm\ 1^o$

$d\dot{Q}_p/\dot{Q}_p = \pm\ 5\%$

$T_s = 380\ ^oR$

$T_w = 40\ ^oR$

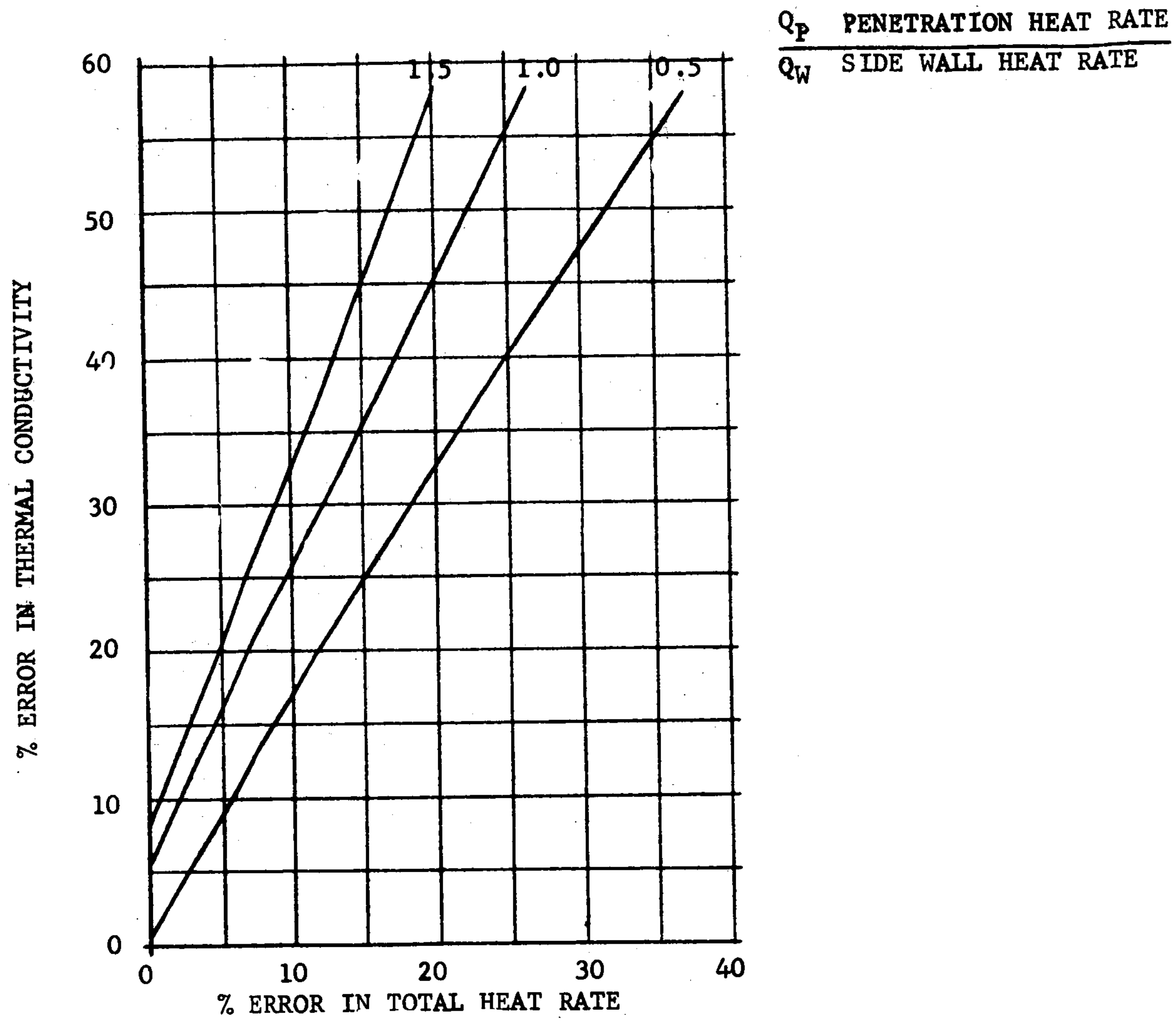

FIG 29 ERROR IN CONDUCTIVITY AS A FUNCTION OF HEAT RATE ERROR AND Q_p/Q_w

This pressure increase will require a stronger and heavier tank than the continuous vent system, and will require more LH_2 for tank chilldown during the propellant transfer experiments. Furthermore, attitude control would cause fluid sloshing in the tank with possible pressure spikes that could cause inadvertent venting of the tank. Since accuracy for this system is time dependent, any interruption in the data collection will degrade the experiment.

3. FIG 29 shows that penetration heat leak can cause considerable error in evaluating insulation conductivity. The vent size of the LH_2 tank will depend on the ground hold performance of the insulation. Presently, the most likely candidate insulation will be a gaseous helium purged system that has relatively high ground hold boiloff and requires a large vent. For a "locked up" tank (no venting), the heat leak through the vent is the same as any penetration of like geometry. Conversely, the continuous venting of gas reduces the heat leak through the vent line. Therefore, the ratio of penetration heat leak to side wall heat leak will be greater for the "lock up" concept than for the continuous vent system.

Advantages for the continuous vent system are as follows:

1. This system does not directly depend on long orbit times for good experimental accuracy. However, orbit times must be long enough to establish quasi-steady state conditions.
2. The structure (tank wall, supports, etc.) will not be as massive as for the closed system, thereby reducing chilldown propellant requirements.
3. This concept measures heating rate directly. Therefore, interruptions in the experiment can be tolerated, and in the case of an abort, after several orbits useful data can still be collected.

The disadvantages for this concept are as follows:

1. For continuous venting, the location of the propellant phases (gas, liquid) must be known in order to prevent venting of liquid. This may require an auxiliary propulsion system for propellant settling.

Summary

Due to time limitations, calculations have not been performed to estimate the effect of a periodic heat flux on conductivity evaluation. This error will be present regardless of the method selected for measuring heating rates (continuous vent, or closed vent systems).

The advantages of the closed vent system are as follows:

1. It will not be necessary to keep the liquid settled during the experiment.
2. It may be possible to study stratification concurrently with the multi-layer insulation experiment.
3. Temperature, pressure, and mass measurements will be the only instrumentation requirements for orbital phase of the multi-layer insulation experiment. However, venting will probably be necessary due to relatively high heat leak during vehicle ascent. If it becomes necessary to vent the tank, the flow rate and quality must be measured.

The disavantages of the closed vent system are as follows:

1. For the propellant mass and low heating rates expected in the multi-layer experiment, orbit time requirements will be on the order of ten days.
2. It has been roughly estimated for the conditions given below that the pressure rise in the LH_2 tank will be approximately 60 psi with a temperature rise of 14° F. This will give the estimated error of $\pm$ 7% mentioned previously.

Conditions for estimating pressure rise are as follows:

a. Initial pressure 10 psia (saturated system)
b. 5% ullage (by mass)
c. Constant density system
d. 3.8 ft. diameter tank, 7.6 ft. long
e. Constant heat rate of 26 Btu/hr (orbital heat rate)
f. System does not deviate from saturated conditions

2. Continuous venting of the gas may affect the stratification mechanism, thus preventing the stratification experiment from being run concurrently with the superinsulation evaluation. However, as stated previously, heat rate errors for this system are not time critical and the superinsulation experiment could possibly be performed after completion of the stratification experiment.

3. Instrumentation for this system will be more complex, because vent flow rate and exit fluid enthalpy must be determined as well as the rate of change of internal energy of the tank and fluid. For the constant pressure system these change rates are dependent on how well the ullage pressure can be controlled.

Based on the above considerations, it is felt that the continuous vent system is the most attractive of the two for obtaining thermal conductivity, provided there is sufficient force to keep the propellant settled. However, it is obvious that considerably detailed investigations must be performed before a firm test plan can be generated for the multi-layer insulation experiment.

Stratification

Booster Flight

Several reliable methods have been developed to predict propellant stratification for acceleration levels of one g and higher. These methods vary from complex boundary-layer flow models to simple empirical models that are accurate to within $0.2^{\circ}R$.

Several dimensionless groups have been developed to correlate such effects as fluid, container geometry, and heating rates. Existing computer programs will be used to assess the boost phase stratification data from this experiment.

The data will be compared with prediction methods applicable to the large LH_2 tanks of the S-IV, S-II, and S-IVB stages. Also, checks will be made with the correlation by Neff, FIG 30.

To prevent venting during booster flight, which can prevail due to increased heat loads from the purged HPI, it may be necessary to operate a stratification destruction device. There are several concepts for this system, one of which is shown in FIG 31. This destruction device must be capable of thoroughly mixing the liquid during boster flight as well as during orbital coast. One method to prevent or delay venting in a near zero-g environment would be to mix gas with the liquid, but this requirement may impose excessive demands in a one g or higher acceleration environment, depending on system design.

Orbital Injection Transients

An area of critical concern is the transition from turbulent to laminar boundary layer flow along the sidewalls. This problem occurs following injection of an insulated tank into orbit, where acceleration levels are reduced by many orders of magnitude (10^{-5} to 10^{-8} g's), and are accompanied by numerous small perturbations from attitude control systems, auxiliary propulsion systems to allow tank venting, and drastic tank heat load decay as the insulation approaches equilibrium.

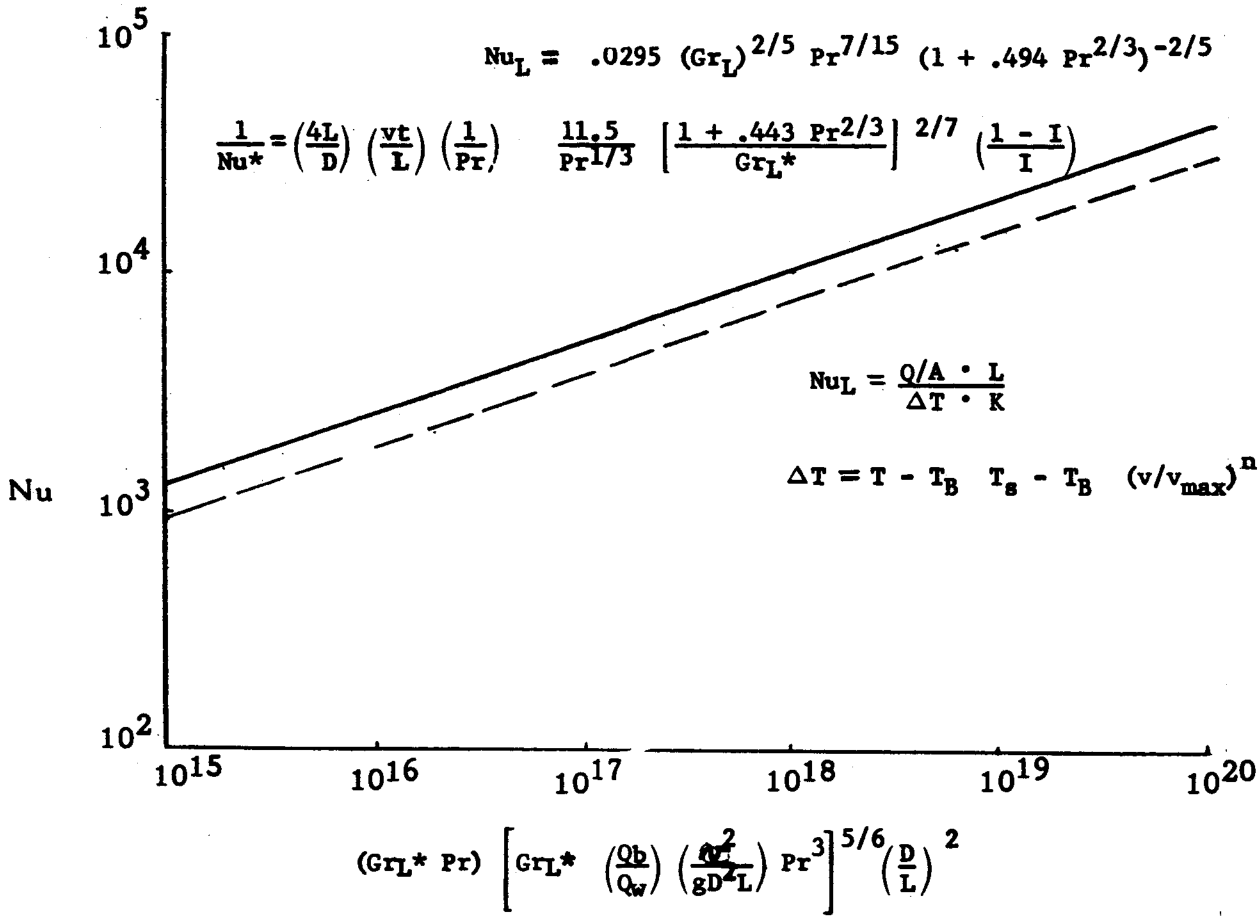

Nu = Nusselt Number

Pr = Prandtl Number

Gr_L = Grasshoff Number

I = Energy Integral

v = Velocity

* = Denotes Modified

FIG 30 NEFF's CORRELATION

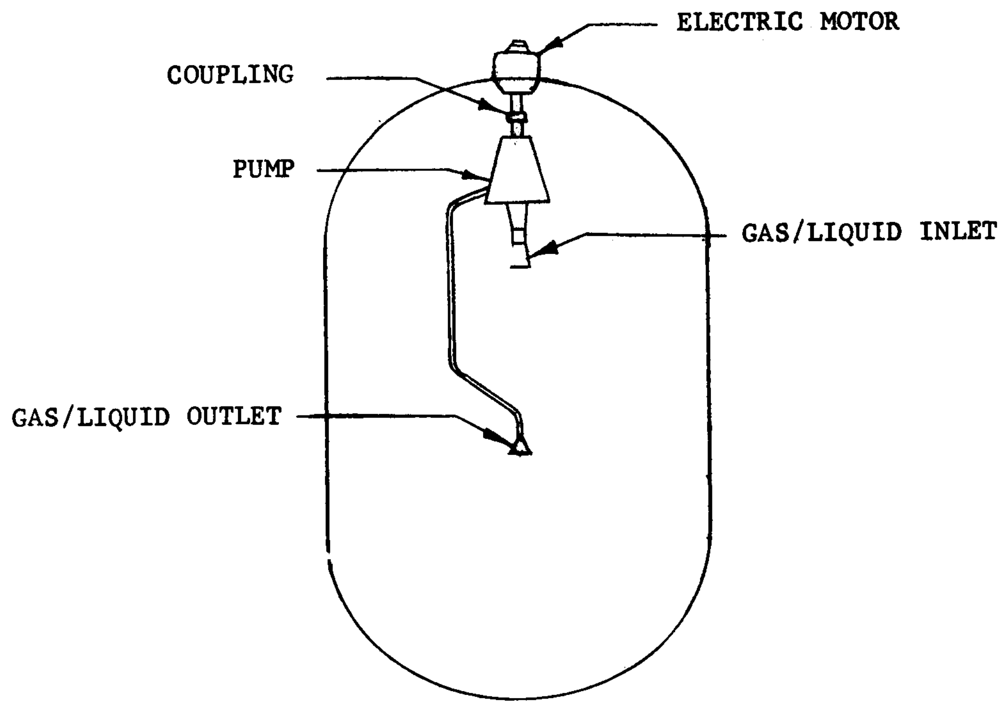

FIG 31 STRATIFICATION REDUCTION DEVICE

These factors cause great difficulty in making accurate predictions of tank pressures that affect auxiliary propulsion and vent system requirements due to stratification of propellants.

Since the heat load will vary in the experimental tank (FIG 19), and since there will be some auxiliary propulsion activity, it may be necessary to operate a stratification reduction device in order to prevent tank venting for integration of the vent and auxiliary propulsion system.

The stratification process under this condition of momentary auxiliary propulsion system operation may be severely affected. Detailed analyses will be required to predict the fluid reactions. These analyses will be performed by a computer program that is a complex treatment to fluid motion in a matrix through Navier-Stokes equations, developed under NASA Contract.

Also, the transients following shutdown of the booster stage are of concern due to the effect of established flow field within the tank, slosh waves, and structural "springback" that could occur at booster shutdown.

Low g

There have been several investigations of low-g fluid behavior. Most of these investigations were primarily analytical using model test data and stage development and test data to validate the analytical models. Several of these analyses are based on computerized Navier-Stokes matrix solutions using iterative computer programs and empirical boundary layer equations. However, most of the studies have resulted in dimensional analysis using modified Rayleigh number and other dimensionless groups that are solved either by computer programs or closed-form approximations.

An example of the correlations is shown in FIG 32, indicating the nature of the boundary layer dependence on modified Rayleigh number. Model tests used to develop the example correlation employed non-cryogenic fluids to simulate modified Rayleigh number at $a/g_o = 1$.

According to these relationships for the low g environment, the current LH_2 tankage should be within the laminar boundary layer

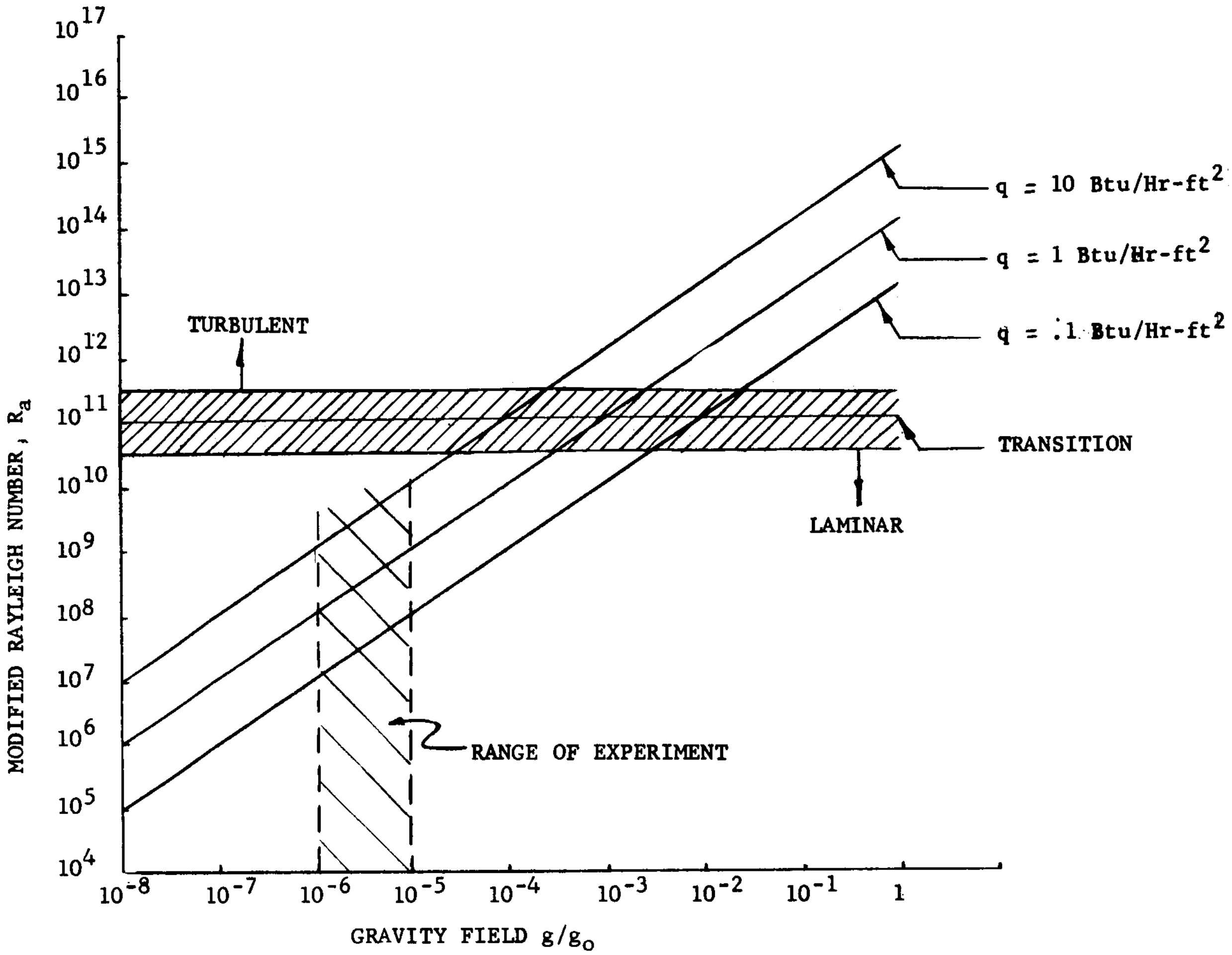

FIG 32 MODIFIED RAYLEIGH NUMBER VS GRAVITY FIELD

regime. Model tests were run at $a/g_o = 1$ but with fluid properties that produce a modified Rayleigh number within the laminar region. However, tests indicate a dependence of Prandtl number, which was not simulated.

Due to the time required for boundary layer development, drop-tower tests are insufficient to demonstrate the processess involved, FIG 33.

The resultant effect on stratified propellant is then correlated by other dimensional groups, which include the effects of geometry and heat load distribution.

One such correlation equation is shown in FIG 34, along with test data at $a/g_o = 1$. The corresponding equations were derived using simplifying assumptions of no perturbation or effects from ullage gas/liquid heat and mass transfer.

Another problem is that of the curvature of the liquid-vapor interface in a low-gravity field. Techniques are available for determining the shape of a liquid meniscus under a reduced-g environment as a function of g, liquid properties, and container geometry. The meniscus shape may have a significant effect upon thermal stratification due to the flow fields, and through mass and heat transfer at the gas-liquid interface. This effect cannot be simulated at $a/g_o = 1$; one typical profile is shown below.

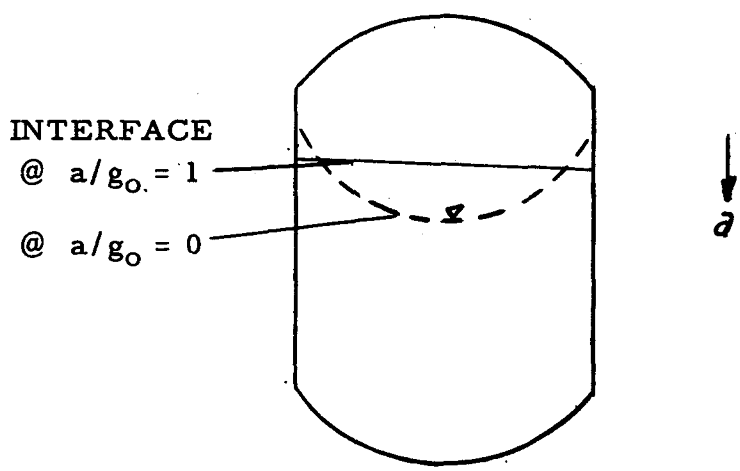

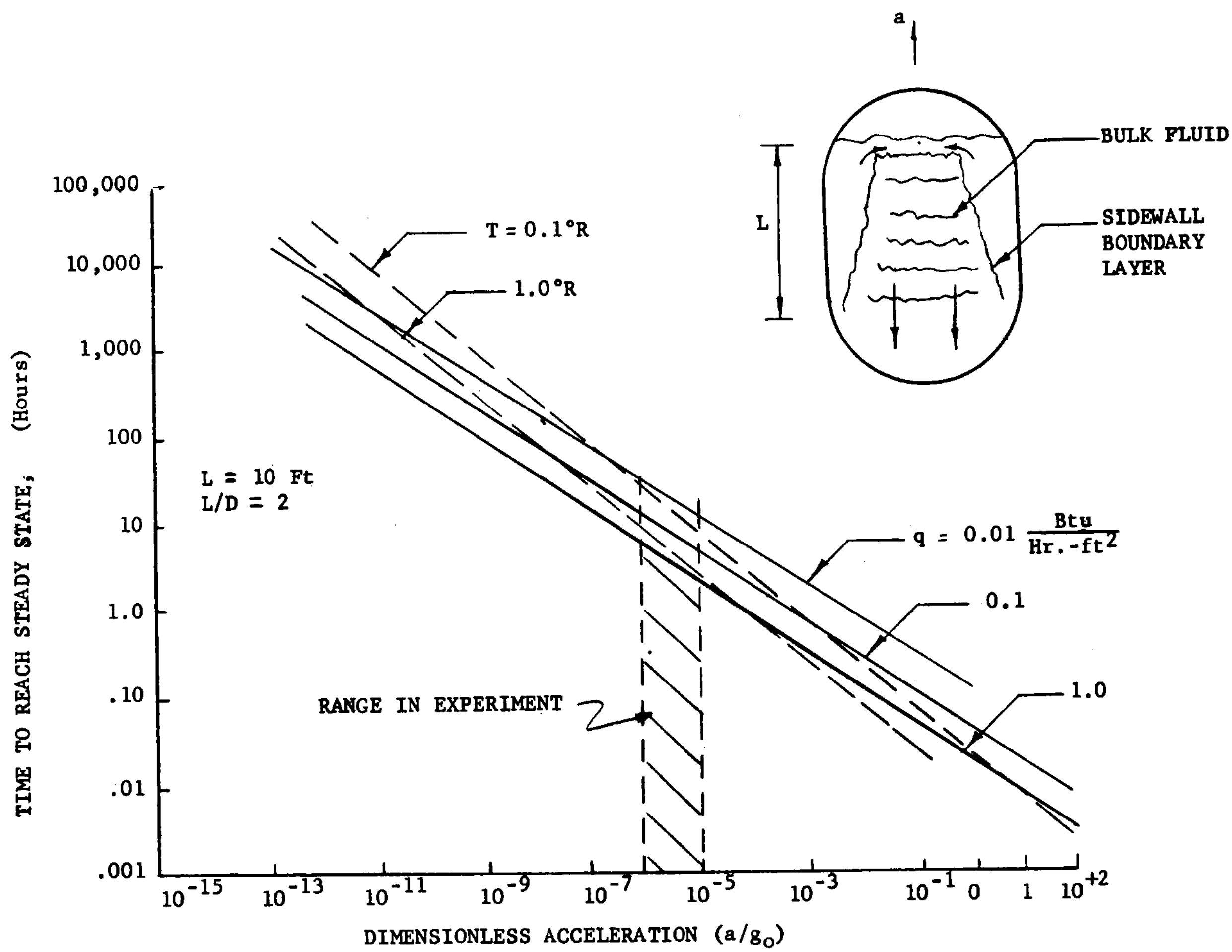

FIG 33 BOUNDARY LAYER DEVELOPMENT TIME

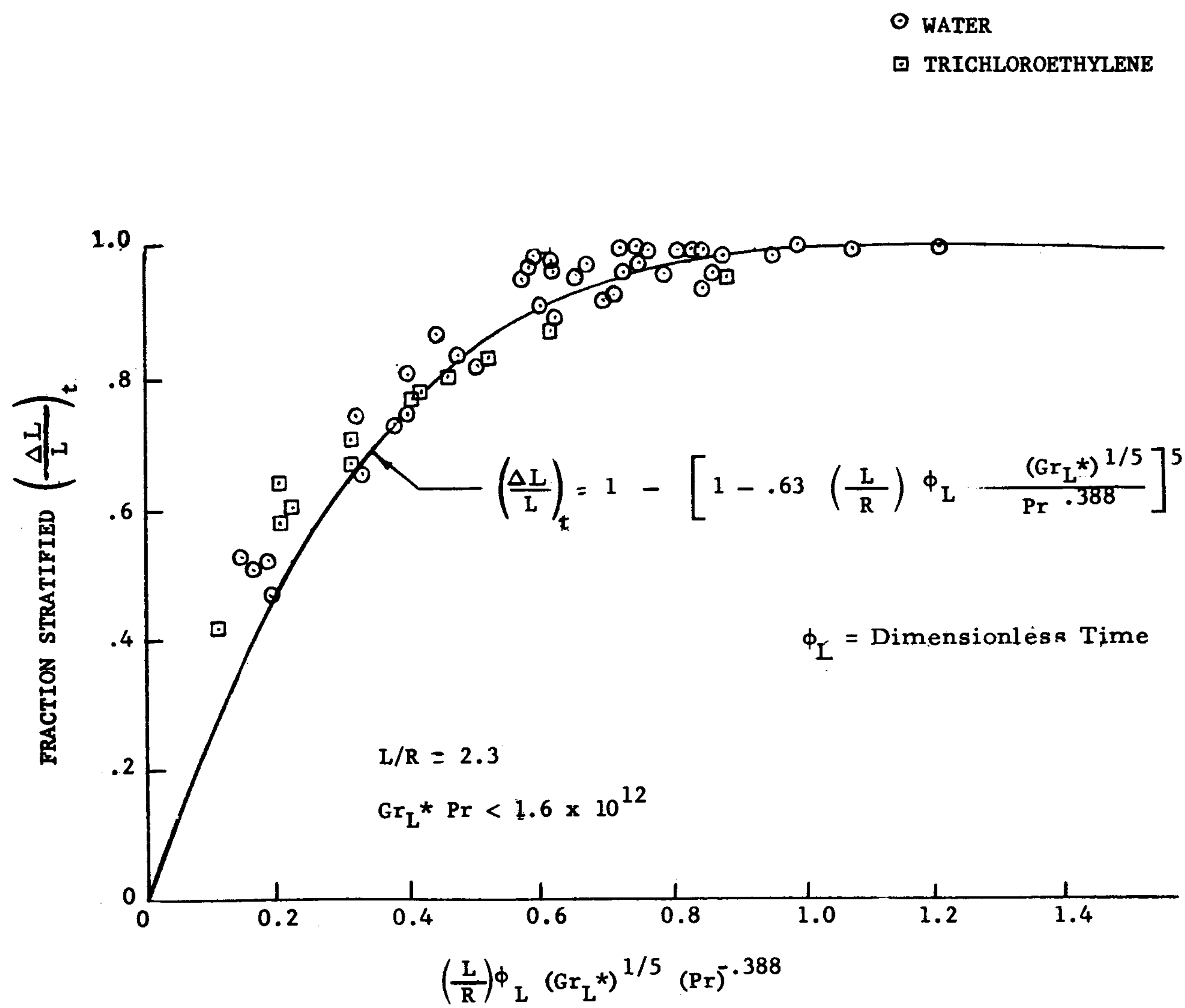

FIG 34 COMPARSION OF OBSERVED & PREDICTED STRATIFIED LAYER GROWTH

Also, bottom heating can have a significant affect on the stratification process. Present models assume that heating from below produces uniform mixing in the fluid bulk. However, as the gravity level is reduced, the tendency for this complete mixing to occur should diminish. In fact, when the gravity level is quite low, the Rayleigh number may be of the order of magnitude of 1000 or less, and the primary mode of energy transport is conduction from an unstable bottom layer that is hotter than the bulk above it. See FIG 35.

Following completion of short-term test objectives, an objective of this experiment will be to impose small heat loads and acceleration forces on the propellant in the HPI tank in order to verify the validity of the several correlations listed above.

This experiment will also include the operation of a stratification reduction device, as shown in FIG 31. A technology program is currently underway to define mechanical mixing devices that would meet the requirements of a long-term storage cryogenic tank.

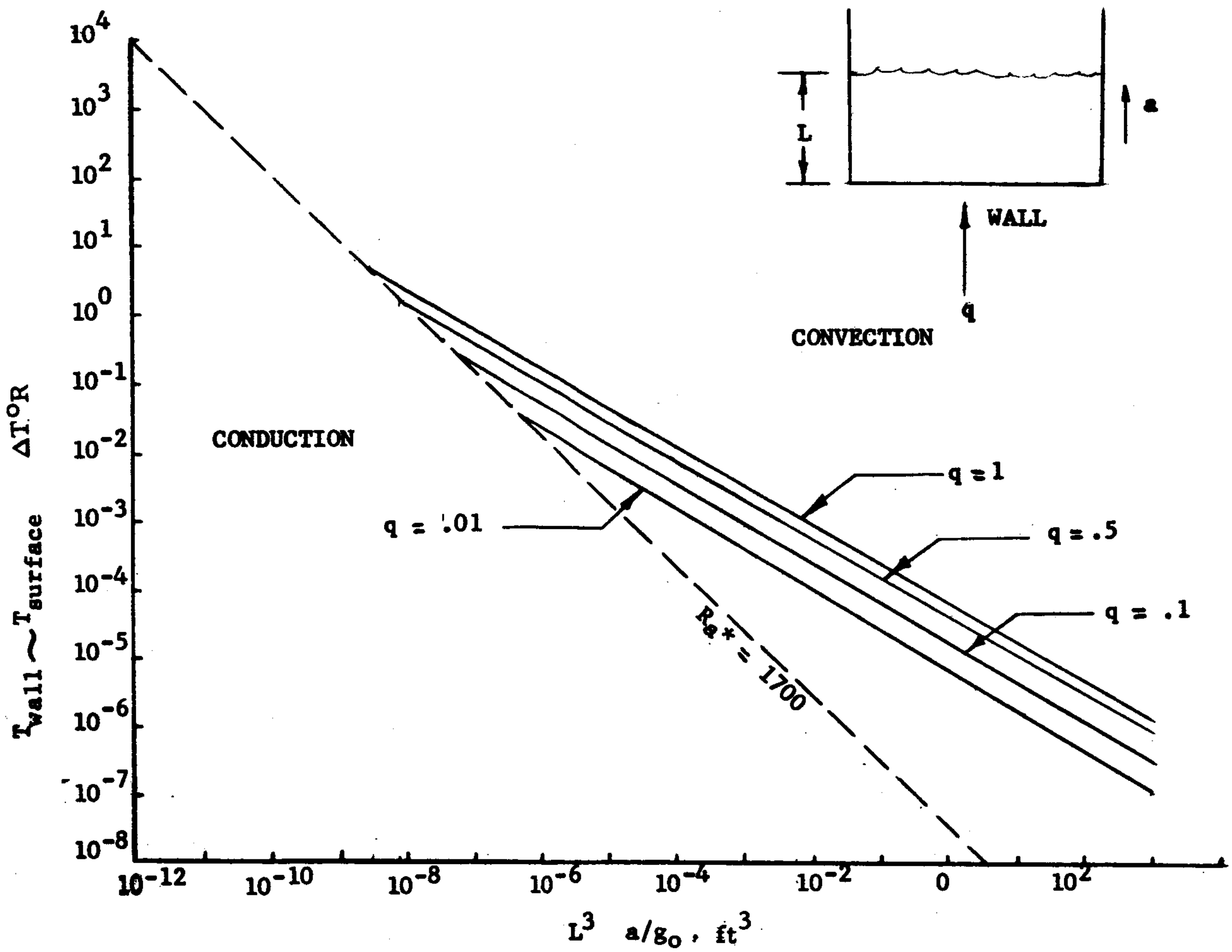

FIG 35 STRATIFICATION RESULTING FROM BOTTOM HEATING

Venting - Heat Exchanger Vent System

The heat exchanger system is designed to operate with either gas or liquid and is, therefore, independent of the local fluid quality. Basically, the vent fluid is throttled to a low pressure and temperature and allowed to exchange heat with the tank fluid before being vented overboard. Assuming a sufficient amount of heat transfer to evaporate all of the liquid originally present in the vent fluid and sufficient heat transfer on the tank side to condense the equivalent quantity of gas, the net effect on the tank pressure is the same as for all-gas venting. A schematic and a T-S diagram of the basic concept are shown in FIG 36.

There have been a number of reports published covering analysis and testing of the basic system concept. The steady-state performance of the system has been demonstrated under one g using Freon-12 (Reference 7) and hydrogen (References 8 and 9); the hydrogen flow rates ranged from 0.07 lb/hr to 6.4 lb/hr. The testing performed at Beech Aircraft (Reference 9) included cycling of the system heat exchanger inlet from gas to liquid and vice versa. Only gas was observed at the heat exchanger outlet; however, it was felt that due to the location of the liquid detection devices, a true indication of whether or not liquid occurred at the exit was not obtained. The testing did point out the need for highly refined techniques when using LH_2, since the very low temperatures involve high possibility of extraneous heat leakage.

This testing was performed using fixed throttling valves sized for gas or liquid heat transfer on the tank side by natural convection. In actual low-g operation, a single valve is desirable for controlling the throttling process when the inlet can be alternately gas and/or liquid If a fixed throttling device were used, the flow rate when operating with a liquid inlet would be approximately seven times that with a gas inlet, and since the valve would need to be sized for the gas case and the heat exchanger for the liquid case, the heat exchanger would need to be large enough to evaporate approximately seven times the nominal rate required. Both Air Research (Reference 10) and Beech (Reference 9) have proposed the use of a regulator to control the pressure in the heat exchanger and provide for throttling of the vent fluid. If the heat exchanger were designed for low pressure drop and a fairly high outlet temperature, fluid conditions out of the heat exchanger would be fairly constant, regardless of the condition of the inlet fluid, and flow control could be accurately maintained downstream of the heat exchanger by a valve sensing tank pressure.

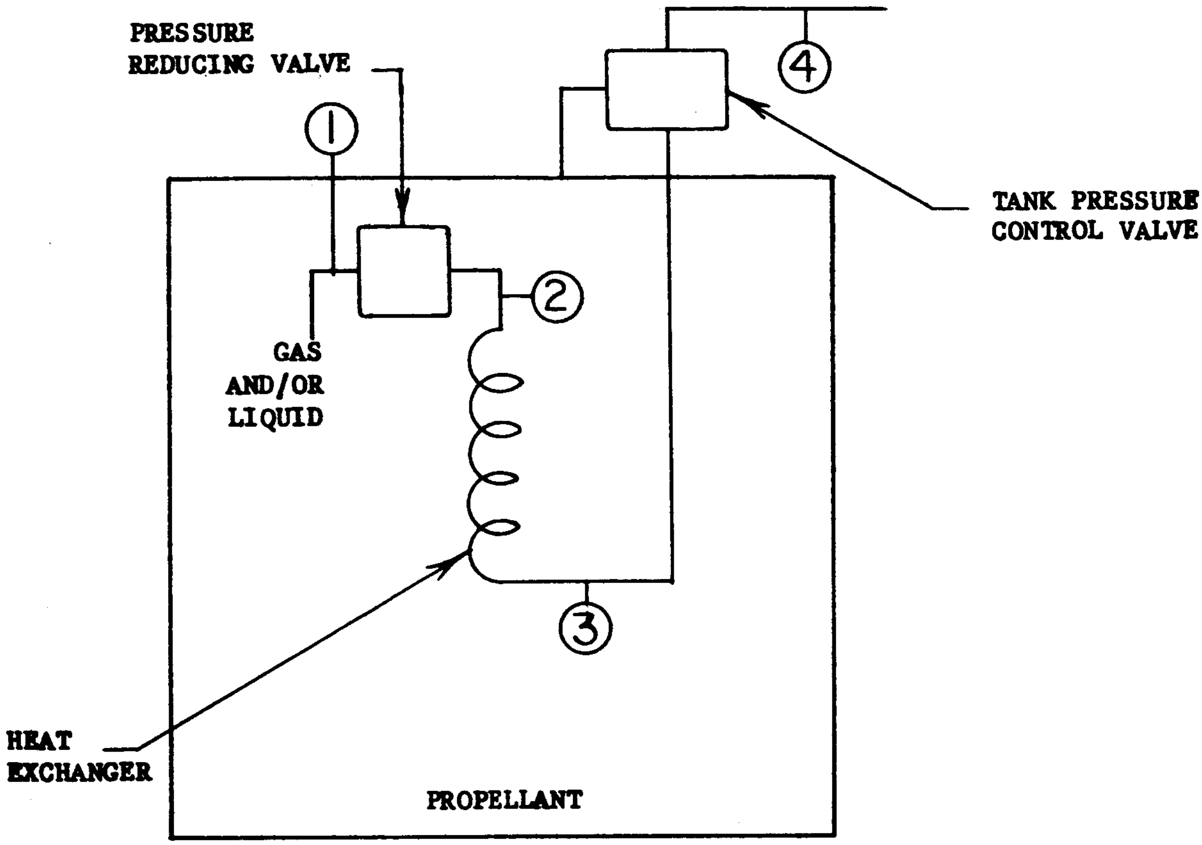

SCHEMATIC

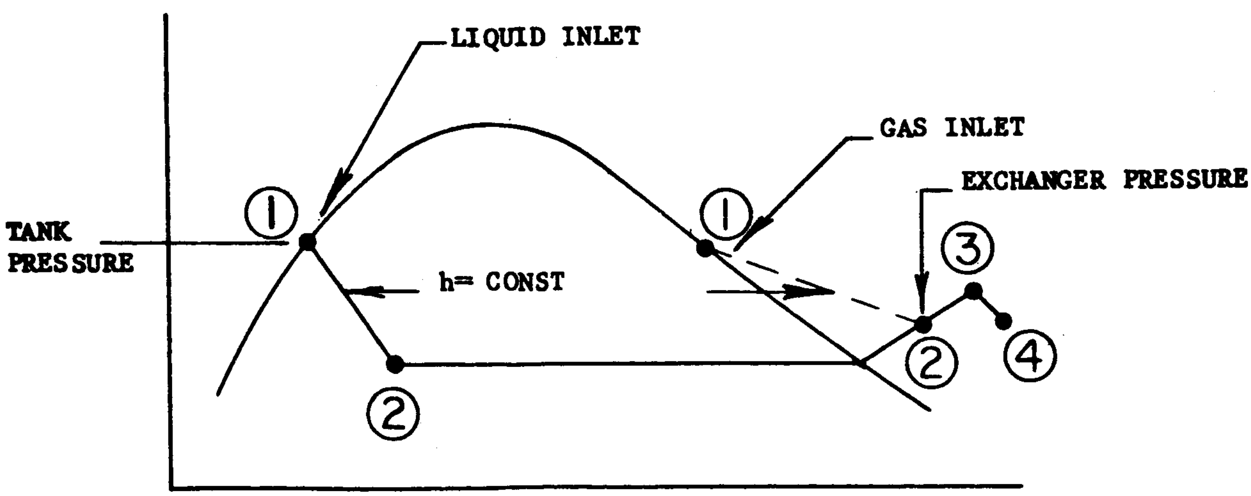

CYCLE DIAGRAM

FIG 36 Heat Exchanger Vent System

Recently, testing was performed at Convair (under a company-funded program) on a system using a downstream pressure regulator as a throttling valve with a fixed restriction downstream of the heat exchanger (Reference 11). The test fluid was Freon-12. The system inlet was cycled from gas to liquid and vice versa with no observable transient loss of liquid, even with the system adjusted for essentially saturated gas outflow (no superheat) at stabilized conditions. The vent flow rate remained essentially constant for a constant tank heating rate regardless of the inlet fluid condition (gas or liquid) during cycling. A standard regulating valve was used for the tests. It was concluded that no serious problems need be expected in a flight system with respect to this component.

A further consideration for system operation at low-g is the heat transfer requirement on the tank side. For the g levels and vent rates normally involved, it is estimated that relying on natural convection heat transfer will require very large heat exchangers. It has been proposed to increase the tank-side heat transfer by using a turbine-driven pump to circulate tank-side fluid through a plate-fin type of exchanger, using the vent gas from the exchanger outlet to drive the turbine (Reference 10).

Conclusions on the present state-of-the-art are:

1. The feasibility of the basic heat exchanger vent system concept has been demonstrated.
2. Operation of the system with hydrogen at low-g needs further evaluation with respect to heat transfer and system transients resulting from venting initiation with liquid hydrogen at the inlet or sudden changes in the vent inlet quality, when a vent-gas-driven turbine is employed for fluid circulation.

During the course of the overall study, several heat exchanger concepts were considered; each iteration included a higher level of refinement. The data presented in this section represent the initial analysis that was developed for comparison purposes only. Subsequent sections refine the results given.

From a review of the available literature and the requirements of the S-IVB and Cryogenic Service Module, a system model consisting of the following components was chosen for the present analysis.

1. Heat exchanger.

2. Circulating pump to circulate sufficient tank fluid over the heat exchanger to provide the necessary heat transfer.

3. Pump drive, which can be a turbine using the vent gas or an auxiliary power source such as an electric motor.

4. Throttling regulator to reduce the vent fluid pressure and temperature and provide a fairly constant pressure in the heat exchanger for gas and/or liquid inlet conditions.

5. Tank pressure control valve, which can be an on-off relief device sensing tank pressure or a continuous regulating vent device sensing tank pressure.

REFERENCES

CRYOGENIC PROPELLANT STORAGE

1. Lockheed Independent Development Program for Multilayer Insulation Systems, Lockheed Missiles and Space Company Report No. LMSC-A650201, May 21, 1964

2. Development of Techniques for Insulation Wrapping of Cryogenic Containers, Fourth Quarterly Progress Report, Contract NAS8-11042, May-July 1964

3. Development of Thermal Protection System for a Cryogenic Spacecraft Module, LMSC Report A703794, October 15, 1964

4. Liquid Propellant Losses During Space Flight, Arthur D. Little, Inc., Report No. 65008-00-03, July 1963

5. High Performance Insulation System Development, Douglas Aircraft Company Report SM-48806, October 1965

6. Cryogenic Thermal Control Experiment, General Dynamics Fort Worth Division, Presentation to MSFC October 28, 1964

7. Salvinski, R. J.; Friedlander, D. I., et al.: Advanced Valve Technology for Spacecraft Engines, Report 8651-6033-SCOOO, Vol II, TRW Space Technology Laboratories Contract NAS 7 - 107, 19 July 1964

8. Kloepfer, W. W.: Liquid Hydrogen Heat Exchanger. General Dynamics/Convair Report 55D-388, August 1960

9. Roos, G. E., et al.: Electrothermal Engine Propellant Storage and Feed System Study, Phase II. Beech Aircraft Corp., NASA Report CR-52, May 1964

10. Fleming, W. T., et al.: Liquid Hydrogen Storage Vessel Relief System for Zero Gravity Operation. AiResearch Manufacturing Co, Report M-754-R, 26 July 1960

11. Start, J. A.; and Casebolt, R. W.: Zero-G Vent Program. General Dynamics/Convair Report GD/C-ERR-AN-811, December 1965

APPENDIX C

PROPELLANT TRANSFER

The primary purpose of the propellant transfer experiment is to provide experimental data required to design orbital transfer systems that guarantee optimized propellant usage. To achieve this goal, the experiment must include sufficient transfer tests to isolate effects of each major factor that influences the propellant transfer. Cursory analysis has determined these influence factors to be transfer mode, gravity level, transfer time (flowrate), venting, and baffling effects. Other influence factors, such as "suction dip," vehicle attitude perturbations, etc., appear to be inherent factors in each transfer test, thereby negating the requirement for individual testing. With these assumptions, the matrix shown in Table X establishes eight transfer tests as a minimum requirement.

Another major consideration for establishing propellant transfer experiment requirements is receiver tank size. The LEM lab, which is currently being used as the main carrier for the experiment during the definition study phase, limits the maximum tank size to a diameter of 3 feet and a length of 6 feet; however, actual tank size will be dependent on chilldown fluid requirements, transfer rates, propellant settling times, and "suction dip." The results of preliminary studies of these parameters is discussed in the following paragraphs. In general, the studies indicate that receiver tanks with diameters of 3 feet, L/D of 2, and wall thickness of 0.03 inches are satisfactory for the experiment, although larger tanks will probably be desirable if space is available.

FIG 37 shows the percentage of propellant received by a hot propellant tank from a supply tank of the same fluid mass capacity. It is shown that for tank diameters above 3 ft. (L/D = 2) and flight type wall thickness, about 95% of the

TABLE X

TRANSFER TESTS CONDITIONS

Test	Transfer Mode		Receiver Tank Entrance			"g" level		Vent		Time	
	Pump	Pressure	Baffle	Nozzle	Normal	g_1	g_2	Yes	No	< 5 min	> 5 min
1	X			X			X		X	X	
2		X	X			X			X	X	
3	X		X				X		X	X	
4		X	X			X		X		X	
5	X		X			X			X	X	
6		X			X	X		X		X	
7		X	X			X			X		X
8		X*			X	X		*	*		X

* Pressure transfer liquid "slugs," allow maximum childown with vents closed, cycle vents to reduce pressure and repeat entire procedure.

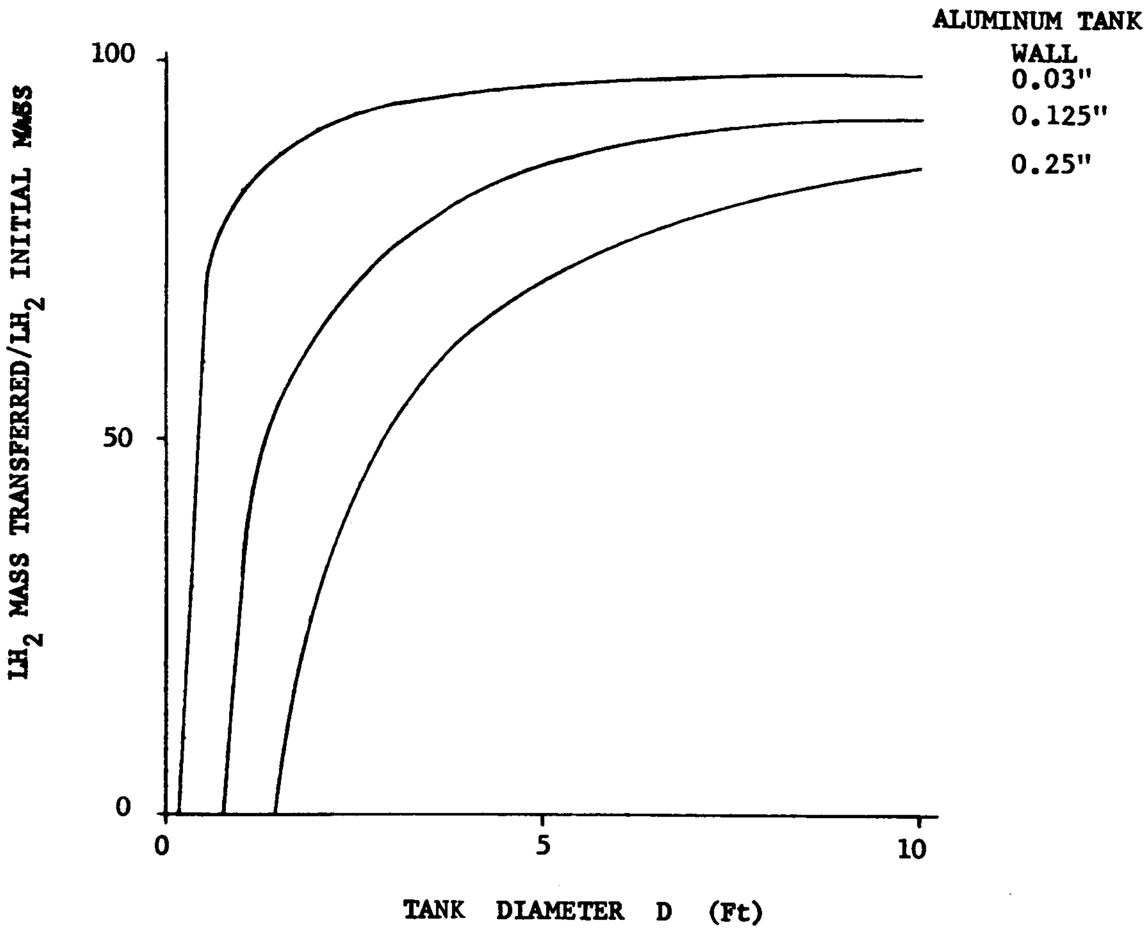

FIG 37 USABLE LH_2 MASS TRANSFERRED VERSUS TANK SIZE

transferred propellant (LH_2) is retained in the receiver tank. FIG 38 shows the condition for a LOX transfer to be less because the product $(\lambda\rho)$ LOX ≈ 7 $(\lambda\rho)$ LH_2.

For the LH_2 transfer experiments, the transfer tanks may be replenished from the cryogenic storage test tank between transfer tests. However, the complexity of this operation and the excessive loss of LH_2 may prohibit this transfer. A more attractive approach appears to be maximum utilization of the initial propellant with a continuing decrease in the quantity that is transferred during a test. FIG 39 shows the amount of LH_2 required to childown a tank with a diameter of 3 feet, L/D of 2, and wall thickness of 0.03 inch as a function of initial wall temperature. By heating the walls to 350°R (maximum) between transfer tests, only 7.8 pounds of LH_2 are required to childown the tank during a transfer test. Other propellant lost during a transfer test will result from suction dip since this propellant must be evaporated prior to the next test when LH_2 is transferred back to that tank. FIG 40 shows maximum suction dip as a function of tank diameter at various acceleration levels. Although the quantity of propellant left in the tank is difficult to estimate, the amount can be minimized by proper design of tank bulkheads and drain lines. It has been assumed that 5 pounds of LH_2 residuals will result from suction dip during each transfer test. Under these conditions, FIG 12 shows the amount of propellant that can be transferred during each of the eight required transfer tests without replenishing between tests.

The power requirements for heating the receiver tank between transfer tests can also be reduced by limiting wall temperatures to 350°R (maximum). As shown in FIG 41, approximately 0.44 kW hr of energy is required to heat the receiver tank from 40°R to 350°R. In addition, 0.28 kW hr of energy is required to evaporate the 5 pounds of LH_2 residuals after each test. For the minimum of eight transfer

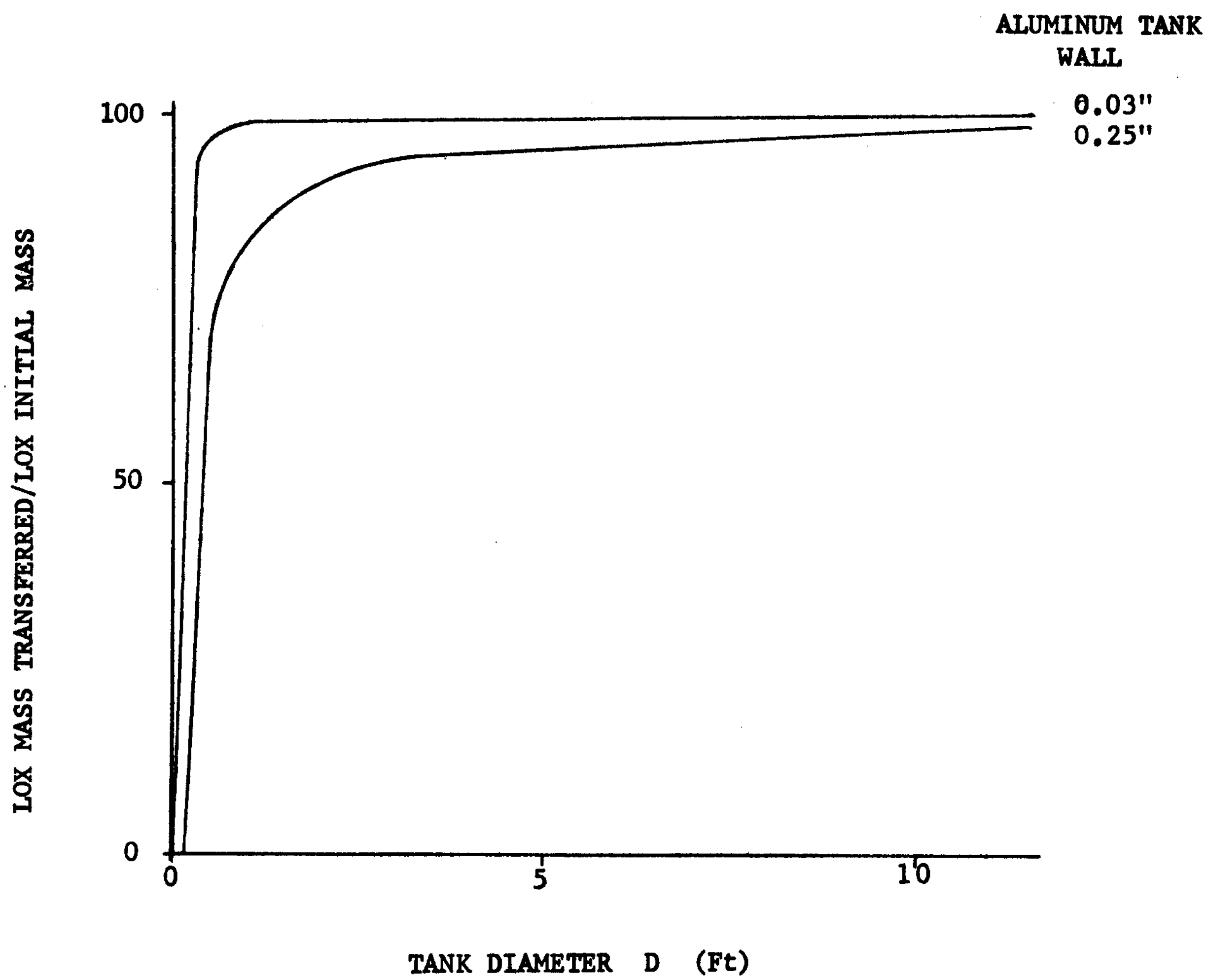

FIG 38 USABLE LOX MASS TRANSFERRED VERSUS TANK SIZE

CONDITIONS:
(1) DIA = 3 ft
(2) LENGTH = 6 ft
(3) WALL = 0.03 inches

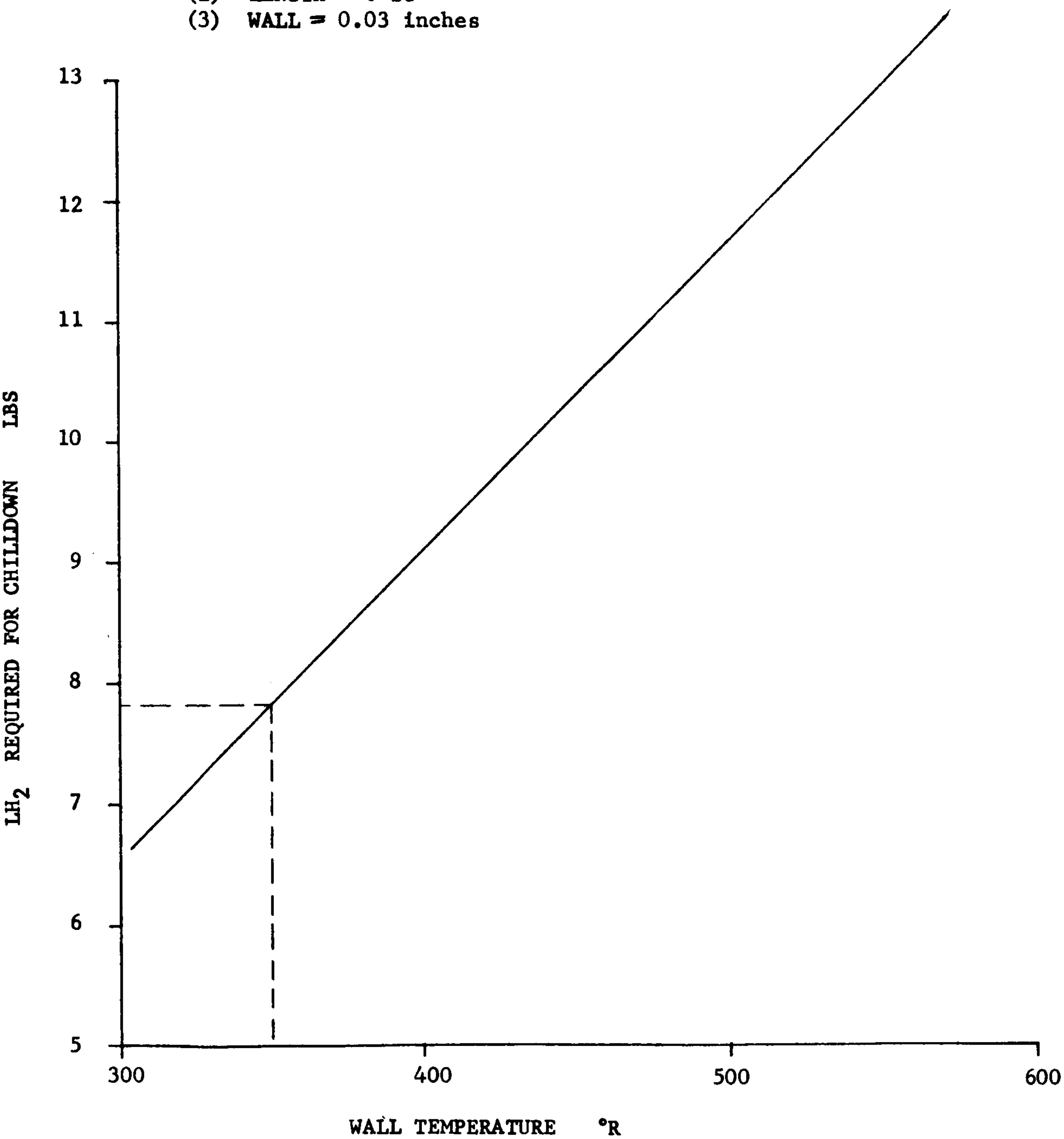

FIG 39 LH_2 CHILLDOWN REQUIREMENTS

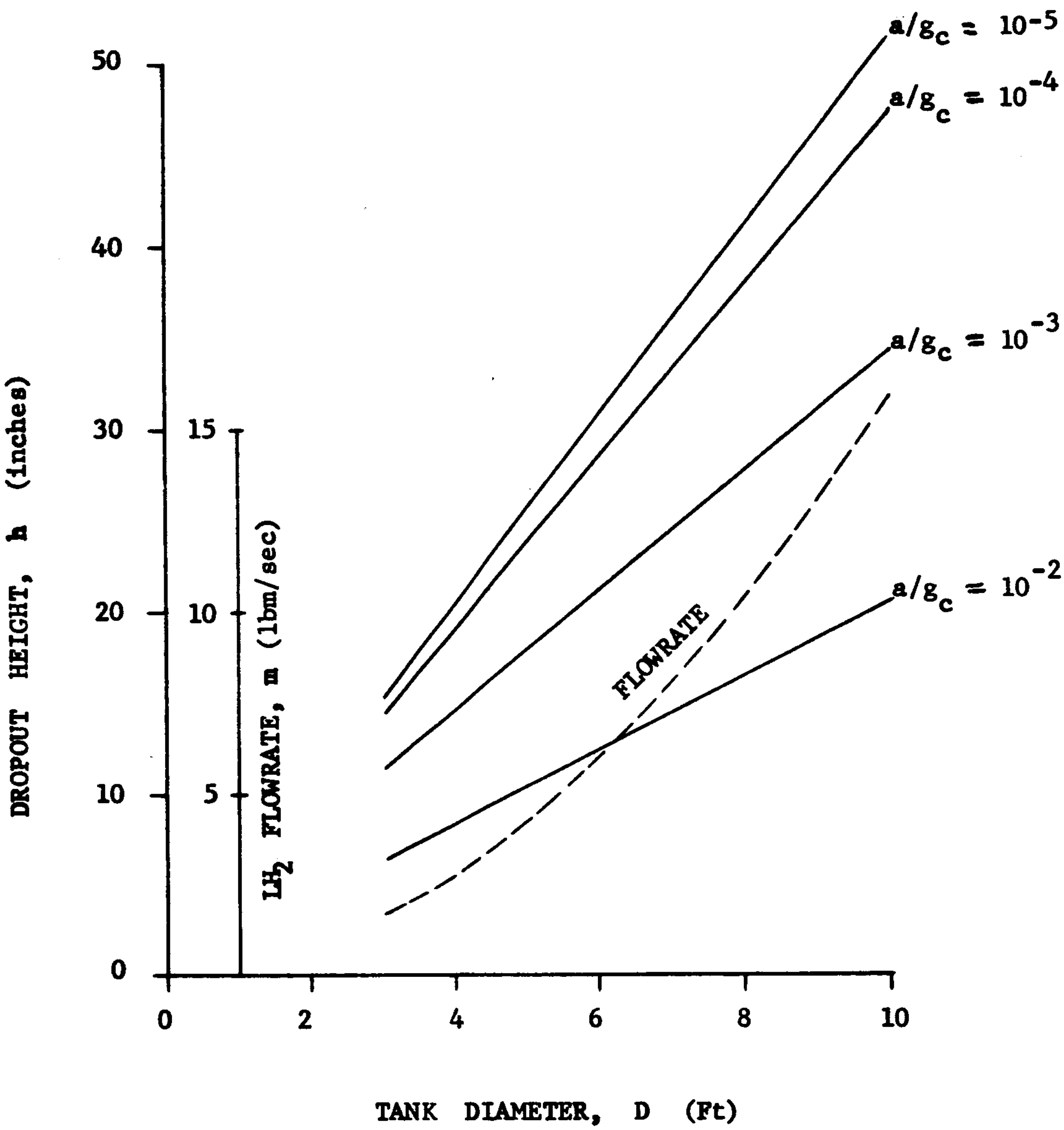

FIG 40 THEORETICAL "SUCTION DIP" HEIGHTS

ASSUMPTIONS:
(1) T_i WALL = 40 °R
(2) D = 3 ft
(3) L = 6 ft
(4) t = 0.03 in.

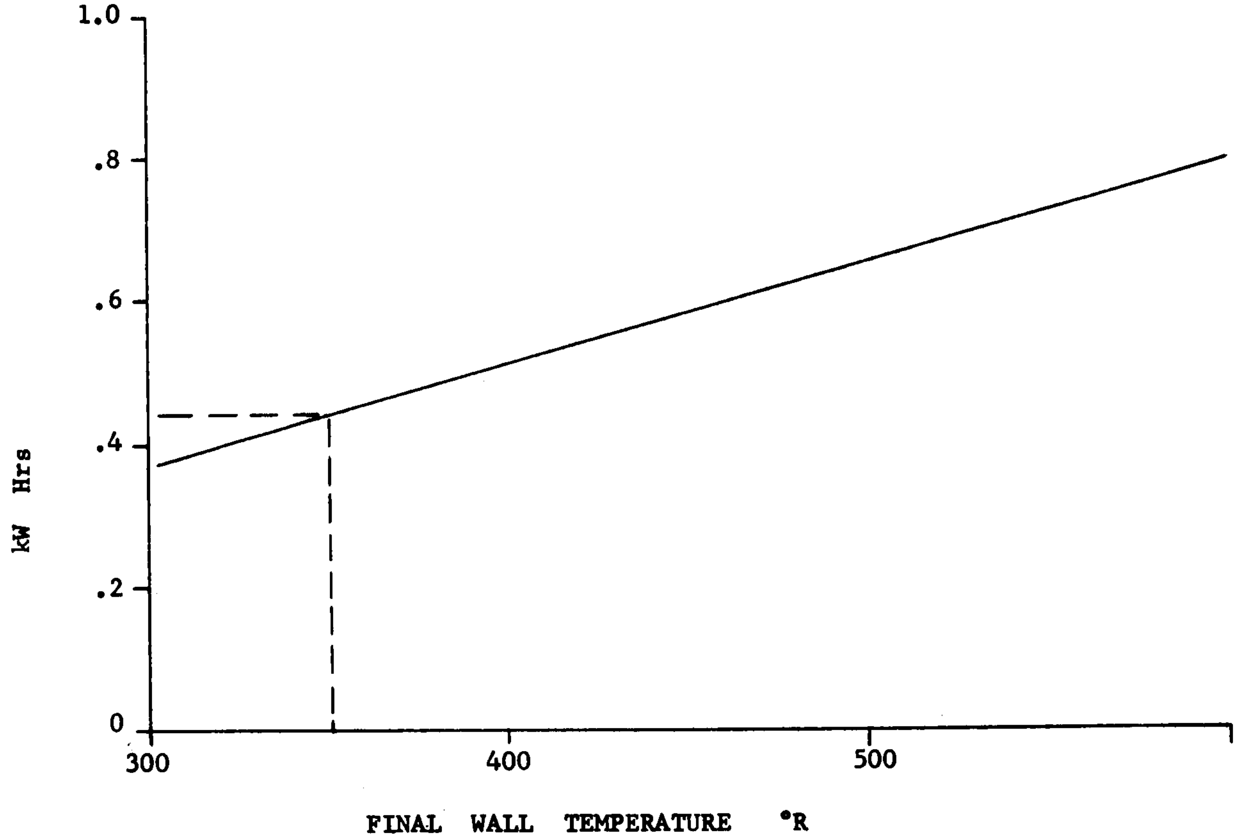

ENERGY REQUIRED TO HEAT WALLS

FIG 41 POWER REQUIREMENTS FOR RECEIVER TANK HEATING tests, this cycle must be repeated seven times requiring a total of 5 kW hr.

Transfer times will probably be determined by optimization of linear acceleration requirements. Assuming that transfer rates are comparable to S-IVB loading rates on the basis of wetted area to volume ratio, FIG 42 is derived. It can be seen that reasonable transfer times (above 100 sec.) are obtained with tank sizes above 3 feet affording ample steady state time for vent and transfer system operation. At this tank size and at approximate S-IVB normalized transfer rates, existing LH_2 pumps can be used (S-IVB recirculation chilldown pump). Approximate flowrates for each transfer test are shown in Table XI.

Another consideration for designing the LH_2 transfer tanks is maximum tank pressure occurring during propellant transfer, especially since propellants will be transferred under nonvent conditions for some tests. FIG 43 shows maximum pressures in a nonvented tank assuming a 5% final ullage and thermodynamic equilibrium. However, it must be realized that higher pressures may result during transfer operations since ullage compression rates can foreseeably exceed vapor condensation rates. Further analysis is necessary before the transient pressures can be predicted. However, equilibrium pressures in a nonvented tank are sufficiently low to encourage attempts to reduce transient pressures during transfer. One method of reducing transient pressure is to increase transfer time. Hence, test 7 (see Tables X and XI) will be a low transfer flowrate over an extended transfer time to investigate this procedure.

Another attractive method for reducing transient pressures is "slug" transfer, whereby a slug of liquid is introduced to the receiver tank with the vents closed; standby lasts until this slug disperses and the vents are cycled to reduce pressure. The procedure is repeated until receiver tank chilldown is achieved. Then the tank is vented to an arbitrary low pressure, the vents are closed, and continuous propellant transfer is initiated. Low transient pressures

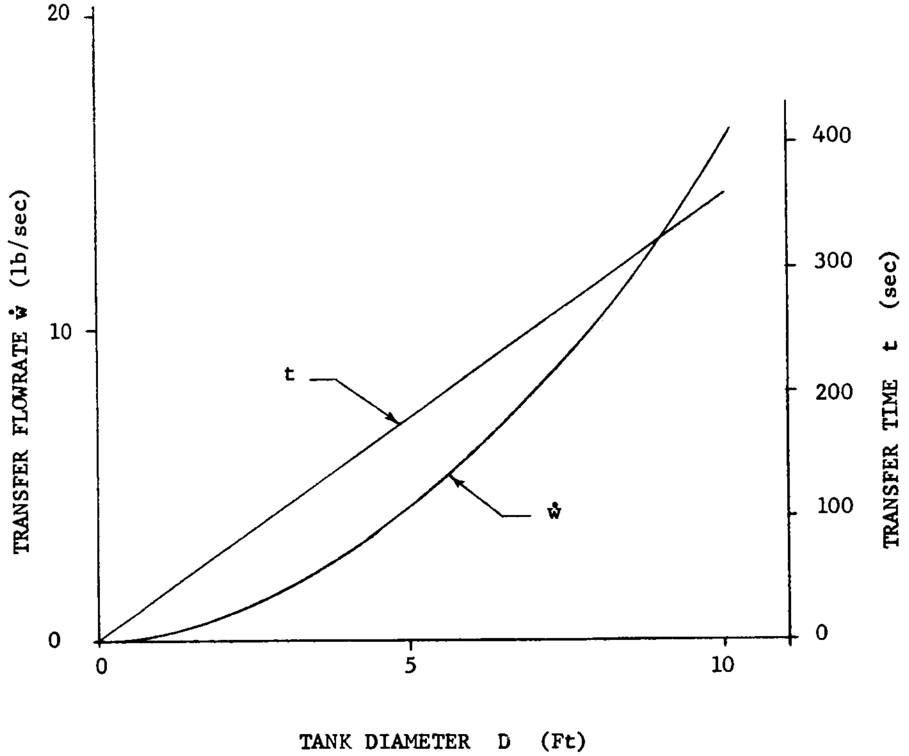

FIG 42 TRANSFER TIME AND FLOWRATE ESTIMATES

TABLE XI

PROPELLANT UTILIZATION

Test	Propellant Transferred (lb)	Transfer Rate (lb/sec)	Transfer Time (sec)
1	153	1.0	153
2	135	1.0	135
3	122	1.0	122
4	109	1.0	109
5	96	1.0	96
6	83	0.8	104
7	70	+	+
8	57	*	*

+ Minimum flowrates

* "Slug" transfer - see footnote of Table X for details

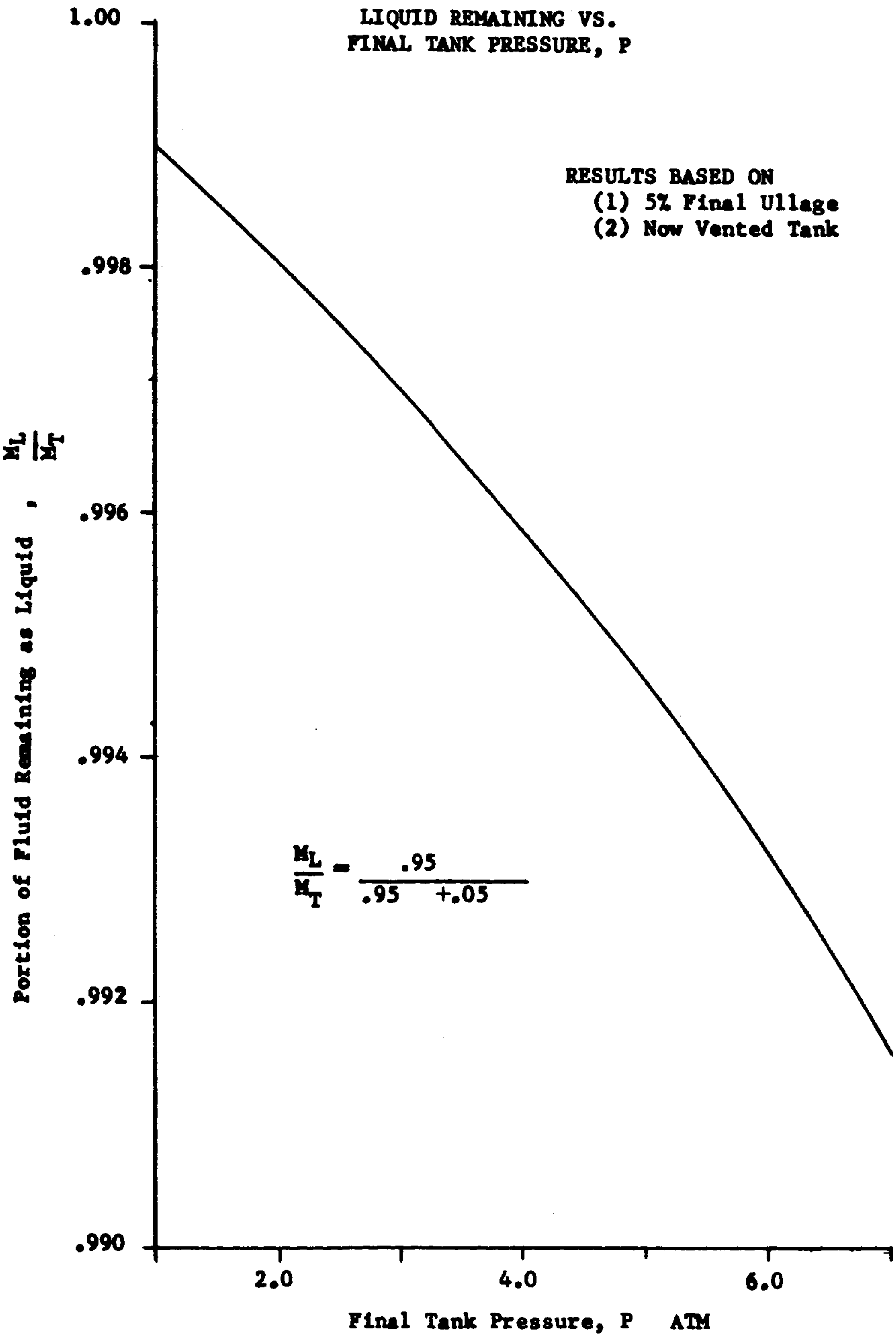

FIG 43 FINAL THERMODYNAMIC EQUILIBRIUM PRESSURE VERSUS USABLE LH_2 MASS

should exist since minimum tank cooling is necessary during actual transfer. Although this procedure requires venting, no zero-g vapor separator is required since there is no liquid in the tank during venting. Test 8 (see Tables X and XI) will be utilized to extablish the effectiveness of tank childown with this procedure.

FIG 44 shows propellant settling times prior to propellant transfer. Theoretically, a three-foot diameter tank (with $L/D = 2$) results in the minimum time required to settle LH_2 with a stable interface. This required time is 150 seconds at an acceleration of 10^{-4} g's. However, experience on the Agena vehicle has indicated that complete propellant settling required six times that calculated for free fall. Using this factor, the required time to settle an 80 percent full LH_2 tank (with $D = 3$ and $L/D = 2$) is 183 seconds. The Bond Number based upon the radius for a three-foot diameter LH_2 tank at 10^{-4} g acceleration is 7.75. If the settling thrust is increased to obtain a high Bond Number for the experiment, the required settling time will be less than three minutes. FIG 44 also shows that bubbles larger than 1/4 in. diameter will clear the surface in less than the required settling time. Thus, the time required to clear the liquid of bubbles larger than 1/4 in. in diameter does not consitute a design criterion.

Table XII presents the proposed instrumentation requirements and locations for the propellant transfer experiment.

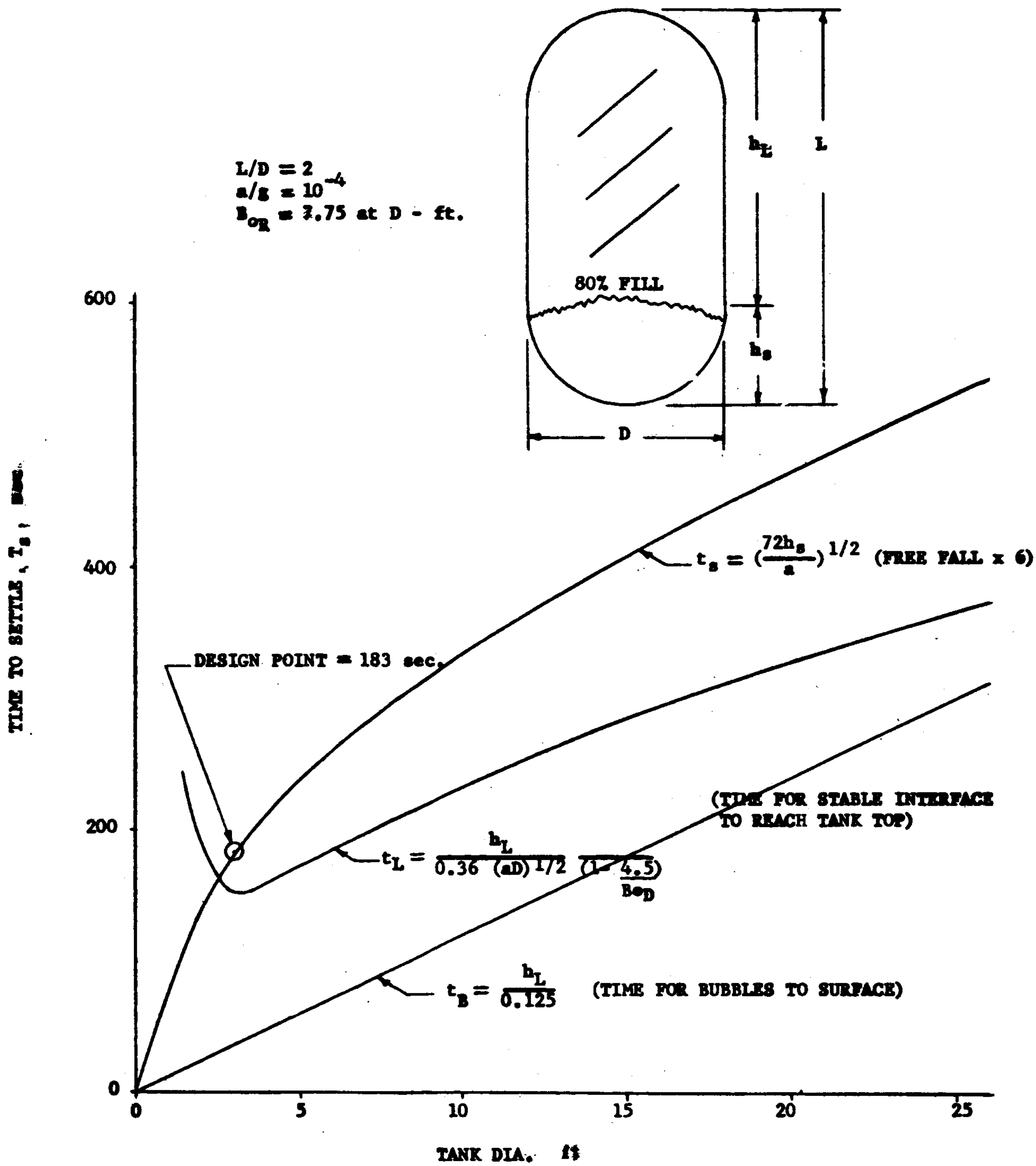

FIG 44 SETTLING TIME FOR PROPELLANT TRANSFER

TABLE XII

PROPELLANT TRANSFER INSTRUMENTATION

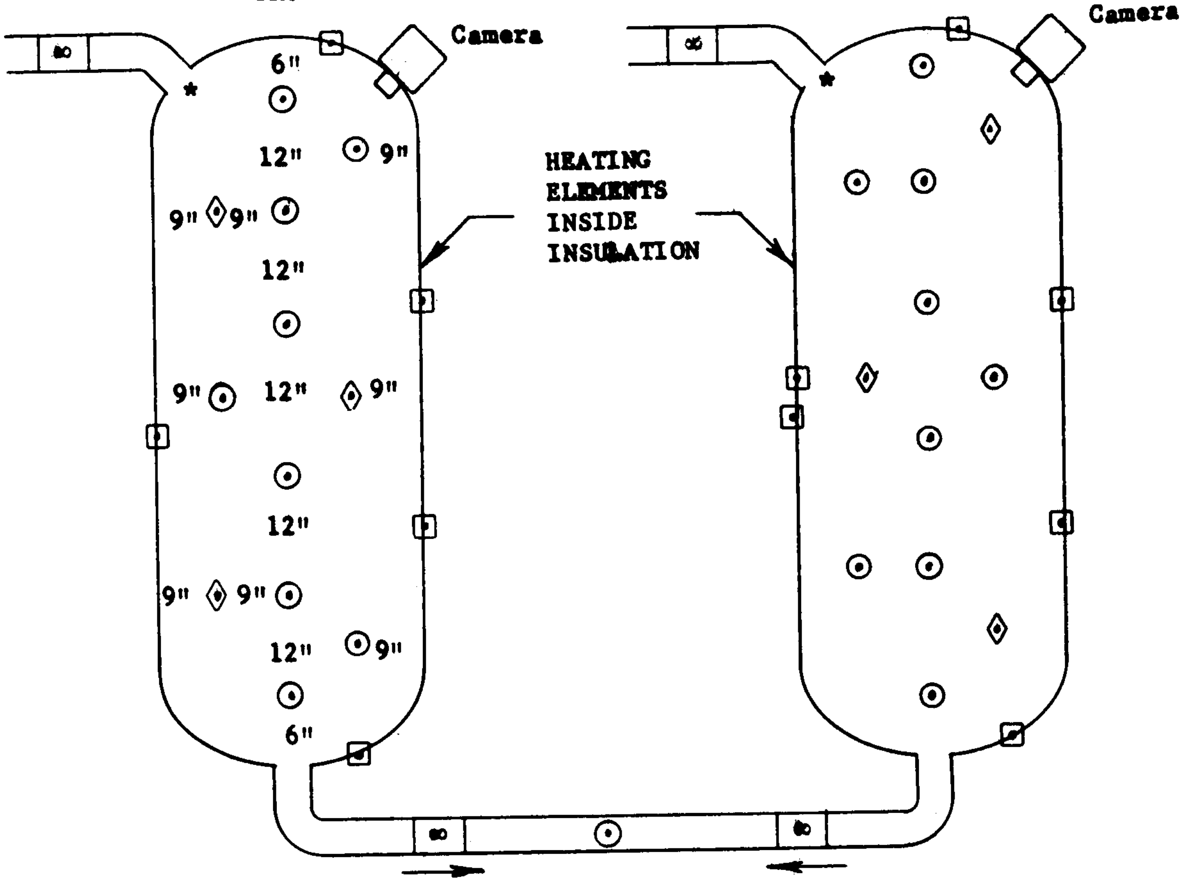

MEASUREMENTS	TYPE	RANGE	QUANTITY
Flowmeters (∞)			2
	GH_2		2
	LH_2	0-5 lb/sec	
Pressure (*)	-	0-60 psia	2
Liquid Level	Capacitance Continuous	6 Ft.	2
Temperature			
	⊡ Copper Constantan	20-400°R	10
	◊ Platinum Resistance	20-400°R	6
	⊙ Platinum Resistance	20-200°R	19
Total			43

APPENDIX D

SUPPORTING RESEARCH

Appendix D is a summation of the supporting research being performed in the area of low-g heat transfer and fluid mechanics by MSFC and other organizations throughout the nation. Also included is a listing of researchers in the pertinent areas that were consulted during the formulation of the experiments.

Contacts Established With Researchers In Pertinent Fields

Boiling Heat Transfer:	Dr. Clark Dr. Merte	U. of Michigan
	Dr. Zuber	UCLA/GE
	Dr. Siegel E. Otto D. Petrash	LeRC
	L. Manson	Rocketdyne
Nuclear Gaging:	Dr. Wright	General Nucleonics
	Dr. Han	Industrial Nucleonics
Insulation System:	D. Norad	LeRC
	Leonhardt	GD/C
	J. Elizalde	TRW
	Dr. Austin	GD/FW
Interface Configuration:	Dr. Bhuta	TRW
	Dr. Satterlee	LMSC
Propellant Transfer:	E. Otto D. Petrash	LeRC
	J. Elizalde	TRW
Stratification:	Dr. Vliet J. Tatum	LMSC
	L. Poth	GD/FW

TABLE XIII (Cont'd)

Technology	Title	Contractor	Scope	Contract No.	Term (CY) 63 64 65 66 67 68
	Ullage Gas Quality Measurement	Industrial Nucleonics	Design, fabricate, and test quality meter for low-g ullage venting		
	Study and Flight Qualified Development of Spacecraft Separation Device	GD/FW	Develop for flight a nucleonic device for measurement of separation rate, angle and distance between two stages	NAS8-11995	
	Ablation Sensor Development	Cook Electric, ERA Inc.	Development of Flight Type Ablation Sensor for Hypersonic Nose Cone Re-entry Tests		
Cryogenic Fluid Behavior					
Heat Transfer	Zero-G Heat Transfer Modes	LMSC	Study and develop analytical models for stratification in low-g, liquid/ullage coupling, and boundary layer thermal convective motion. Perform tests to verify analysis results	NAS8-11525	
	Mass Determination Under Reduced Gravity Using Nucleonic Radiation	Giannini	Study and develop breadboard nucleonic mass gaging system for LH_2 tank of S-IV size volume, to be used for filling, PU and low-g mass determination	NAS8-11311	
	Analytical Method for Prediction of Residual Cryogenic Propellant Behavior in Orbital Vehicles	GD/C	Study to develop analytical model for predicting propellant behavior subsequent to orbital injection, accounting for effects of ascent slosh energy, thermal convection boundary layer velocity, and dry wall flashing		

TABLE XIII (Cont'd)

Technology	Title	Contractor	Scope	Contract No.	Term (CY) 63 64 65 66 67 68
	Research in Low Gravity Cryogenic Fluid Boiling	U. of Mich.	Study and experimentally determine the effects of reduced gravity on the cryogenic fluid boiling phenomena utilizing various test configurations. Supply theoretical correlations to predict pool boiling conditions under low and high levels	NAS8-20228	
	Boiling Heat Transfer with LOX, LN_2, LH_2	Rocketdyne	Compile and catalogue pertinent U. S. and foreign literature on boiling heat transfer with cryogenics and assess the suitability of the available correlations. Present in a summary the recommended equations	NAS8-5337 NAS8-11367	
	Study of Zero Gravity Liquid-Vapor Separators	GD/C	Study theoretically to compare venting systems for cryogenic fluids under zero gravity	NAS8-20146	

SUPPORTING RESEARCH

In-House	MSFC	Participating Labs
Superinsulation		R-P&VE-ME
Instrumentation		R-P&VE/ASTR/TEST
Fluid Behavior		R-P&VE-TEST

Out-of-House	MSFC	Contracts
Insulation/Tank Support		11
Instrumentation		9
Cryogenic Fluid Behavior		4
Propellant Positioning		2
Venting and Reliquification		4
Thermal Protection and LH_2 Slush		2

NASA/AF/	Aerospace Co's.	Research Monitored
Insulation and Tank Supports Instrumentation		2
Cryogenic Fluid Behavior		5
Propellant Positioning		6
Venting and Reliquification		3
Thermal Protection and Slush		5
Transfer		7

TABLE XIII

Summary of Cryogenic Technology Contracts Sponsored by MSFC
(Studies, Hardware Development, and Flight Tests)

Technology Thermal Protection	Title	Contractor	Scope	Contract No.	Term (CY) 63 64 65 66 67 68
Insulation/Tank Support	Design of High Performance Insulation Systems	LMSC	Study thermal models, design data, insulation system optimization for vehicle applications	NAS8-11347	
	Structures-Cryogenic Insulation System Integration	NAA	Study multi-layer insulation performance vs payload weight, attachment designs, system concepts	NAS8-5300	
	Structures-Cryogenic Insulation System Integration	Martin	(Study parallel to above)	NAS8-5268	
	Cryogenic Insulation Research	Martin	Test and evaluate several candidate multi-layer insulation systems. Install the (2) test systems on MSFC 105" tank	NAS8-5268 (follow-on)	
	High Performance Insulation Study	DAC	Study feasibility of applying external multi-layer insulation to the S-IVB stage	NAS 7-101	
	Thermal Protection Systems for Cryogenic Propellants on Interplanetary Space Vehicles	GD/FW	Study multi-layer insulation/ tank support systems. Determine optimum systems for selected missions and vehicles	NAS8-1161	
	Liquid Hydrogen Suction Line Insulation Research and Development	GD/C	Study, design, fabricate and test alternative multi-layer insulation systems for LH_2 and LO_2 suction lines	NAS8-20167	
	Cryogenic Storage System Study (AES Payloads)	(not yet assigned)	Study and evaluate various multi-layer insulation/tank support concepts for 6 months storage of LH_2 on lunar surface	(not yet assigned)	

TABLE XIII (Cont'd)

Technology Thermal Protection	Title	Contractor	Scope	Contract No.	Term (CY) 63 64 65 66 67 68
Insulation/Tank Support	Development of Techniques and hardware for insulation wrapping of cryogenic containers	Linde Co.	Provide tooling materials and assistance for insulation of a 70" diameter tank	NAS8-11041	
	Superinsulation systems for cryogenic test tanks	Linde Co.	Provide tooling, materials and design assistance for insulation of a 105" diameter tank	NAS8-11740	
	Development of techniques and hardware for insulation wrapping of cryogenic containers	NRC	Provide tooling, test equipment, designs and application techniques for 70 and 105" diameter tankage	NAS8-11042	
Thermal Disconnects	Cryogenic storage system study (AES Payloads)	(Not yet assigned)	Study several active disconnect designs. Incorporate selected designs in thermal protection/support system mockups.	(Not yet assigned)	
Shadow Shields	Study of lightweight inflatable shadow shields for cryogenic space vehicles	GS/FW	Study requirements for and design of practical shield systems. Test candidate materials for structural reinforcement and thermal control	NAS8-11317	
LH_2 Subcooling and Slush	Slush hydrogen applications	(Not yet assigned)	Study of mission/vehicle applications for slush hydrogen	(RFP in preparation)	
Open-loop Refrigeration	Extraterrestrial cryogenic propellants reliquefaction	Marquardt	Study feasibility of using open-loop LH_2 reliquifiers for deep space missions	NAS8-5298	
	Cryogenic storage system study (AES Payloads)	(Not yet assigned)	Study the design of vapor-cooled radiation shields with and without multi-layer insulation	(Not yet assigned)	

TABLE XIII (Contd)

Technology	Title	Contractor	Scope	Contract No.	Term (CY) 63 64 65 66 67 68
Ullage Control and Venting					
Vent Gas Thrusters	Saturn IB liquid hydro gen orbital experiment	DAC/ MSFC	Perform orbital flight test on vehicle SA-203 to obtain data on performance of S-IVB continuous orbital vent and propellant settling system and engine restart	(N.A.)	65–66
Dielectrophoretic Systems	Research and Design of a practical and economical dielectrophoretic system for control of liquid fuels under low gravity conditions	(Not yet assigned)	Design, fabricate, and test system to suppress slosh, orient and separate ullage and prevent pull-through during orbital propellant transfer	(Not yet assigned)	
Centrifugal Phase Separators	Zero-Gravity Vapor-Liquid Separator for Saturn S-IVB Stage	Pesco	Design and test centrifugal separators (self-powered and electrically powered) for S-IVB continuous vent and rapid blowdown system		63–65
Mechanical Mixing Devices	Investigation of Mechanical Mixing Devices to Reduce Thermal Stratification	(Not yet assigned)	Study and develop mixer concepts. Perform parametric analysis of the mixing process in low-g. Limited small scale tests to verify analysis	(Not yet assigned)	
Liquid Quantity Sensors	Investigation and Development of R-F Liquid Level Sensing Techniques	LMSC	Experimental Program, including design, fabrication and testing of prototype units		64–66
Mass Flow Meters	Investigation and Development of R-F Liquid Level Sensing Techniques	Giannini	Design and fabricate prototype mass flow meter for ground tests of S-IVB tanking		
	Investigation and Development of R-F Liquid Level Sensing Techniques	Bendix	Design, fabricate, and test prototype mass flow meter	NAS8-5218	65–66

Table XIII (Cont'd)

Technology	Title	Contractor	Scope	Contract No.	Term CY 63 64 65 66 67 68
	Study of Mass Flowmeter Principles Based on Nuclear Radiation Techniques	Industrial Nucleonics Corp.	The objective is to study nuclear radiation methods for measurement of cryogenic mass flowrate	NAS8-20189	
	A Study of Surface Barrier Silicon Detector	Oak Ridge Technical Enterprises	To Provide a Ten Channel LH_2 Point Density System using Beta Sources and Silicon Detectors	NAS8-11080	
	A Prototype Cryogenic Density Measuring System	Franklin GNO Corp., W. Palm Beach, Florida	To Develop a Portable cryogenic density measuring system using Ionization type detectors and x-rays as the radiation source	NAS8-11710	

Table XIV
Summary of Cryogenic Technology Contracts Sponsored
by non-MSFC Groups
(Studies, Hardware Development, and Flight Tests)

Technology Thermal Protection	Title	Contractor	Scope	Sponsor	Contract No.	Term (CY) 63 64 65 66 67 68
Insulation/Tank Support	Development of Thermal Protection System for a Cryogenic Spacecraft Propulsion Module	LMSC	Design, fabricate, insulate, and test 82.6" spherical tank	LeRC	NAS3-4199	
	System Effects on Cryogenic Propellant Storability and Vehicle Performance (Phase VI, VIII)	DAC	Study various multi-layer insulation/tank support systems (Phase VI), design, fabricate, insulate, and test 74" cyl, LH_2, LN_2 tanks (Phase VIII)	AFRPL	AFo4(611)10750	
Thermal Coatings	System Effects on Cryogenic Propellant Storability and Vehicle Performance (Phase IV)	DAC	Study available candidate coatings. Apply selected optimum coating to test apparatus	AFRPL	AF04(611)10750	
LH_2 Subcooling and Slush	Research on Rheologic and Thermodynamic Properties of Solid and Slush Hydrogen	Linde	Laboratory studies of LH_2 slush properties and characteristics	AFAPL	AF33(657)10248 AF33(657)11098	
	Liquid-Solid Mixtures of Hydrogen Near the Triple Point	NBS	Laboratory studies of methods for production, storage, and pipeline transport of slush H_2	NASA-KSC		
	Production and Rheology of Fluid Hydrogen Slush	AFAPL	Engineering study of production and handling methods, utilizing 1000 gal. production tank and (2) 500 gal. storage tanks	AFAPL	(In House effort)	
Open-loop Refrigeration	Development Study of Vent Gas Heat Exchangers (Vapor cooled shields)	LMSC	Study and test vapor-cooled radiation shields inserted within multi-layer insulation	LMSC	(In house ID effort)	

Table XIV (Cont'd)

2

Technology	Title	Contractor	Scope	Sponsor	Contract No.	Term (CY) 63 64 65 66 67 68
Ullage Control and Venting						
Vent Gas Thrusters	Hydrogen-Oxygen Catalytic Reaction Control System	NAA	Study and test application of cryogenics to secondary propulsion systems	LeRC		
Dielectrophoretic Systems	Design Study of a Liquid Oxygen Converter for Use in Weightless Environments	Dynatech	Study, design, fabricate test apparatus for KC-135 flight tes.	WP AFB	AF33(657)9423	
	Zero Gravity Control of Hydrogen and Cesium by Electrical Phenomena	Dynatech	Study feasibility of separation and orientation of two phase hydrogen in long-duration, large scale, zero-g storage tanks	WP AFP	AF33(657)10784	
	In-Space Propellant Orientation and Venting Experiments	LMSC	Study, design and fabricate dielectrophoresis experimental payloads for flight test on MOL or Titan IIIC	AFRPL	(Not yet assigned)	
Liquid Removal Systems (open-loop Refrigeration)	System effects on Cryogenic Propellant Storability and Vehicle Performance (Phase III)	DAC	Study application of a liquid removal system (thermal conditioning) as a means of controlling tank pressure without ullage venting	AFRPL	AF04(611)10750	
		TRW	Design, fabricate, test, a liquid removal thermal conditioning system utilizing heat exchangers in tank walls	LeRC		
	Liquid Propellant Thermal Conditioning System	LMSC	Design, fabricate, test a thermal conditioning unit for a reference kick stage mission. Correlate lg test data to zero-g conditions	LeRC	Not yet assigned	

Table XIV (Cont'd)

Technology	Title	Contractor	Scope	Sponsor	Contract No.	Term (CY) 63 64 65 66 67 68
Containment Screens	System effects on Cryogenic Propellant Storability and Vehicle Performance (Phase III)	DAC	Study feasibility of using capillary devices (e.g. containment screens) for passive orientation of cryogenics under low-g environment	AFRPL	AF04(611)10750	
Pressurization and related areas						
Pressurization Systems	System effects on Cryogenic Propellant Storability and Vehicle Performance (Phase II)	DAC	Study and evolve analytical model for pressurization. Calculate pressurant requirements of candidate systems for specified duty cycles. Perform pressurization tests (Phase VIII) in test apparatus	AFRPL	AF04(611)10750	
Cryogenic Pressure Vessels	Extended loading of Cryogenic Tanks	Boeing	Experimental test program to study flow propagation in Al and Al/Ti alloys under sustained loads at both room and cryogenic temperatures. Correlate results for pressure vessel design criteria	LeRC		
Propellant Feed Systems						
Boost Pumps	System effects on Cryogenic Propellant Storability and Vehicle Performance (Phase I)	DAC	Study candidate systems and perform pre-design of optimum system selected. Compare performance with pressure-fed system for the specified duty cycles	AFRPL	AF04(611)10750	
LH_2 Bladders	Cryogenic positive Expulsion Bladders	Beech	Study and develop design concepts for LH2 bladders. Design, fabricate, and test bladders for several selected concepts	LeRC		

Table XIV (Cont'd)

4

Technology	Title	Contractor	Scope	Sponsor	Contract No.	Term (CY) 63 64 65 66 67 68
Propellant Feed Systems	Subcritical Cryogenic Expulsion System (Tasks II-V)	Arda-Portland	Design, fabricate, test a LH_2 expulsion system using collapsible metallic containers for separation of LH_2 from He pressurant	AFSC (R&TD)		
LOX Bladder	Liquid Oxygen Bladder Development	(not yet assigned)	Study and develop design concepts for LO_2 bladders. Design, fabricate, test bladders for several selected concepts	LeRC	(not yet assigned)	
Propellant Utilization Systems	System Effects on Cryogenic Propellant Storability and Vehicle Performance (Phase V)	DAC	Study and determine the P.U. system required to obtain maximum stage performance for each of the specified duty cycles. Survey existing systems for application to the duty cycles selected for the study.	AFRPL	AF04(611)10750	
Liquid Quantity Sensors	Development of Liquid Sensor for Cryogenic Propellants	Acoustics	Study feasibility of extending current designs for storables (e.g., UDMH, H_2O_4) to cryogens. Fabricate and test prototypes	AFRPL		
Feed System Line Losses	System Effects on Cryogenic Propellant Storability and Vehicle Performance (Phase II)	DAC	Study and evaluate engine feed line propellant losses for a conventional design. Investigate methods for maintaining losses, and perform pre-design for selected approach	AFRPL	AF04(611)10750	
Fluid Dynamics	Analytical Study of Interface Dynamics	LMSC	Study and develop analytical techniques for calculating slosh frequencies under applied forces of varying magnitude and direction	LeRC	NAS3-7119	

Table XIV (Cont'd)

Technology	Title	Contractor	Scope	Sponsor	Contract No.	Term (CY) 63 64 65 66 67 68
Fluid Dynamics	Lockheed Independent Technology Program for Cryogenics	LMSC	Test program for fluid dynamics encompasses drop tower tests for study of nucleate bubble growth and stability, liquid sloshing and rebound, suction dip, etc.	LMSC in-house I.D.	(N.A.)	66–68
	Research into Fundamental Properties of Low Temperature Fluids	AGC	Test program for study of formation of foam and bubbles during liquid flow	NBS	In-house program	66–67
	Behavior of Liquid-Vapor Interface During Liquid Removal	TRW	Study of liquid-vapor interface dynamics during liquid removal (open loop refrigeration system)	LeRC		66–67

February 10, 1966 APPROVAL TM X-53395

PROGRAM PLAN FOR EARTH-ORBITAL LOW G HEAT TRANSFER AND FLUID MECHANICS EXPERIMENTS

By M. E. Nein and C. D. Arnett

The information in this report has been reviewed for security classification. Review of any information concerning Department of Defense or Atomic Energy Commission programs has been made by the MSFC Security Classification Officer. This report, in its entirety, has been determined to be unclassified.

This document has also been reviewed and approved for technical accuracy.

C C Wood

C. C. WOOD
Chief, Fluid Mechanics and Thermodynamics Branch

H G Paul

H. G. PAUL
Chief, Propulsion Division

F. B. Cline

F. B. CLINE
Director, Propulsion and Vehicle Engineering Laboratory

DISTRIBUTION

DIR	Dr. von Braun
DEP-T	Dr. Rees
I-DIR	Brig. Gen. O'Connor
I-SE-CH	Dr. Mrazek
I-I/IB-MGR	Mr. James
I-V-MGR	Dr. Rudolph
I-E-MGR	Mr. Belew
R-DIR	Mr. Weidner
R-DIR	Dr. McCall
R-DIR	Dr. Johnson
R-RP-DIR	Dr. Stuhlinger
R-SA	Mr. Dannenberg
R-A	Mr. Williams
R-A	Mr. von Tiesenhausen
R-A	Mr. Oliver
R-AERO-DIR	Dr. Geissler
R-ASTR-DIR	Dr. Haeusserman
R-COMP-DIR	Dr. Hoelzer
R-ME-DIR	Mr. Kuers
R-QUAL-DIR	Mr. Grau
R-TEST-DIR	Mr. Heimburg
R-TEST-C	Mr. Grafton
R-P&VE-DIR	Mr. Cline
R-P&VE-DIR	Mr. Hellebrand
R-P&VE-DIR	Mr. Palaoro
R-P&VE-M	Dr. Lucas
R-P&VE-S	Mr. Kroll
R-P&VE-V	Mr. Aberg
R-P&VE-V	Mr. DeSanctis
R-P&VE-V	Mr. Pedigo
R-P&VE-P	Mr. Paul
R-P&VE-P	Mr. McCool
R-P&VE-PA	Mr. Thomson
R-P&VE-PA	Mr. Reed
R-P&VE-PAA	Mr. Chandler
R-P&VE-PAA	Mr. Lombardo
R-P&VE-PAS	Mr. Long
R-P&VE-PT	Mr. Wood
R-P&VE-PT	Mr. Connell
R-P&VE-PT	Mr. Nein (25)

DISTRIBUTION (Cont'd)

R-P&VE-PT	Mr. Swalley
R-P&VE-PTF	Mr. Platt
R-P&VE-PTP	Mr. Vaniman
R-P&VE-PTD	Mr. Hopson
R-P&VE-PTE	Mr. Moses
R-P&VE-PTE	Mr. Arnett
R-P&VE-PM	Mr. Fuhrmann
R-P&VE-PM	Mr. Voss
R-P&VE-PMD	Mr. Muller
R-P&VE-PMC	Mr. Schnelle
R-P&VE-PMS	Mr. Burson
R-P&VE-PMP	Mr. Edwards
R-P&VE-PE	Dr. Head
R-P&VE-PE	Mr. Bergeler
R-P&VE-PP	Mr. Heusinger
MS-IP	Mr. Remer
MS-IL	Miss Robertson (8)
MS-H	Mr. Akens
MS-T	(6)
CC-P	
R-P&VE-RT	Hofues

Scientific and Technical Inf. Facility (25)
Attn: NASA Rep. (S-AK-RKT)
P.O. Box 33
College Park, Maryland